

Conceptual Composite Wing Design

by

Martin C. Blair

A Thesis Presented in Partial Fulfillment
of the Requirements for the Degree
Master of Science

Approved July 2021 by the
Graduate Supervisory Committee:

Timothy Takahashi, Chair
Raghavendra Murthy
Ruben Perez

ARIZONA STATE UNIVERSITY

August 2021

ABSTRACT

Automation has become a staple in high volume manufacturing, where the consistency and quality of a product carries as much importance as the quantity produced. The Aerospace Industry has a vested interest in expanding the application of automation beyond simply manufacturing. In this project, the process of systems engineering has been applied to the Conceptual Design Phase of product development; specifically, the Preliminary Structural Design of a Composite wing for an Unmanned Air Vehicle (UAV). Automated structural analysis can be used to develop a composite wing structure that can be directly rendered in Computer Aided Drafting (CAD) and validated using Finite Element Analysis (FEA). This concept provides the user with the ability to quickly iterate designs and demonstrates how different the “optimal light weight” composite structure must look for UAV systems of varied weight, range, and flight maneuverability.

DEDICATION

This Thesis is dedicated to my best friend and wife, who has supported me through the arduous path of getting a graduate degree. I also dedicate this Thesis to my mother and father, who have never let me down, and to the Flinn Foundation, who invested in my education and enabled me to attend university. Thank you all for your support and aid along the way.

ACKNOWLEDGEMENTS

Thank you, Dr. Takahashi, for not only being an exemplary teacher, but also being a mentor and friend. Without his guidance, this thesis project would not have made it all the way to fruition. A special thanks to Dr. Murthy for joining this committee midway through the project and being instrumental in the ANSYS modeling component.

TABLE OF CONTENTS

	Page
LIST OF TABLES.....	vi
LIST OF FIGURES.....	vii
LIST OF SYMBOLS/ NOMENCLATURE.....	x
CHAPTER	
1. INTRODUCTION.....	1
2. PRIOR ART	5
Aircraft Design Principles.....	5
Composite Materials	9
Wing Load Testing	12
Wing Stress Box Simplification.....	16
Buckling Load Limitations and Composite Failure Criteria.....	19
Factor of Safety and Balanced Design.....	22
Computational Structural Sizing in Industry, Government, and Academia	23
3. BUILDING THE MODEL.....	27
Critical Variables	27
Wing Geometry and Load Build Up.....	28
Enumerating Potential Composites.....	30
Composite Laminate Build Up & Skin Thickness.....	32
Composite Layup Analysis.....	34
Rib Placement	35

CHAPTER	Page
4. MODEL VALIDATION.....	38
CAD Modeling.....	38
ANSYS ACP (Pre/Post).....	40
Finite Element Analysis.....	41
5. RESULTS	44
UAV Analysis.....	44
Jet with Low Aspect Ratio Wing Analysis.....	73
6. CONCLUSION.....	86
REFERENCES	88
APPENDIX.....	92
A. MATERIAL PROPERTIES TABLES.....	92
B. EXCEL MODEL EXAMPLES	96

LIST OF TABLES

Table	Page
1. Wing Structural Layup Output from Model	39
2. UAV User Design Inputs	46
3. Composites Layups Enumerated in a Set of Twenty	49
4. Composite Layups for the Twenty Enumerated Options.....	50
5. Model Output Failure Criteria for UAV Wing	51
6. Model Output Structural Description for UAV Wing	52
7. Carbon-Epoxy Failure Strength	55
8. Normal Stress Maximum Stress Criterion Tabulated	72
9. Jet User Design Inputs	74
10. Jet Wing Model Composite Failure Check.....	76
11. Model Output Structural Description for Jet Wing.....	77

LIST OF FIGURES

Figure	Page
1. Example of a Work Breakdown Structure.....	5
2. Example of the Design Cycle	8
3. Composite Laminate Coordinates.....	9
4. Types of Composites.....	10
5. Long Fiber Laminate Composites.....	10
6. BOEING 787 FUSELAGE w/ RIVETED RIBS & SKINS All in Composite.....	12
7. V-N Diagram 14 CFR § 04.2110.....	13
8. N _z cert VS. Weight Limit 14 CFR § 25.337.....	13
9. B787 WING FLEX.....	15
10. Potex 25 Wing Structure.....	17
11. Wing Stress Box Simplification as Shown in ANSYS.....	18
12. Wing Beam Approximation as Shown in ANSYS	18
13. Panel Buckling Under Compressive Edge Loading.....	20
14. Simply Supported Panel Buckling Example.....	21
15. Example of Aero Load Development Over the Wing Section.	29
16. FBA Code Used to Select for Panel Buckling Failure or Composite Compression Failures.....	36
17. Sample Model Output for a Wing Structure	38
18. CAD Wing Model.....	40
19. SOLIDWORKS Wing Model with Shear Concentration	41
20. ANSYS Boundary Conditions	42

Figure	Page
21. ANSYS Pressure Distribution	43
22. UAV Fuselage and Wing Visualization.....	47
23. SOLIDWORKS Static Stress Analysis with Point Shear Loading.....	53
24. SOLIDWORKS Wing Model Static Loading Failures Analysis with Distributed Pressure.....	54
25. UAV Wing Total Deformation [In]	55
26. UAV Wing Equivalent Stress [Psi].....	56
27. UAV Panel 1 Equivalent Stress Top 90 Deg. Ply [Psi]	57
28. UAV Panel 1 Equivalent Stress Top 45 Deg. Ply [Psi]	58
29. UAV Panel 1 Equivalent Stress Top 0 Deg. Ply [Psi]	58
30. UAV Panel 1 Equivalent Stress Top -45 Deg. Ply [Psi].....	59
31. UAV Panel 1 Equivalent Stress Foam Core [Psi].....	59
32. UAV Panel 1 Equivalent Stress Bot -45 Deg. Ply [Psi]	60
33. UAV Panel 1 Equivalent Stress Bot 0 Deg. Ply [Psi].....	60
34. UAV Panel 1 Equivalent Stress Bot 45 Deg. Ply [Psi].....	61
35. UAV Panel 1 Equivalent Stress Bot 90 Deg. Ply [Psi].....	61
36. UAV Panel 2 Equivalent Stress Top 90 Deg. Ply [Psi]	62
37. UAV Wing Normal Stress [Psi].....	63
38. UAV Panel 1 Normal Stress Top 90 Deg. Ply [Psi]	63
39. UAV Panel 1 Normal Stress Top 45 Deg. Ply [Psi]	65
40. UAV Panel 1 Normal Stress Top 0 Deg. Ply [Psi]	65
41. UAV Panel 1 Normal Stress Top -45 Deg. Ply [Psi].....	66

Figure	Page
42. UAV Panel 1 Normal Stress Core [Psi]	66
43. UAV Panel 1 Normal Stress Bot -45 Deg. Ply [Psi].....	67
44. UAV Panel 1 Normal Stress Bot 0 Deg. Ply [Psi]	67
45. UAV Panel 1 Normal Stress Bot 45 Deg. Ply [Psi].....	68
46. UAV Panel 1 Normal Stress Bot 90 Deg. Ply [Psi].....	68
47. UAV Wing Composite Safety Factor	69
48. UAV Wing Composite Safety Factor Panel 1 Top 90 Deg.	69
49. UAV Wing Eigenvalue Buckling 0.97887	70
50. UAV Wing Eigenvalue Buckling 1.0127	70
51. UAV Wing Eigenvalue Buckling 1.0469	71
52. UAV Wing Eigenvalue Buckling 1.0664	71
53. UAV Wing Eigenvalue Buckling 1.0788	71
54. Jet Wing Profile Visualization	75
55. Jet Wing Total Deformation [In]	78
56. Jet Wing Total Deformation (Bottom of Wing) [In]	78
57. Jet Wing Equivalent Stress [Psi].....	80
58. Jet Wing Equivalent Stress (Bottom of Wing) [Psi].....	80
59. Jet Wing Normal Stress [Psi]	82
60. Jet Wing Normal Stress (Bottom of Wing) [Psi]	82
61. Jet Wing Composite Safety Factor	83
62. Jet Wing Composite Safety Factor (Bottom of Wing).....	83
63. Jet Wing Eigenvalue Buckling 1.675.....	84

LIST OF SYMBOLS/ NOMENCLATURE

a	= Characteristic Length (spanwise)	[in]
Aero load		
B	= 50% of Chord	[in]
CL	= Coefficient of Lift	
$Chord_{avg}$	= average chord length	[in]
D	= length wing center to composite center	[in]
Design lift	= Maximum flight weight	[lbf]
E	= Young's Modulus	[lbf/in ²]
I	= Area Moment of Inertia	[in ⁴]
K	= Compressive Buckling Coefficient	
k	= Composite Strain Coefficient	
L	= Length	[in]
Load %	= Load Percentage Carried by Area	
M	= Applied Torsional Moment	[lbf-in]
N	= Applied Force	[lbf]
N_z	= Load Factor	[gee's]
P	= Pressure	[lbf/in ²]
S_{ref}	= Wing Reference Area	
T	= Torsional Force	[lbf-in]
t	= Thickness	[in]
W	= Weight	[lbf]

ρ_{air}	= Density of Air	[lbm/in ³]
ν	= Poisson's Ratio	
ε°	= Composite Strain	
σ	= Composite Stress	[psi]

CHAPTER 1

INTRODUCTION

The world and the natural laws that drive it are exceedingly complex. To describe this complexity and distill from the chaos an order, keen thinkers define models which fit it. They may not perfectly describe the phenomena or have built in limitations to their accuracy, but they allow any person to become a student of reality. What follows is the record of the creation of one such model.

Engineers are often tasked with developing products from nothing, inventing solutions to problems where no prior experience, intuition or standard exists. It is in these clean sheet design challenges that an engineer is called to bring to bear their full arsenal of tools, and as with all things where efficiency is paramount, a process has been developed for success. In this case, the design process can be leveraged to develop something from nothing. This is a structured approach where the product concept moves through several phases of design. Each phase has the targeted goal of refining some part of the product. For instance, in the conceptual design phase the goal is to develop several high-level concepts for the product and its desired functionality. From these, an optimal concept is selected and refined in following design phases.

The aerospace industry is functionally different than most other fields of engineering. Aerospace engineers are constrained by the high demand placed on their products, from exceedingly long-life cycles, finer factors of safety, stricter regulatory compliance, certifications, and regulation on the communication of design qualities. All this restricts the innovation in the industry and presents a greater challenge to any new company looking to produce a product. Aircraft must be safe, reliable, maintainable and

producible. Consider that a Boeing 737 is typically airborne more than 2500 hours a year; over its 25-year lifetime it will be airborne for more than half a million hours. If the “millionth chance” were good enough for aviation, half of commercial airliners built could end in a fiery crash. Thus, we must design structures to be light enough to fly yet strong and maintainable enough never to fail in expected and “unexpected” operating conditions.

The development of a new airframe is a monumental task likely only rivaled by the design of space fairing vessels. As a comparison, new companies enter the automotive industry yearly, attempting to sell their product and gain traction in an ever-evolving community of competitors. In contrast, commercial aircraft manufacturing is fairly stagnant and is dominated by a few major players; Boeing and Airbus. While barrier of entry is lower to unmanned systems, “drones” are not supposed to crash randomly either – hence they must be designed to similarly high standards

A crucial part of the design of an aircraft is the design of the wing. Firstly, the shape of the wing needs to be selected to meet the needs of the aircraft, which include flight loads, speed, altitude, and other factors. These factors influence the development of both airfoil and the wing’s structural geometry. The design of wing structure is further complicated by the inclusion of modern structural materials in the form of composites. Composites present a unique design challenge when compared to traditional construction materials, such as metals or wood. Due to their ply-by-ply nature, composite materials present a more complex set of design constraints that must be accounted for. The large-scale structural integrity of a given panel needs to be modeled considering the statically indeterminate stresses that form within the composite layup.

Analysts alone cannot design an airframe. Due to the high degree of skill required of Finite Element Analysis (FEA) specialists, a variety of engineers and test pilots all work in integrated product teams (IPT) to complete the design cycle. These teams allow for the distribution of work to specialists, meaning that any individual is not required to take the product or component through the entire design cycle. First, requirements are needed – what does the aerostructure need to look like externally? An understanding of the loads expected in typical flight, as well as the loads expected in “atypical” flight is required. Second, a list of candidate materials that can be used to fabricate the aerostructure must be developed. Finally, the thicknesses of the external panels and the nuance of all internal stiffeners, ribs, etc. needed to construct a safe, reliable and maintainable aerostructure must be identified.

The goal of this project is to develop a tool which compresses the pooled intuition of a large team and the design process into a streamlined, single-step process to assist in the iterative development of a wing. This structural approximation can be extremely useful to an engineering design team, as it can provide fairly accurate approximation for the final wing weight, the potential space within the wing for flight control componentry, and fuel consumption. Furthermore, it provides the engineer with the ability to quickly edit the structure for new design constraints. The parametric design model selects an “optimum” design by choosing skin and rib materials from an enumerated list of possible engineering materials. A wide range of composite layups can be considered using this approach by varying the number and orientation of plies, the thickness of plies and the possibility of “sandwich” materials. By sorting through the possibilities, discarding those which do not satisfy certification loading requirements and ranking the remaining in terms of predicted

weight, the model provides the competent designer a good starting point for a final structural configuration.

CHAPTER 2

PRIOR ART

a. Aircraft Design Principles

Aircraft are complex machines developed by extensive teams of experts spanning various facets of the machine. Often, the teams stretch across multiple fields and potentially even companies. For any particular aircraft, the construction and design are split by the Prime, which functions as the interface between the customer and the sub-contractors. The customer describes what they need from the potential aircraft design and what they are willing to pay for the product. From this outline of needs, the Prime can develop the high-level requirements for the design and potentially begin development of the product in-house. As the Prime is faced with design challenges they may be under-equipped to complete or manufacturing requirements they do not have the capabilities to complete, they will seek out sub-contractors to design and build those components. This relationship can be drawn in a work breakdown structure (WBS) ^[1]. An example of a WBS is shown in fig. (1); this practice is pulled directly from MIL-STD 499 ^[1].

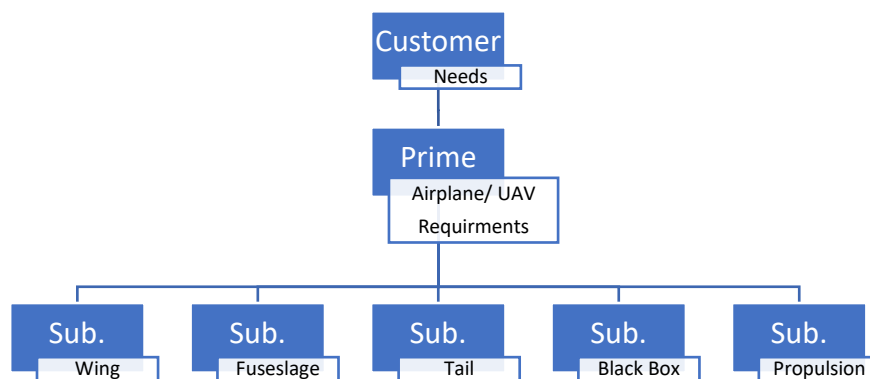


Figure 1: Example of a Work Breakdown Structure.

A WBS forms an organizational structure between the Prime and sub-contractors for the work to be completed. Further, it outlines the relationship between each company involved and the entity that owns the rights to individual designs. After the Customer approaches the Prime with design needs, the Prime will develop the Requirements of the design. Needs are the high-level capabilities of the aircraft: its mission, payload, range, deployment method, etc., while the Requirements are the individual specifications of the aircraft to meet those needs, for example aircraft weight, range, size, engine thrust and wing lift. Often, needs can be directly translated into requirements. However, more commonly, the customer has broad system demands and expects the Prime to translate those into a product. In the case of government contracts, multiple Primes could be competing with the same set of needs and develop largely different aircraft with different requirements.

Once the Prime knows the Requirements for the aircraft, they must take the product through two different design cycles: The Preliminary Design Phase and the Detail Design Phase. In the Preliminary Design Phase, the Prime develops the conceptual design for the product and works with potential end users to refine that design toward a clearer set of design variables. In the case of an aircraft, this would involve discussion with potential pilots of the aircraft about their desires for its function and form. Further, prior designs that fit the use case of the product can be reviewed through trade studies. This process serves to further narrow the scope of the design and arrive at a concept of what the final product would be. This process is closed out with the Preliminary Design Review where the conceptual design is validated and green-lit for further development.

The second design cycle is the Detailed Design Phase, in which the conceptual design is refined into a potential product that could be manufactured. Included in this phase is the prototyping process, where full proof of concepts could be built and tested for function. This phase ends with a Critical Design Review, where the design is assessed for its manufacturability, cost, and function. Further this phase concludes with the assessment of the products final form or a design freeze where particular qualities, dimensions, or requirements of the product can no longer be changed without significant effort.

Nested within these phases is the sub-process for the design of each component of the aircraft. While there are many flavors of the design process current practice for designing aircraft is to follow a procedure which cycles back on itself to reaffirm checks. This process begins with the end user describing a set of requirements or needs that the aircraft will have to meet. This process recurs a multitude of times in the design of an entire airframe. As subsystems, and potentially even minor components, have their own nested design cycles. This process can be seen in fig. (2).

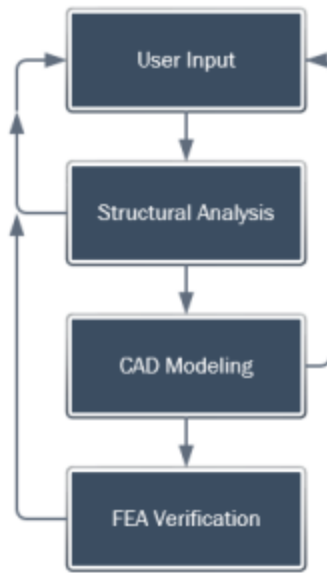


Figure 2: Example of the Design Cycle

The sub-components of the aircraft are drawn in Computer Aided Design (CAD) based on the requirements and the engineering team's intuition. This design is verified in Finite Element Analysis (FEA). Throughout this process as checks are failed, the inputs are refined, the design is altered, and the analysis is repeated to eventually arrive at a final working design. Here it is critical to design components which can easily be analyzed. Overly complex designs can lead to extended modeling times and potentially raise concerns with the accuracy of any given computational test. The process of taking the requirements and iterating through a potential geometry and its testing will repeat throughout both the Conceptual and Detailed Design phases. The results of these tests can also prove invaluable in the final validation of the product when transitioning into the manufacturing stage. The goal of this project is to step into the Conceptual Design Phase and provide detailed design insights earlier in the aircraft's development cycle.

b. Composite Materials

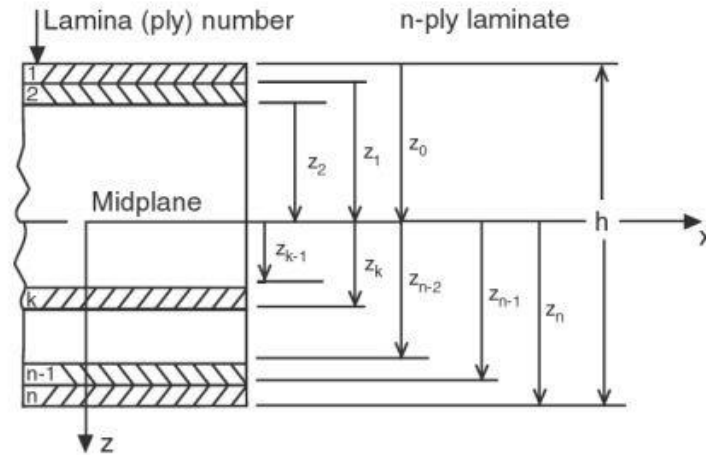


Figure 3: Composite Laminate Coordinates ^[4]

Composites involve the mixing of dissimilar materials to create a part with the joint properties of both those materials, and they have been used in the construction of tools for ages ^[5]. A natural example of a composite is wood, which takes advantage of long “fiber” cellulose strands held together by a lignin “matrix”. The Hungarian horse bow is a more complex example of a composite, which combines a wood core with sinew laminate to create a lighter, stronger bow. One of the most widely known composites is carbon fiber. Carbon fiber uses long strands of carbon fibers bound together with an epoxy resin. Sheets of carbon fiber are then stacked to increase their strength. In the modern age, composites have become a favored construction material for instances where strength to weight ratios is paramount and cost is a secondary concern. This is because composites have extremely high tensile strength and rigidity, while also being light in comparison to their metallic or polymer counterparts. This theoretical weight savings is extremely appealing for aircraft designers, who are constantly balancing the need for rigidity, strength and stability of structures against its impact on airframe weight.

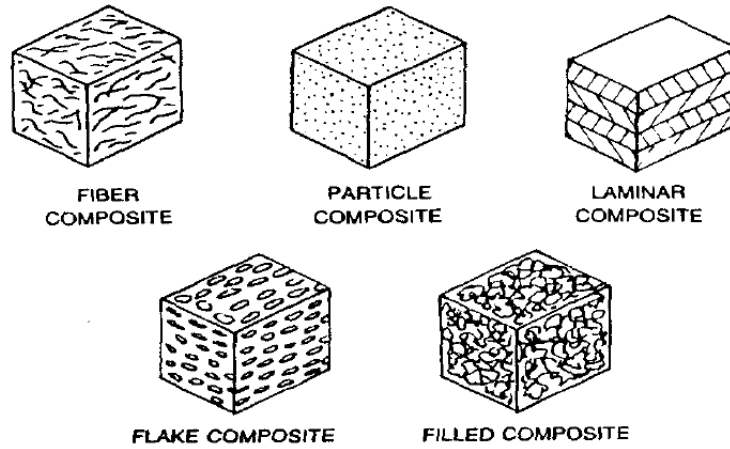


Figure 4: Types of Composites ^[4]

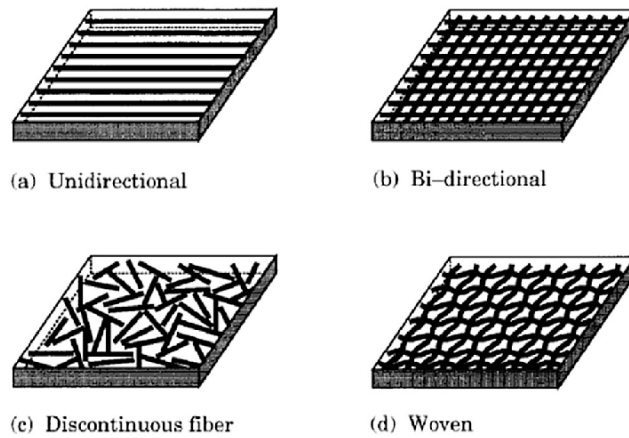


Figure 5: Long Fiber Laminate Composites ^[4]

Composites can be broken into several sub types all characterized by the presence of a supporting matrix and higher strength filler media. The simplest composite is the laminar type, which is the bonding of sheets of material, plywood is an excellent example of this composite type. Particle, flake and fiber composites are analogous in their creation, as seen in fig. (4). Each has a supporting matrix which provides the dimensionality and structure to the composite while a filler media is used to enhance the material properties of the structure. Filled composite is similar to these, but has a much higher fiber to matrix ratio. The final composite type shown in the above fig. (5) is long strand fiber composites, which

uses long strands of the composite fiber in sheets that are often woven to further increase the performance. In practice, composite types are often combined, as in our example of carbon fiber where a long strand composite sheets are then stacked to create a laminar composite, as seen in fig. (3).

Boeing's 787 is an example of the use of composites in aircraft design to take advantage of their high tensile strength. Where Boeing used a combination of conventional aircraft building materials and composites to build the primary structures of the aircraft. Composite panels were built up over composite ring frames affixed with fasteners, calling this manufacturing method "black aluminum". These parts are made from graphite-reinforced composites configured in the same geometric manner as a conventional aluminum structure, as seen in fig. (6). However, composites are not without disadvantages. While their extreme tensile strength and rigidity is appealing, composites are weak in compression cases. To expand on this, see fig. (5), and note the fiber supported by a matrix. The fiber in this analogy can be consider as a rope, and the matrix is a glue which holds the ropes in a "fixed" arrangement and direction. Now consider a rope in hand when pulled from each end; the rope is taught and strong. However, as you attempt to compress the rope it droops and loses shape, providing little to no resistance. A fiber matrix composite behaves much the same way. In tension, the fibers of the composite support the majority of the load. However, in compression the load is supported by the matrix, which is comparatively weak [2, 3, 4, 7, 8].



Figure 6: BOEING 787 FUSELAGE w/ RIVETED RIBS & SKINS all in composite ^[40]

c. Wing Load Testing

The method of proof testing aircraft structures to a certification flight weight with a multiplier has been practiced since the earliest days of Federal Regulation. The concept of a load-factor vs flight speed design envelope emerges in the initial edition of the Code of Federal Regulations, published 1938. 14 CFR § 04 “Airplane Airworthiness” (1938) ^[9] which is the direct precursor to the modern 14 CFR § 23 ^[10] and 14 CFR § 25 ^[11] regulatory framework. This early CFR establishes the $V-N$ diagram seen in fig. (5) in its present form and fully encapsulates the modern approach to structural sizing.

The wing of an aircraft must support several different types of load cases, which reflect different phases of flight. Two essential load cases comprise 1) maneuvering flight at the maximum flight weight (the MTOW or maximum takeoff weight) where the lift of the wing greatly exceeds the weight of the aircraft, and 2) a hard landing where the aircraft maintains an appreciable sink rate at the moment of touch down ^[12, 6, 13, 14, 15]. The maximum flight load condition is defined by the “ $V-n$ ” diagram fig. (7); the limiting load cases are typically found at a load factor, N_z fig. (8), between 2.5 and 3.8-gees for

commercial aircraft [15] and anywhere from 3.0 to 6.0 gees for maneuvering military aircraft [16].

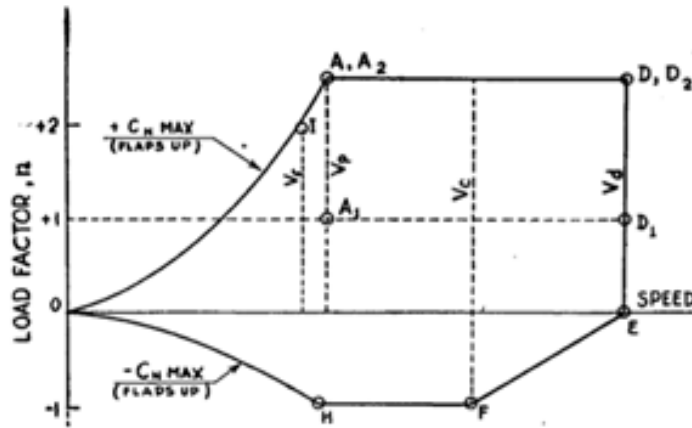


Figure 7: V-N Diagram 14 CFR § 04.2110

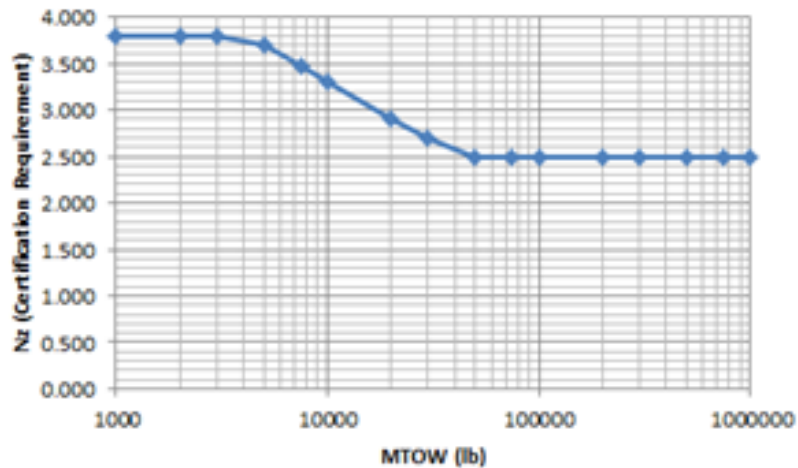


Figure 8: Nz cert VS. Weight limit 14 CFR § 25.337

The 1945 CFR states in 14 CFR § 04.200 that “strength requirements are specified in terms of limit and ultimate loads. Limit loads are the maximum loads anticipated in service. ... when not otherwise described, loads specified are limit loads. Unless otherwise provided, the specified ... loads shall be placed in equilibrium with inertia forces, considering all items of mass in the airplane. All such loads shall be distributed in a manner

closely approximating or conservatively representing actual conditions. If deflections under load would significantly change the distribution of external or internal loads, such redistribution shall be taken into account.”^[17]

The 1945 CFR states clearly under 14 CFR § 04.201 that “the factor-of-safety shall be 1.5 unless otherwise specified.”^[18] This is the precursor to the same statement now made in modern regulation 14 CFR § 25.303.^[19] 14 CFR § 04.202 states the structure to be “capable of supporting limit loads without suffering detrimental permanent deformations. At all loads up to limit loads the deformation shall be such as not to interfere with safe operation of the airplane. The structure shall be capable of supporting ultimate loads without failure for at least 3 seconds”^[20] under a test which 14 CFR § 04.203 requires to represent “all critical loading conditions.”^[21] This sets the precedent under which flight testing is a pass or fail metric. If the requirements are met, the test the aircraft is deemed airworthy, even if those requirements are met in the slightest margin.

The certification load is first defined in 14 CFR § 04.210 stating that “flight load requirements shall be complied with at critical altitudes ... at all weights between the minimum design weight and design take-off weight with any practicable distribution of disposable load within prescribed operating limitations stated in the airplane operating manual.”^[22] 14 CFR § 04.2130 stipulates that “a sufficient number of points on the maneuvering and gust envelopes shall be investigated to ensure that the maximum load for each member of the airplane structure has been obtained. ... all significant forces acting on the airplane shall be placed in equilibrium in a rational or conservative manner ... (including) linear inertia forces in equilibrium with wing and horizontal tail surface (aerodynamic) loads.”^[23]

This concept of a maneuvering and gust “envelope” supports the graphical foundation of the *V-N* diagram and associated gust envelope. These novations are introduced in 14 CFR § 04.2111 which holds that “the airplane shall be assumed to be subjected to symmetrical maneuvers resulting in the following limit load factors except were limited by maximum (static) lift coefficients. ^[24, 25]

Unchanged since 1945, the modern 14 CFR § 25 states “strength requirements are specified in terms of limit loads (the maximum loads to be expected in service) and ultimate loads (limit loads multiplied by prescribed factors of safety). Unless otherwise provided ... loads must be placed in equilibrium with inertia forces, considering each item of mass in the airplane. These loads must be distributed to conservatively approximate or closely represent actual conditions. ... If deflections under load would significantly change the distribution of external or internal loads, this redistribution must be taken into account.” ^[26] An example of extreme wing flex can be seen in fig. (9).

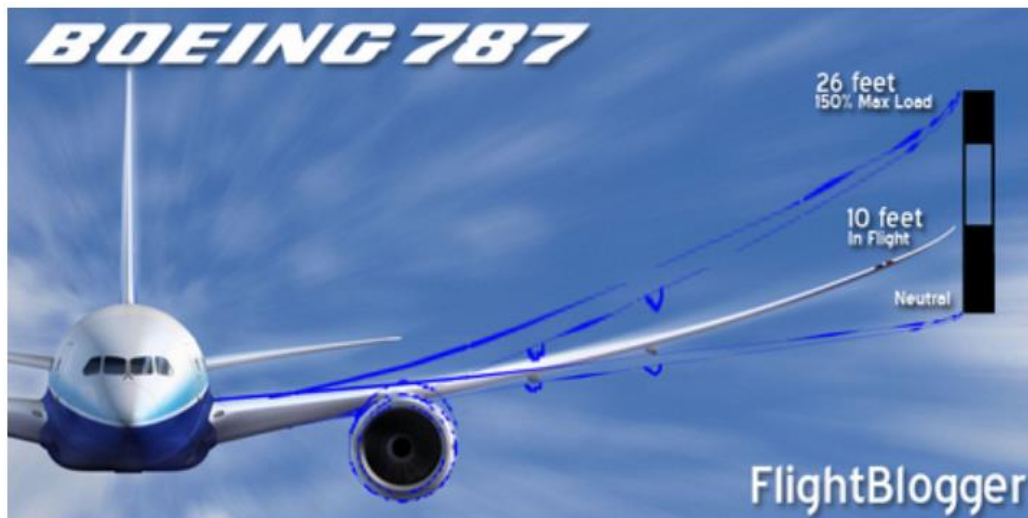


Figure 9: B787 WING FLEX ^[41]

The distributed pressure and/or landing gear loads impart both transverse and torsional loads to the airframe structure. For primary structural sizing, the transverse (bending) torques are much greater than the torsional (twisting) torques. The deformation of the wing when viewed in total is great, however at the composite laminate level each cell is experiencing minimal deformation. Here we can apply linear elasticity theory, where the relationship between the strain and stress in the material is linear. This approximation for the deformation of the material allows for the bending and torsional load cases to be decoupled and solved independently ^[27, 13]. Furthermore, this relationship also allows for the independent solutions to be superimposed after post processing.

The geometry of a high-performance wing will have spanwise variation in the defining airfoil sections. As we move from the side-of-body to the wingtip, the planform may taper so that the chord (the distance from leading-edge to trailing-edge) will decrease as we move outboard. In addition, the defining airfoil sections may vary in camber and thickness-to-chord ratio as we move from side-of-body to wingtip. Finally, the wing may be twisted, so that the local incidence of each defining airfoil relative to the reference “waterline” datum will vary as we move from side-of-body to wing tip.

Because linear elasticity theory decouples the effects of transverse bending from torsional twisting, we can decouple our bending model from twist ^[27, 13]. This greatly simplifies the enumeration of the wing structure and its subsequent validation in computational analysis.

d. Wing Stress Box Simplification

The substructure of current wings has become too complex to be analyzed using traditional analytical techniques. To overcome this, a major simplification to the wing structure has been made. This simplification will inform several other assumptions made

throughout this project. A wing is made up of 3 primary structures: the ribs are chord wise structural members which serve as breaks to buckling loads and define the airfoil shape; the spar, which can be singular or exist in a set, is a spanwise structure that supports the majority of the structural loads imparted on the wing; the skin is the outer layer which defines the outer perimeter of the wing. An example of a complex wing structure can be seen in fig. (10).

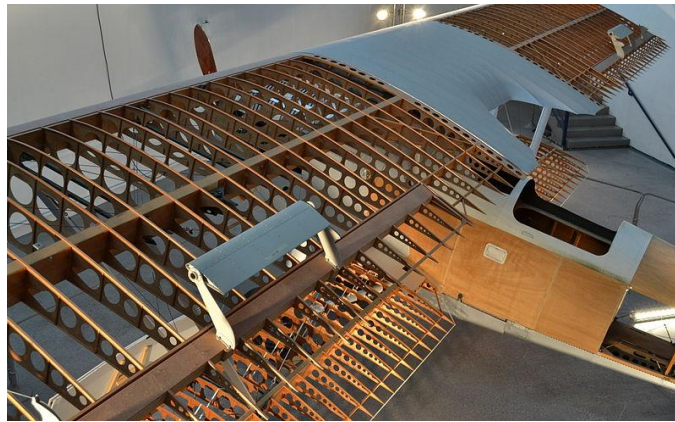


Figure 10: Potex 25 Wing Structure on display at the Musée de l'Air et de l'Espace in Le Bourget, Paris.

A stress box can be created by isolating two adjacent ribs and the top and bottom skin of the wing, ^[6, 13, 27] seen in fig. (10). When used in conjunction with the beam simplification for the wing, this becomes a powerful tool for understanding the shear flow in the ribs and skin of the wing. As the wing is exposed to a non-uniform spanwise loading defined by the lift case, the local shear at any point on the wing can be found. This can then be used to define force couples in each of the stress boxes, which then provides the tension and compression forces that are applied to the skins.

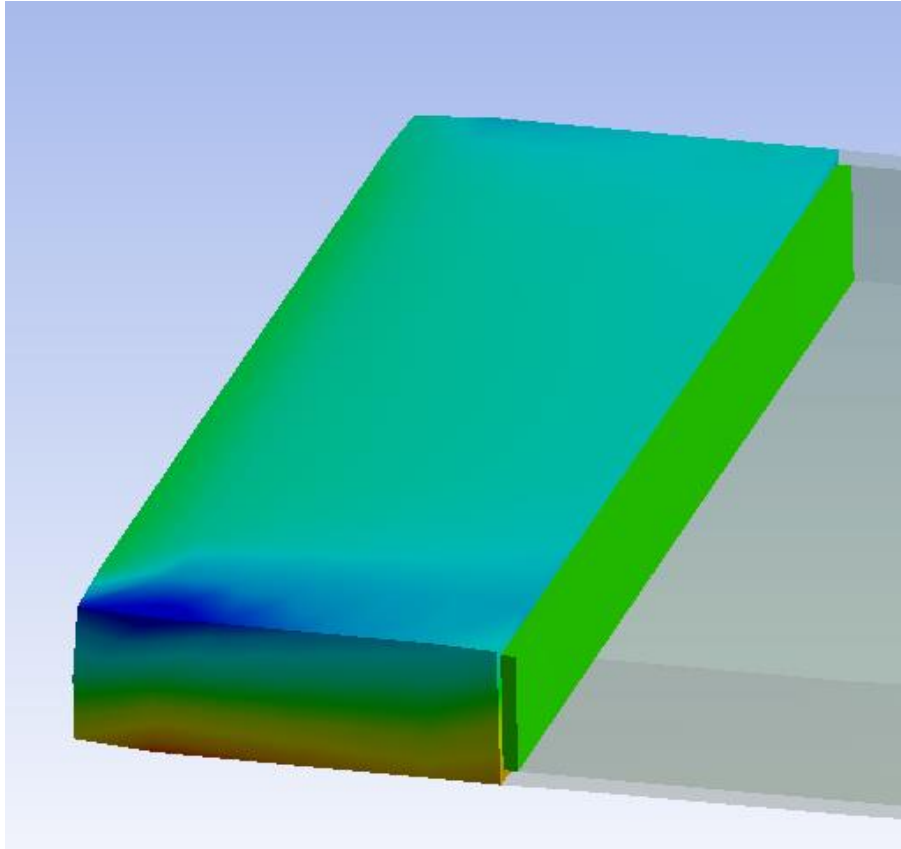


Figure 11: Wing Stress Box Simplification as Shown in ANSYS

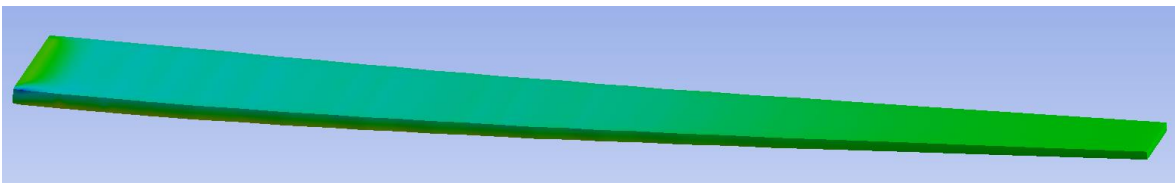


Figure 12: Wing Beam Approximation as shown in ANSYS

The force couples can further be used to find the critical buckling loads under which any wing panel would fail. Note that this simplification greatly reduces the complexity of the wing structure, which serves to expedite the modeling and analysis time involved in each iteration of the wing. It also allows for the use of analytical solutions with the inclusion of empirical correction constants. However, this simplification in conjunction with others made in the creation of the model could lead to the structure being overly

pessimistic or optimistic when finally analyzed. In other words, the model could accurately under- or over-predict the requirements of the wing, leading to a structure which is linearly over- or under-engineered. This case would require the application of a scaling factor to bring the structure inline during computational post processing.

e. Buckling Load Limitations and Composite Failure Criteria

The materials used in aircraft construction are typically stronger in tension load cases than in compression load cases. This behavior is shared by long strand fiber matrix composites^[4]. The reason for this behavior in the case of a composite panel would be two-fold. Firstly, as expressed earlier in the rope analogy, tension cases align the fibers in the matrix and disproportionately rely on the stiffness of the fiber to support the structure. In compression cases, the fiber easily collapses, transferring load to the supporting matrix, which does not share the extreme material properties of the fiber. The second case is due to the increased number of potential failure modes in compression cases when compared to tension cases such as buckling, crimping, shear, panel wrinkling and others. This is a byproduct of material choice and construction methodology^[3]. Of the potential failure modes, buckling is the most empirically tested and has been distilled into analytical functions for the appropriate support cases. It would follow that the limiting factor to aircraft design, and in this case wing design is the compression case^[6].

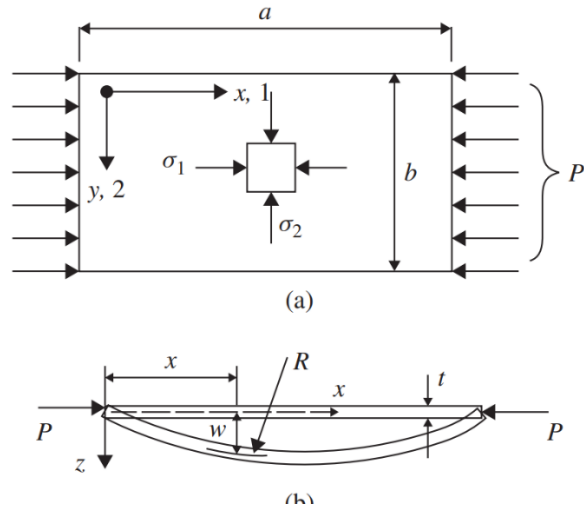


Figure 13: Panel buckling under compressive edge loading from *Mechanics of Optimal Structural Design: Minimum Weight Structures* David W. A. Rees pp. 526

Fig. (10) demonstrates the complexity of an aircraft wing. For the purposes of this analysis, several simplifications can be made to create the construction seen in fig. (13). These simplifications, which are representative of the construction of small frame aircraft, include the omission of stringers and stiffeners, which are specific to metallic wing construction. Using this construction methodology, the majority of the bending loads applied to the wing will be supported by the top and bottom skins of the wing, which can be approximated using a panel simplification ^[6, 28], as seen in fig. (11).

As previously noted, the panel is much more likely to fail in compression than in tension, as any loading of the wing will result in the top and bottom panel having opposing loading cases. The compression case is taken as the critical loading case and the tension case is omitted from the iterative development of the wing structure. Areas of the wing under tension will be analyzed computationally to confirm that the wing does not fail under that type of loading. Unfortunately, compressive failure is more difficult to analyze as there are several ways in which the panel could fail in this load case. Due to

the thinness of the panel, the most likely failure will be buckling, where the panel is not rigid enough to support the applied load and deflects catastrophically, no longer supporting the applied force. An example of panel buckling analysis can be seen in fig. (14).

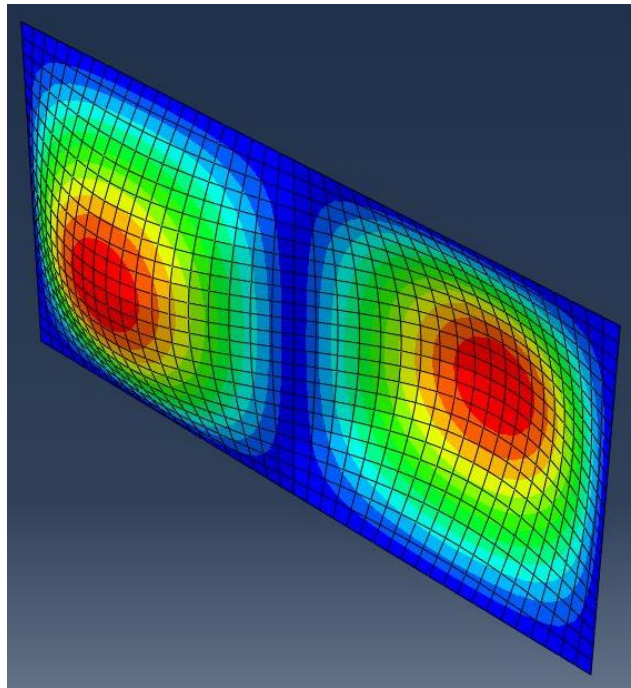


Figure 14: Simply Supported Panel Buckling Example

Buckling is not the only failure criteria used to build up the wing structure. While buckling is useful to describe the failure of any particular panel on the aircraft, it does not describe the stresses and strains developed within the individual plies of the laminate [2, 4, 8]. Failure of composite laminate can be defined using several composite failure criteria. The failure criteria used in this case include maximum strain, maximum stress, and Tsai-Hill. For the buildup of the wing in the compressive case both the panel buckling and the composite failure criteria need to be checked.

f. Factor of Safety and Balanced Design

Aircraft are designed to a much tighter tolerance than many other products of engineering. In all engineering practices a factor of safety is used to provide a ceiling for the acceptable loads on a structure ^[19]. This is achieved by applying a multiplier to the intended load a structure will support. This multiplier serves as the safety net between what the structure is designed to support and what it can support in an emergency. The modern industry standard for an aircraft's primary structure from 14 CFR § 25.303 is 1.5x on limit loads ^[19]. While automobiles are typically designed for a factor of safety of 3. In aircraft design the worst-case limit load as identified in as per 14 CFR § 25.337 and then multiplied by 1.5 ^[15]. The structure is then tested with the enhanced load and to test for failure. This test is a binary pass or fail. Success results in certification while failure leads to increase development costs. Manufactures tend to design closely to this limit within 5-10% of failure, leading to tighter margins than in other industries.

In the case of this project, a factor of safety of 1.5 was used for the iterative development of the wing. The lower factor of safety is a product of several factors, primarily the need for a lightweight structure to maximize flight capabilities. As factor of safety is increased, the structural weight also increases. A factor of safety this close to one comes with the requirement of high confidence in all calculations and testing as the margin of error is significantly reduced. Furthermore, the potential stakes of an engineering blunder cannot be over-stressed.

To build up the limit loads for the wing, the critical flight lift is defined by multiplying together a Factor of Safety with the maximum maneuvering gees of the aircraft and the maximum flight weight. In the case of civil aviation, gees would range from 2.5 to 3.8 gees

^[15], while in the case of a maneuvering aircraft they could go as high as 6 gees ^[15]. The wing will have to support this load without permanent deformation or compromise to the structural integrity of the wing. Note that this limit load is a hard cap, meaning that it represents the absolute peak loading the wing is expected to support. Failure would be expected at just over this limit.

The structure of the wing will not be balanced for all failure cases ^[7]. As discussed, the wing is designed around compressive failure modes, specifically the panel buckling case ^[3] and the composite failure criteria ^[4]. The wing will assuredly be overdesigned for the tension load case, and also will not be balanced between the buckling and composite failure cases, likely being overdesigned for one of the cases. This is not an issue as in all manufacturing there will be a weak link that serves as the limitation of the capabilities of a product.

g. Computational Structural Sizing in Industry, Government, and Academia

The development of structural sizing tools is not a new practice. In fact, since the late 90's the development of sizing tools, which directly output CAD models, has been common. As computational modeling has increased in capability, so has the potential use cases and power of this type of tool. Further, the integration of composite laminates into these tools is of great interest to the industry due to the proliferation of composites use in practice. One of the earliest of these tools is GENISIS developed by Garret Vanderplaats. This is a FEM based structural optimization tool with the potential to also develop composite structures ^[34]. The paper titled "Discrete Optimization Capabilities in GENISIS Structural Analysis and Optimization Software" discusses composite laminate optimization with the ability to determine ply orientations and count in a composite layup

^[34]. Since the time of writing (2002), the capabilities of GENESIS have progressed significantly with the addition of further functionality and the integration of composite optimization tools. In fact, GENESIS is now capable of optimizing structures for additive manufacturing, and it “can perform topology optimization with additive overhang angle constraints to build the structures with minimum support material.”^[38]

Likely the most prolific of the industry-used structural sizing tools is HyperSizer developed by NASA/Langley^[31]. Beginning as ST-SIZE at the NASA/Langley research center in 1988, Craig Collier further developed the program into HyperSizer, stating “Its purpose was to do a very fast weight-reduction using different design concepts and configurations of vehicles...”^[35]. The program is now in use by industry-leading companies such as Northrop Grumman, Lockheed Martin, and The Boeing Company in the development of aircraft^[35], as well having been used by NASA in the development of the Orion space capsule with hopes of carrying the next humans to the moon in 2024^[37]. HyperSizer succinctly describes their product’s functionality with “HyperSizer is CAE software that couples with FEA to analyze and optimize structures. Use HyperSizer to predict and avoid critical failures with advanced metal and composite strength and stability theories simultaneously, while finding the lightest weight for your design, in the shortest amount of time.”^[36] They further state that HyperSizer removes the need for hand calculation and the use of spreadsheets^[36].

While the tools developed in academia do not share the same refinement as industry and government applications, they do often provide insight into the potential hurdles faced by computational structural design. Often the development of such tools begins in

academia, where the public dissemination of information promotes the iterative and collaborative development of applications.

The foundation of this project traces back to a paper written by Hutchins, Missoum & Takahashi titled, “Fully Parametrized Wing Model for Preliminary Design” which sets the precedent for analyzing a “fully parameterized” FEA wing structure in ANSYS. By using the pressure data collected from VORLAX a “generalized subsonic/supersonic vortex lattice panel method code” ^[39] to analyze the stress, pressure loads, and natural frequencies developed in the wing structure ^[29].

A paper written by Lemonds & Takahashi titled “Prediction of Wing Structural Mass of Transport Category Aircraft Conceptual Design” outlines the practices of direct CAD integration ^[30] is more specific to the structural development of wings. Using a spreadsheet-based enumeration method with empirical functions, the model develops a wing structure made of conventional aerospace materials. The tools specifically aim to accurately predict the weight of the wing structure in transport aircraft, providing conceptual design insights early in the design process. The tool is built on the panel buckling failure mode for metal wing skins with the inclusion of stiffeners and stringers to place ribs in the wing structure.

The practice of sizing a wing structure using the compressive failure modes and subsequently predicting the weight of the wing developed in the Lemonds & Takahashi paper sets the direct foundation for the work conducted here. The key addition is the reduction in aircraft size to unmanned UAVs as well as the shift from conventional aerospace materials to composite laminates. Composite laminates present several specific challenges to structural sizing, specifically in the non-orthotropic behavior and the

importance of ply orientation to the overall structural performance. The prior development of structural sizing for composite structures largely approaches the problem via a strength-based analysis. In contrast, this work builds on compressive failure modes which dominate in light aircraft. This approach should yield more conservative structural sizing as composites excel in tension tests while struggling under compressive loads.

CHAPTER 3

BUILDING THE MODEL

a. Critical Variables

The goal of this design tool is to streamline the design process of a composite wing by providing a tool to develop a credible, lightweight structural concept (a “preliminary design”) from an initial aerodynamic shape, design MTOW and V-N diagram. To accomplish this task, the concept of a “napkin” sketch was used, where a design team would have a high-level understanding of the customer’s needs and requirements which could be translated into a rough set of design constraints. In the conventional design process, the design constraints would then be taken through a rigorous design cycle to arrive at the first prototype design. Subverting this design cycle is the goal of this project in its entirety.

The process of building a model for the construction of a composite wing begins with an approximation of the aerodynamic properties of the airfoil. This begins with defining the aforementioned “napkin” sketch of the aircraft ^[13]. Key dimensions for the fuselage and wing will be decided upon as well as the target design factors ^[12].

When defining fuselage, the length, width, and height are key dimensions. However, the design of the fuselage is of secondary concern in this project and its dimensions play a minor role in the design of the wing. These dimensions serve as the “check” for the overall sizing of the airframe and provide an intuitive start when sketching the aircraft for its mission.

Defining of the wing is critical for the function of this model. The adage “garbage in garbage out” holds truth in this case. Providing the model with a wing geometry that has

grounding in reality is required for the model to function optimally. This is one of the few areas where the operator will need some background in aerospace engineering and the performance of wings to match a comparable wing to the airframe requirements. The critical wing dimensions include the wing reference planform area (S_{ref}), wingspan (b), taper ratio (TR), and sweep. These dimensions are used to create the geometry of the wing.

Finally, the overall design depends on aircraft lift, target Mach number, flight altitude and expected peak gee loading. This limited set of design variables are used to develop the lift distribution across the wing, which is later enumerated into the stresses the wing will face. The required list of variables is the minimum set needed to define the wing and set a lower limit for its performance. Each of these variables can be approximated on the initial runs of the model and later refined as the design of the aircraft comes to fruition.

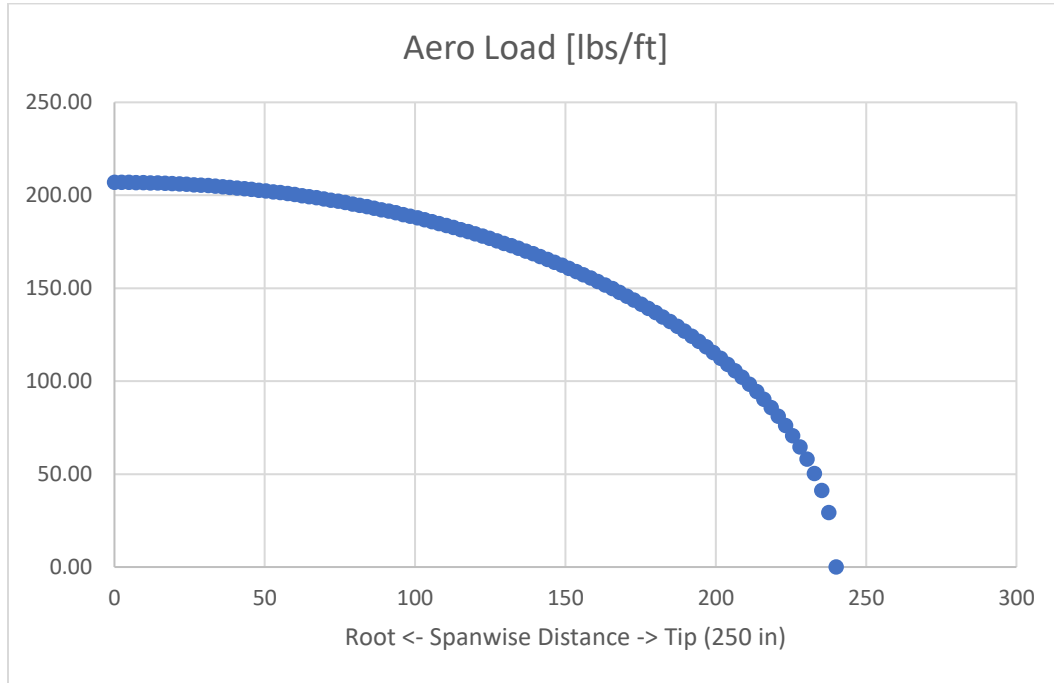
b. Wing Geometry and Load Build Up

After defining the overall aircraft dimensions, the next task is to build up the wing geometry by breaking the wing into a set of spanwise elements with corresponding cords. While simple, this step is crucial to the function of the model as it serves as the foundation for all future enumeration. In this case, the wing has been broken into a hundred spanwise elements which provide a fine enough incrementation for later failure analysis. Each element was assigned a lift load percentage as a function of the spanwise location as a ratio of the total wingspan as seen in equation (1). A ratio of the design lift to the total wing area was then found. These were then translated to an aero load in pounds-force per foot, as a piece of a total lift required in a three-gee maneuver. Here, a 1.5 factor of safety is applied increasing the load per element.

$$\frac{W}{S} [\text{Lbs}/\text{ft}^2] = \frac{\text{Design Lift}}{S_{ref}} \quad (1)$$

$$\text{Load \%} = 1.226 \sqrt{1 - \left(\frac{Y}{\text{Span}}\right)^2} \quad (2)$$

$$\text{AeroLoad} [\text{lbs}/\text{ft}] = \text{Load\%} * \text{Chord}_{avg} * \frac{W}{S} * N_{z \text{ Max}} * \text{Factor of Safety} \quad (3)$$



Figur: Example of Aero Load development over the wing section.

The aero load was then used to find the shear and moment at each spanwise increment. This was done by work from the tip to the root of the wing building up the shear per spanwise element. The moment was then used to find the force couple through the top and bottom panels at each increment. This was done be applying the moment over half the corresponding wing thickness. The cross-sectional area of the wing skin was found by taking the cord of the wing and multiplying it by the skin thickness. This area and the force couple were used to find the stress at each spanwise location. This stress was used in the calculation of the critical buckling load as well as the laminate failures.

c. Enumerating Potential Composites

For a given wing geometry, there are several properties that can be tuned to optimize the structure for weight and strength. Note again that the goal of this model is to quickly optimize the structure of the wing in the form of the placement of ribs around a multitude of composite layup options. In this case, the options a user could use to define the composite layup are core material, core thickness, ply material, number of ply's, ply thickness and ply orientation. Each of these variables can have significant impact on the structural properties of the composite.

Beginning with the choice of a Core material and its thickness, a core can also be omitted if a composite with no filler is required. However, this would not be advised due to the advantages of including a core. The inclusion of a core in a composite layup provides an extremely lightweight “filler” which thickens the layup without adding significant mass. The increase in thickness adds stability in compression by increasing the moment of inertia of the panel. Further, it greatly increases the cross-sectional area of the composite panel, which provides the same benefits. The performance of the core can be further tuned by selecting its material for either compressive strength or weight.

Defining the ply's material, thickness, orientation, and count is a complex process. The number of variables creates a computational issue in that it would not be productive to enumerate all the potential combinations for the composite layup^[5]. The ply thickness and count serve a similar function by linearly increasing the total thickness of the composite layup. Thus, the ply thickness should be defined early in the enumeration process, the user would select the thickness based of their supplier's availability. Ply material could also be selected in this way, depending on whether cost or performance is of greater concern, since

the structural weight will be a direct product of the materials properties. Ply orientation is used to provide structural integrity against inter-ply shear and fatigue failures. For compression and tension load cases, the majority of the plies were aligned in the spanwise direction, while surface plies were aligned in 45-, -45-, and 90-degree orientations for the previously stated reasons. The ply layup was also made symmetrical about the core. Finally, the ply count was used as the primary source of enumeration within a composite material selection, where addition zero-degree plies were added incrementally to increase the composite strength until the stress and buckling tests were passed.

Initially the process of enumeration involved testing twenty different composite layups where the composite layup was maintained over the entire span of the wing. This follows with the design of metallic skinned aircraft where small airframes used a standard skin thickness over the whole wing. Intuitively the maximum stress the wing skin will have to support will be felt at the root. Thus, the skin thickness is designed around this point. Furthermore, metallic skinned wings rely heavily on their spars and stiffeners for structural integrity. In the case of composites, stiffeners are omitted due to the increased thickness of the skin, and the skin is expected to provide the wings structural rigidity. Due to this difference, the constant composite layup approach was providing wings of outrageous weight.

To address the issues involved with the composite material selection, a varied skin thickness approach was employed. In this approach, twenty ply layups were defined each identical in all variables except the ply thickness. Note, ply thickness was used in this case due to the limitation of twenty symmetrical plies around the core, both ply thickness and count scale the composites performance in the same manner. As such, for final production

of the wing an equivalent layup can be defined around thickness or ply count constraints. The twenty potential layups were then cycled through beginning at the wing tip and checking for inner ply failures as well as panel buckling failures. This process will be discussed in further detail in following sections.

d. Composite Laminate Build Up & Skin Thickness

The properties of the composite layup were built using the conventional matrix approach to fiber matrix composites. To do this, the enumerated composite layup was translated into a detailed layup including the ply orientation, thickness, and core properties. Here, each ply was assigned a Z coordinate to describe the distance from the center of the layup to the top of the given ply. For each ply orientation a stiffness matrix (Q) was created. This was first done for the zero-degree plies where the three-by-three stiffness matrix was assembled using the set of equations (4-9) below based off the provided material properties of the composite. The stiffness matrix for the remaining orientations were created by applying the rotational transposition equations (10-15) where theta is angle of orientation for the given ply. These stiffness matrices and the accompanying Z coordinates were then used to generate the Extensional Stiffness (A), Coupling Stiffness (B), and Flexural Stiffness (D) matrices using equations (16, 17, 18).

$$\nu_{21} = \nu_{12} \frac{E_2}{E_1} \quad (4)$$

$$Q_{11} = \frac{E_1}{1 - \nu_{12}\nu_{21}} \quad (5)$$

$$Q_{22} = \frac{E_2}{1 - \nu_{12}\nu_{21}} \quad (6)$$

$$Q_{12} = \frac{\nu_{12}E_2}{1 - \nu_{12}\nu_{21}} \quad (7)$$

$$Q_{16} = Q_{26} = 0 \quad (8)$$

$$Q_{66} = G_{12} \quad (9)$$

$$\bar{Q}_{11} = Q_{11} \cos^4 \theta + Q_{22} \sin^4 \theta + 2(Q_{12} + 2Q_{66}) \sin^2 \theta \cos^2 \theta \quad (10)$$

$$\bar{Q}_{22} = Q_{11} \sin^4 \theta + Q_{22} \cos^4 \theta + 2(Q_{12} + 2Q_{66}) \sin^2 \theta \cos^2 \theta \quad (11)$$

$$\bar{Q}_{12} = (Q_{11} + Q_{22} - 4Q_{66}) \sin^2 \theta \cos^2 \theta + Q_{12} (\cos^4 \theta + \sin^4 \theta) \quad (12)$$

$$\bar{Q}_{66} = (Q_{11} + Q_{22} - 2Q_{12} - 2Q_{66}) \sin^2 \theta \cos^2 \theta + Q_{66} (\sin^4 \theta + \cos^4 \theta) \quad (13)$$

$$\bar{Q}_{16} = (Q_{11} - Q_{12} - 2Q_{66}) \cos^3 \theta \sin \theta - (Q_{22} - Q_{12} - 2Q_{66}) \cos \theta \sin^3 \theta \quad (14)$$

$$\bar{Q}_{26} = (Q_{11} - Q_{12} - 2Q_{66}) \cos \theta \sin^3 \theta - (Q_{22} - Q_{12} - 2Q_{66}) \cos^3 \theta \sin \theta \quad (15)$$

$$A_{ij} = \sum_{p=1}^n (\bar{Q}_{ij})_p (z_p - z_{p-1}) \quad (16)$$

$$B_{ij} = \frac{1}{2} \sum_{p=1}^n (\bar{Q}_{ij})_p (z_p^2 - z_{p-1}^2) \quad (17)$$

$$D_{ij} = \frac{1}{3} \sum_{p=1}^n (\bar{Q}_{ij})_p (z_p^3 - z_{p-1}^3) \quad (18)$$

The Laminate stiffness is the composite of the individual stiffness matrices arranged as per equation (19). The six-by-six matrix provided in conjunction with equation (19) describes the comprehensive reactions of the matrix to all input forces and moments. Having found this matrix, the inner-ply performance of the composite can be described, allowing for failure analysis to occur both at the macro panel buckling level and at the micro composite laminate level.

$$\frac{N}{M} = \begin{bmatrix} A & B \\ B & D \end{bmatrix} \frac{\varepsilon^0}{k} \quad (19)$$

e. Composite Layup Analysis

The analysis of the wing panel in this case is done from two competing frames, including the panel buckling frame, which encompass the performance of the composite as a homogeneous structure, and the composite laminate frame, which observes the interactions between each ply of the composite. The composite as a panel may have the properties to not buckle, while still having individual ply failures that would lead to long term degradation of the panel and potentially catastrophic failure due to poor design.

The analysis of the composite at the individual ply level stems directly from the six-by-six matrix developed in the previous section. By applying a load in equation [00], the composite strain can be determined. The strain of the composite can then be translated into the appropriate strain and stress for each ply orientation in the stack. There are three primary methods for checking for failure within the composite plies, including: Maximum Stress Criterion, Maximum Strain Criterion, and the Tsai-Hill Criterion ^[4, 5, 6]. Note that all the methods work for approximating failure in both tension and compression load cases. All three-failure criterion were employed as checks while cycling through the potential composite layups.

The zero-degree plies became the limiting factor for the composite layup because they are aligned with the applied compressive load. The spanwise alignment causes the zero-degree plies to experience the full strain of the composite leading to individual fiber shearing. Further, Tsai-hill was used as the second limiting factor as it is the most restrictive failure criterion. These in conjunction provided the necessary checks for a composite layup to be used.

Maximum Stress Criterion:

$$\sigma_1 > S_{1T}, \quad \sigma_2 > S_{2T}$$

$$|\tau_{12}| > |S_{12}|, \quad |\sigma_1| > |S_{1C}|, \quad |\sigma_2| > |S_{2C}|$$

Maximum Strain Criterion:

$$\varepsilon_1 > \frac{S_{1T}}{E_1}, \quad \varepsilon_2 > \frac{S_{2T}}{E_2}$$

$$|\gamma_{12}| > \frac{S_{12}}{G_{12}}, \quad |\varepsilon_1| > \frac{|S_{1C}|}{E_1}, \quad |\varepsilon_2| > \frac{|S_{2C}|}{E_2}$$

Tsai-Hill Criterion:

$$\frac{\sigma_1^2}{s_1^2} - \frac{\sigma_1\sigma_2}{s_1^2} + \frac{\sigma_2^2}{s_2^2} + \frac{\tau_{12}^2}{s_{12}^2} > 1(\text{failure})$$

f. Rib Placement

The ultimate step to fully defining the wing structure is solving for the panel length limit, as set by the critical buckling load and placing a rib. The foundation built prior to finally enumerating through the potential composites has been building to solving for the panel buckling as a function of the increasing panel length. Equation (20) was used to determine the critical buckling load ($P_{critical}$) on the panel at each increment [8, 12]. As established in earlier sections, there are 100 increments over the wing. The process begins at the wing tip where the 50% of the cord is assigned to the variable (b). Then a step is made toward the root and this incremental distance is assigned to the variable (a). At each increment, the $P_{critical}$ is checked against the stress in the panel. If the stress is greater than $P_{critical}$ a rib is placed at the previous increment and the process begins again for the new panel.

$$k = 3.6 \text{ to } 4.0$$

a = rib spacing, b = 50% of Chord, c = 100% of Chord

$$P_{critical} = k * E_{Compression} * b * T_{composite} * \left(\frac{T_{composite}}{a}\right)^2 \quad (20)$$

Concurrently to checking the $P_{critical}$ against the internal stress of the panel, the composite ply failures are also being checked. To expand on the process used to simultaneously place ribs and select the composite layup, recall the process of enumeration used for the composite. 20 potential composite layups are input by the user of linearly increasing layer thickness. For the initial run, the “thinnest” layer thickness is used. If at any point before placing a rib, any of failure criterion output a value greater than 1 the composite layup selected fails and it is thrown out and the next composite layup with a thicker skin thickness is used to rerun the rib placement. The selection process can be seen in Fig. (16) below, which shows how the model creates develops and checks the critical buckling load against the panel force couple. Further note the presence of the addition checks for composite failure, or premature buckling in the panel.

```

k = 3.6 '3.6 to 4.0
Pcr = k * E_Comp * b * T_thick * (T_thick / a) ^ 2 'b 50% of cord, a is rib distance
Force = Abs(Sheet5.Cells(J_2%, 15))
rib_height = Sheet5.Cells(J_2%, 2)

s = J_1% - J_2% - 1

If (Pcr < Force) And (Sigma_1_0 < 1) Then
  If s <= 2 Then
    Debug.Print "Premature Buckling problem - change material type"
    s = 0: i% = i% + 1: If i% > 20 Then GoTo 2000 Else GoTo 1000
  End If

  Debug.Print "Buckling Failure without Compression Failure":
  Debug.Print "***** PLACE RIB *****":
  Exit For

ElseIf (Sigma_1_0 > 1) Then

  Debug.Print "Premature Compression Failure without Buckling - change material type"
  i% = i% + 1 'increment material type
  s = 0
  If i% > 20 Then GoTo 2000
  GoTo 1000

End If

```

Figure 15: FBA code used to select for Panel Buckling Failure or Composite Compression Failures

$$Mass_{Front\ Spar} = T_{skin} * \rho_{skin} * a * rib\ height + T_{core} * \rho_{core} * a * rib\ height \quad (21)$$

$$Mass_{Back\ Spar} = Mass_{Front\ Spar} / 2 \quad (22)$$

$$Mass_{Rib} = ((c * ribheight * T_{skin} * \rho_{skin}) + (c * ribheight * T_{core} * \rho_{core})) * 0.6 \quad (23)$$

$$Mass_{panel} = ((a * c * T_{skin} * \rho_{skin}) + (a * c * ribheight * T_{core} * \rho_{core})) * 2 \quad (24)$$

The iterative process repeats over the entire wingspan, placing ribs and increasing the layup thickness as the panels approach the root. While the structure of the wing is built, the mass of the wing structure is also being calculated by taking the summation of the spars, ribs, and skin masses as seen in equations (21-24). The mass of the wing is a critical metric which can be used in the comparison of different structures developed. It provides an early warning to the model efficacy and the potential draw backs of a created wing structure.

CHAPTER 4
MODEL VALIDATION

a. CAD Modeling

To confirm the efficacy of the model and the structure it produces, the output needs to be confirmed. The confirmation process begins with modeling the structure in a CAD modeling program. In this case, two modeling programs were used firstly in SOLIDWORKS and secondly in ANSYS. SOLIDWORKS was used for its simplicity and speed. However, it was only used for preliminary checks of the developed wing structures and not for in depth analysis of their performance or feasibility. ANSYS primarily for the generous element and node limitations of the student version and importantly the built-in solver ANSYS Composite PrepPost (ACP). ACP allows the user to describe the exact layup and material properties of a composite material and assign them to sections of a model, creating the opportunity for high quality composite laminate analysis.

Model Output Structural Layout

Total Mass [lbm] of wing	291.89										
Ply Count	7.000	7.000	7.000	7.000	7.000	7.000	7.000	7.000	7.000	7.000	7.000
Effective Ply Count	7.000	7.700	8.400	9.100	9.800	10.500	11.200	11.900	12.600	13.300	14.000
Total Layup Thickness	0.203	0.217	0.231	0.245	0.259	0.273	0.287	0.301	0.315	0.329	0.343
Ply Thickness	0.010	0.011	0.012	0.013	0.014	0.015	0.016	0.017	0.018	0.019	0.020
Composite Material	3.000	3.000	3.000	3.000	3.000	3.000	3.000	3.000	3.000	3.000	3.000
Core Thickness	0.063	0.063	0.063	0.063	0.063	0.063	0.063	0.063	0.063	0.063	0.063
1	194										
2	168										
3	144										
4	124.8										
5		105.6									
6			81.6								
7						55.2					
8								24			
9											0

Figure 16: Sample Model Output for a Wing Structure

Table 1: Wing Structural Layup Output from Model

Rib #	Distance to Root [in]	Chord [in]	Rib Heigh [in]	Panel Thickness [in]	Shear at Rib [lbf]
1	0 "Root"	27.90	2.79	0.343	413.18
2	24.0	27.90	2.79	0.301	530.59
3	55.2	26.68	2.62	0.273	436.69
4	81.6	24.96	2.48	0.245	381.66
5	105.6	23.94	2.34	0.217	291.21
6	124.8	22.81	2.22	0.200	275.21
7	144	21.68	2.10	0.200	315.82
8	168	19.50	1.94	0.200	300.26
9	194.4	18.33	1.79	0.200	324.68
10	240 "Tip"	15.00	1.50	0.200	0

The structural geometry was built using the output of the enumerated model. After inputting the structural requirements and enumerating the composites, the model produces a log of the rib placements as well as the failure modes that caused any particular composite to be replaced along the span. Observe fig. (17) for the output of the model after fully running through a wing development cycle. Note that only 11 potential composites were assessed before completely defining the wing. Each rib is placed at a corresponding distance from the root and is accompanied by the composite, which makes up the structure of that panel section.

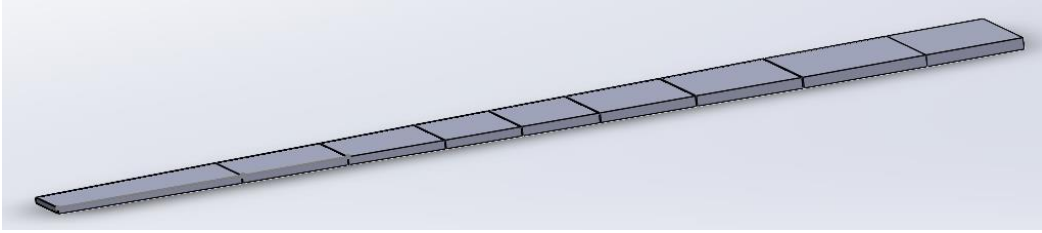


Figure 17: CAD wing model

The geometry of the wing as simplified to stress boxes can be seen in the table (1), where each section between two ribs is drawn as a trapezoidal prism. Should the wing structure pass validation as a prism, the airfoil could be introduced for final structural refinement. However, it is unnecessary for the preliminary check conducted here, or to validate the efficacy of this model. The table (1) created from the output of fig. (17) is used to produce the CAD model seen in fig. (18).

b. ANSYS ACP (Pre/Post)

A major challenge in defining the material used for the panels within the modeling software came with the nature of composite layups. To overcome this, different approaches were used in the respective softwares. ANSYS allows the user to input a composite layup with a core, defining the exact properties of each ply in the laminate. This allowed for the efficient application of the laminate properties over the wing model. SOLIDWORKS required a more creative approach, where the laminate properties were calculated using the laminate stiffness matrix. As SOLIDWORKS was used for cursory evaluation of the wing structure, the approximations made are of minimal consequence.

The ACP module of ANSYS allows the user to fully define the composite laminate used to construct the structure. To do this, the user must first define the raw materials to be used. Then the user works through defining the fabrics used by their thickness and material.

The process progresses through defining stackups, sub laminates. These can then be assigned to individual sections of the model in the case of a variable composite buildup over the span.

The ACP further adds the functionality for reviewing the reactions within the individual plies of the laminate. This functionality will be crucial in confirming the developed structure and whether it passes each of the composite failure criteria.

c. Finite Element Analysis

Having created solid models of the wing geometry in both SOLIDWORKS and ANSYS, the next process would be to define the loads and boundary conditions on those models. Boundary conditions serve to fix a model in space. They provided the “grounding” for the model and describe its interactions with nearby parts. In SOLIDWORKS the boundary conditions consisted of simply bounding the roots panels face as a fixed surface. This was done to approximate the wing having a rigid connection to the aircraft fuselage, the remainder of the wing was left free of boundary conditions, as it would freely deflect under applied flight loads. This boundary condition can be seen in fig. (19) as double green arrows.

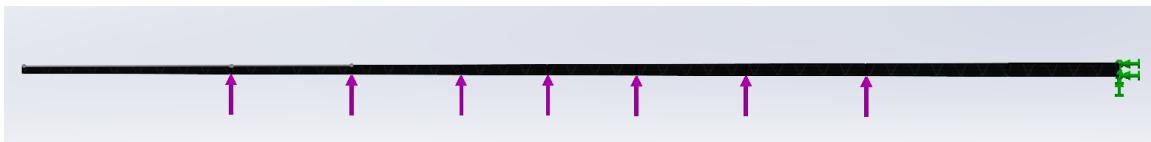


Figure 18: SOLIDWORKS wing model with Shear Concentration

For the ANSYS model, a more complex approach was used that would more accurately simulate the fixity conditions between the wing and the aircraft fuselage. Four conditions were set; firstly, the right and top edges of the root panel were assigned

constrained deflections in the Y and Z coordinates, which are the chordwise and thickness directions, respectively. The whole face was given a frictionless support and finally the trailing edge vertex was assigned as a fixed support. The support assignments and locations can be seen in fig. (20). This support strategy was used to sufficiently bound the wing structure while also minimizing the presence of stress singularities at the root of the wing. By allowing the edges of the panel to expand and contract with the deformation of the wing, the stress concentrations created by the angular geometry were reduced.



Figure 19: ANSYS Boundary Conditions

After bounding the root of the wing, the next step to analyzing the deflection of the wing is to apply loads. As a preliminary check in SOLIDWORKS, loads were applied to the wing as shear concentrations at each rib. For the ANSYS model, the loads were built up by applying a pressure distribution across each wing panel. The pressure and shear used were calculated directly in the model as a product of the flight loads. While a non-uniform pressure distribution over each panel could have yielded more accurate results, it was deemed unnecessary for the required validation. The pressure distribution is fairly constant over the span, changing dramatically at the wing tip, which is an area of minimal concern as stress concentrations will occur at the root.

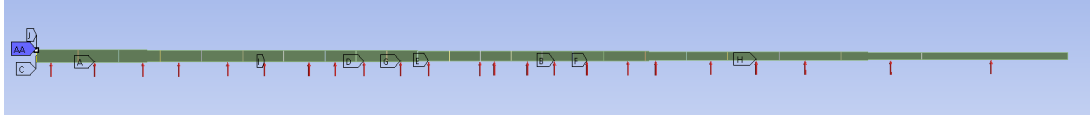


Figure 20: ANSYS Pressure Distribution

The goal of doing Finite Element Analysis is to both validate the final structure produced for structural integrity, but also to progressively refine the modeler to produce an optimized structure. For example, in the Eigenvalue Buckling, if the first buckling mode occurs at a 1.9 force multiplier, this would indicate that the modeler is overly pessimistic of the structures requirements and develops an overly strong wing. With that information, the modeler can be derated to build a more physically accurate wing. This also works with a force multiplier less than one, where the modeler would have to be scaled up to build a sufficiently strong wing. The application of fudge factors is common in empirical equations where the stacking approximations lead to precise inaccuracy. The fudge factor works to zero the model onto the appropriate target wing strength. In this case, it is a buckling force multiplier of 1, as the Factor of Safety is built into the wing developed.

Finite Element Analysis is critical to validate the structure but also to check the wing for its global reactions to the applied loads. The approach used to develop the wing works incrementally inward from the wing tip panel by panel ensuring each panel supports the in-plane force couple for both buckling and composite laminate failure. Modeling the structure in FEM not only confirms the structure will support the applied load, it also confirms that the 2D approach to developing the wing can function in a 3D application.

CHAPTER 5

RESULTS

The design tool was developed with the ability to handle a wide range of aircraft shapes and sizes. This was achieved by taking advantage of robust design principles and using failure criteria that are independent of size class or panel thickness. A potential advantage of the composite material is its “flexibility” in its application due to the nearly infinite variations capable in layup pattern and composite mixing. Thus, the tool had to be designed with this flexibility in mind. Working for the end user rather than against them, the tool provides the end user with the ability to tune the composite layup to their needs and the respective use case of the wing. To exemplify this attribute of the model, two different airframe classes were tested: 1) a small frame lightweight aircraft with low speed and altitude requirements which would represent an Unmanned Aerial Vehicle (UAV), and 2) a short, winged aircraft with exceptionally low aspect ratio representing a maneuvering jet. These two would encompass the bounds of the model’s application, due to the limitations on the model complexity making it unrealistic for the analysis of larger aircraft. This is due to “large” aircraft having increasingly complex wing structures that cannot be represented accurately by the simplifications made in this model. After developing the structure for both aircraft using the built tool, they were modeled in CAD and finally validated in FEA.

a. UAV Analysis

The first airframe to be run through the simulated design cycle is a small lightweight aircraft. The design inputs were developed to represent a UAV. This design case would test the lower limits of the model and its ability to develop a lightweight and structurally sound wing. Having a high aspect ratio, the panels of the wing would have to support greater buckling loads while having functionally less area to support the in-plane stresses.

These factors make this airframe an ideal candidate as a test subject for the validity of this model. As a general rule for all airframes, the wing should make up no more than a third of the structural weight of the aircraft. In this case it would be a third of the design lift. However, this was not used as a design ceiling but more as a consideration when observing the structure developed by the model.

1. Design Inputs

The first step to wing development through the use of this model is to define the aircrafts geometry and design requirements. The design variables listed in table (2) are the key inputs required to define the aircraft and its flight characteristics. These variables can intuitively be developed by a IPT with minimal experience and knowledge of the end users' requirements. Making them a robust set, easily developed by the model's user. Particularly important design requirements include the design lift, Mach and upper G limit for the aircraft. These are especially critical as they define the wings critical loading and set the flight capabilities of the aircraft.

For the UAV these design inputs were created to fit the generalized design requirements for such an aircraft. The airspeed is set to 150 knots with an altitude ceiling of 10,000 feet and lift of 1500 lbf. This aircraft is exceptionally small with a high efficiency wing for sustained low speed flight. Thus, the maximum gee requirement of the wing is 3 gee's, which encompasses even the most strenuous of climbing and landing cases, and emergency flight maneuvers^[15, 17]. The Fuselage is approximated as a twenty-foot cylinder with a two-foot diameter. A forty-foot wingspan with no sweep approximates the high aspect wing typical in aircraft with this mission type. The full set of wing dimensions and requirements can be seen in table (2).

Table 2: UAV user design inputs

Fuselage Length	20	ft
Fuselage Width	48	in
Fuselage Height	48	in
Wing Area, Sref	75	sq. ft
Wingspan, b	40	ft
Wing TR	0.5	
Wing LE-Sweep	0	deg
Wing LE-FS	100	in
Aspect Ratio	21.33	
Aircraft Lift	1500	Lbf at 1 gee
Design Mach #	0.227	
Design Alt	10000	ft
Design KTAS	150.0016	knots
Design G	3	G
Design Lift	6750	Lbf at 3 gees

As an aside, the wing and fuselage geometry has been drawn as a 2D sketch for the readers convenience. Note that the fuselage dimensions serve as a place holder in this model and are not considered in calculations. They are included to press the user to consider the aircraft design wholistically and provide the opportunity of later integration of this model with a model that creates the fuselage structure.

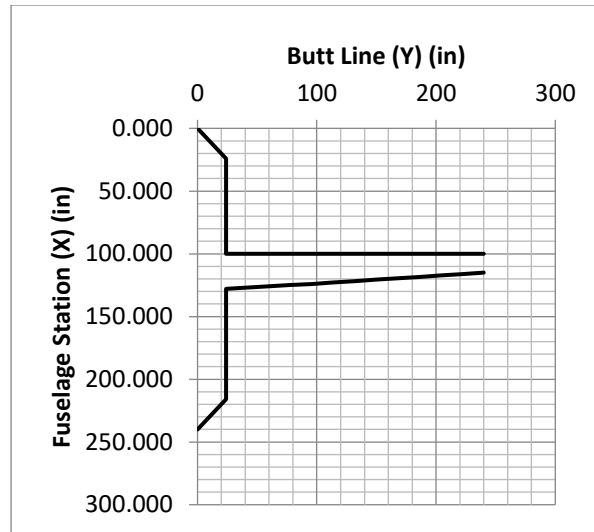


Figure 21: UAV Fuselage and Wing visualization

2. Composite Enumeration

After defining the wings geometry and performance requirements, the next set of variables the user must define is for the composite layup. Included in the model are the material properties of several commercially available composite laminates and foam cores as can be seen in table (3). The selection of composite will typically be driven by outside factors, such as performance in various temperatures, supplier availability, cost and user manufacturing capability. Thus, various composites were included primarily for user convenience and to increase the flexibility of the model.

Table 3: Potential Composite Laminates

Composite Laminate Material Properties												
Mat.	Name	E1 x [psi]	E2 y [psi]	v12	v21	G12 [psi]	S_1T	S_1C	S12	S_2T	S_2C	Density [lbm/in ³]
1	Test	20000000	1200000	0.3	0.018	1000000	1000	600	70	50	120	
2	Boron-E B(4)/5505	29587752	1775265.1	0.3	0.018	700000	182748	362595	9717.55	8847.32	29297.7	0.0722546
3	Carbon-E T300/N5208	26251878	1493891.4	0.28	0.01593	700000	217557	217557	9862.58	5801.52	35679.3	0.05780368
4	Carbon-E AS/H3501	20015244	1200914.6	0.3	0.018	700000	209870	209870	13488.5	7541.98	29877.8	0.05780368
5	Carbon-E IM6/epoxy	29442714	1766562.8	0.32	0.0192	700000	0	0	0	0	0	0.05780368
6	AS4/APC2	19435092	1166105.5	0.3	0.018	700000	0	0	0	0	0	0.05780368
7	Kevlar 49/Epoxy	11022888	661373.28	0.3	0.018	700000	203053	34083.9	4931.29	1740.46	7687.01	0.05274586
8	Glass-epoxy	5598467	335908.01	0.3	0.018	700000	0	0	0	0	0	0.06502914
Form Core Material Properties												
11	PVC Foam Core	217557	13053.42	0.3	0.018	0	0	0	0	0	0	0.00162
12	FR-3703 Polyurethane	1250	1250	0.3	0.3	2000	75	45	40	75	45	0.00173611
13	FR-3740 Polyurethane	72200	72200	0.3	0.3	61000	2750	4500	2000	2750	4500	0.02314816
14	FR-6710 Polyurethane	10000	10000	0.3	0.3	10900	280	560	225	280	560	0.00578704
15	FR-6725 Polyurethane	51300	51300	0.3	0.3	35600	1100	3100	1000	1100	3100	0.0144676

The composite layup is defined using an upper and lower threshold. The user defines an upper and lower bound for the ply thickness to be used. Understand that this is a theoretical bounding for the function of the model. In order for the model to succeed, the entire structure must be built within the user provided range of allowable composites. In a case where the application does not complete building the structure before exhausting the twenty potential composites, an error will be thrown requesting the user redefine their composite enumeration. The material selection will be made on a case-by-case basis informed by the availability to the manufacturer or other reason previously stated in the case of the UAV materials selected for the laminate is a Carbon Fiber/Epoxy more specifically T300/N5208 or composite material 3. The core is a high-density polyurethane foam certified for flight applications or Foam core material 13. Next the composites layup was defined with a ply thickness ranging from 0.01 inches to 0.03 inches as shown in table (4). In practice, this composite thickness can be achieved by either using progressively thicker laminate sheets or by using more laminate sheets of the minimum thickness as seen in the “effective ply count” row of table (4) which has been rounded to the nearest whole

ply. For enumeration, the layup for all twenty composites has been set to seven plies. This can be adjusted if the user needs to vary ply counts. Finally, the user must select what ply orientations they are going to include by either placing a one or zero in the appropriate slot. In this case, all ply orientations have been used for the entire set of composite layup options.

Table 4: Composites Layups Enumerated in a Set of Twenty

	Composite Layup Enumeration																			
Composite Layup	1	2	3	4	5	6	7	8	9	10	11	12	13	14	15	16	17	18	19	20
Core Material											12									
Material											3									
Ply Thickness	0.01	0.01	0.01	0.01	0.01	0.02	0.02	0.02	0.02	0.02	0.02	0.02	0.02	0.02	0.02	0.03	0.03	0.03	0.03	0.03
Number of Plies (S)											7									
0 Degree											1									
90 Degree											1									
45 Degree											1									
-.45 Degree											1									
Effective Ply Count	7	8	9	10	10	11	12	12	13	14	14	15	16	17	17	18	19	19	20	21

Having specified the ply thicknesses and orientations as well as the materials to be used, the user must then explicitly write out the layup for the composite. In this example, the process is simple as the layup remains fixed throughout the twenty composite options with a [90,45,0,0,0,0, -45] symmetrical layup pattern as seen in table (4). This layup pattern was used to decrease the likelihood of delamination between plies [6]. In the center of the composite a 1/16th inch core has been placed to increase buckling resistance. Core thickness can also be varied throughout the twenty options, however for a small aircraft has been designed here a constant core thickness is more likely due to manufacturing complexity. As previously mentioned, the number of laminates in the layup and their respective orientation can be altered on a case-by-case basis. This can be used to “tune” the structure throughout the span of the wing for particular structural concerns or potentially the inclusion of a payload such as landing gear in the wing. Note if a payload is added to the

structure, the wing loading would have to be adjusted at the point of the bearing load addition.

Table 5: Composite Layups for the Twenty Enumerated Options

Composite Layup	
Ply	
10	1 1
9	1 1
8	1 1
7	90 90
6	45 45
5	0 0
4	0 0
3	0 0
2	0 0
1	-45 -45
0.0625 Inch Core Thickness	
Chick	
1	-45 -45
2	0 0
3	0 0
4	0 0
5	0 0
6	45 45
7	90 90
8	1 1
9	1 1
10	1 1

3. Model Outputs

After developing the design inputs for the model, the application will be ready to be run for the first time. A successful run of the model will yield table (6) and table (7) these tables describe the failure criteria for the composite panels as well as the rib placement within the wing respectively. Table (6) is critical as it shows where the composite failure occurred resulting in that layup being replaced by the subsequent panel. This information is valuable for two primary reasons. Firstly, it provides insight into the likely areas of fatigue failure in the panel as well as which laminate in the stack will fail if pushed beyond the safe loading. Secondly, if the application were to error without fully developing the structure there would not be insight into where the composite layup needs to be strengthened. Note the values saved are for when the composite fails and is replaced, these

values are not indicative of the failure criterion results of the actual structural panels. Only the last column of values is representative of the failure criterion of the panel. In this case, for the panel closest to the root which coincidentally will be supporting the highest compressive loads of any panel in the wing.

Table 6: Model Output Failure Criteria for UAV Wing

	1	2	3	4	5	6	7	8	9	10	11
Tsai Hill Failure Criteria 0	1.056345	1.019422	1.042176	1.052957	1.014014	1.0531	1.035317	1.052957	1.046639	1.041887	0.865004
Tsai Hill Failure Criteria 90	1.051279	1.014532	1.037178	1.047907	1.009151	1.048049	1.030351	1.047906	1.041619	1.036889	0.860855
Tsai Hill Failure Criteria 45	1.115278	1.076295	1.100319	1.111701	1.070585	1.111852	1.093076	1.1117	1.10503	1.100013	0.913262
Tsai Hill Failure Criteria -45	1.115278	1.076295	1.100319	1.111701	1.070585	1.111852	1.093076	1.1117	1.10503	1.100013	0.913262
0 Degree											
Sigma 1 > S1C	1.024	1.006	1.017	1.023	1.004	1.023	1.014	1.023	1.02	1.017	0.927
Sigma 2 > S2T	0.072137	0.070866	0.071652	0.072022	0.070678	0.072027	0.071417	0.072023	0.071806	0.071643	0.065279
Tau 12 > S12	0	0	0	0	0	0	0	0	0	0	0
$\epsilon_1 / (S1/E1)$ [Compression]	1.024829	1.006759	1.017933	1.023184	1.004085	1.023254	1.014577	1.023184	1.02011	1.017791	0.927379
$\epsilon_2 / (S2/E2)$ [Tension]	0.684165	0.672102	0.679562	0.683068	0.670317	0.683114	0.677322	0.683068	0.681016	0.679468	0.619111
ν_{12}	0	0	0	0	0	0	0	0	0	0	0
90 Degree Plies											
Sigma 1 > S1T	1.02429	1.00623	1.017398	1.022646	1.003557	1.022716	1.014044	1.022646	1.019574	1.017256	0.926892
Sigma 2 > S2C	0.01173	0.011523	0.011651	0.011711	0.011492	0.011712	0.011612	0.011711	0.011676	0.011649	0.010614
Tau 12 > S12	0	0	0	0	0	0	0	0	0	0	0
$\epsilon_1 / (S1/E1)$ [Tension]	-1.02483	-1.00676	-1.01793	-1.02318	-1.00408	-1.02325	-1.01458	-1.02318	-1.02011	-1.01779	-0.92738
$\epsilon_2 / (S2/E2)$ [Compression]	0.111246	0.109285	0.110498	0.111068	0.108995	0.111075	0.110134	0.111068	0.110734	0.110483	0.100668
ν_{12}	0	0	0	0	0	0	0	0	0	0	0
45 Degree Plies											
Sigma 1 > S1C	0.275935	0.271069	0.274078	0.275492	0.270349	0.27551	0.273174	0.275492	0.274664	0.274039	0.249696
Sigma 2 > S2C	0.665569	0.653833	0.66109	0.664501	0.652097	0.664546	0.658911	0.6645	0.662504	0.660998	0.602281
Tau 12 > S12	0.791375	0.777422	0.78605	0.790105	0.775357	0.790159	0.783459	0.790105	0.787732	0.785941	0.716125
$\epsilon_1 / (S1/E1)$ [Compression]	0.352112	0.345903	0.349742	0.351546	0.344984	0.35157	0.348589	0.351546	0.35049	0.349693	0.31863
$\epsilon_2 / (S2/E2)$ [Compression]	0.122179	0.120024	0.121356	0.121983	0.119706	0.121991	0.120956	0.121982	0.121616	0.12134	0.110561
ν_{12}	0.395688	0.388711	0.393025	0.395053	0.387679	0.39508	0.39173	0.395053	0.393866	0.392971	0.358062
-45 Degree Plies											
Sigma 1 > S1C	0.275935	0.271069	0.274078	0.275492	0.270349	0.27551	0.273174	0.275492	0.274664	0.274039	0.249696
Sigma 2 > S2C	0.665569	0.653833	0.66109	0.664501	0.652097	0.664546	0.658911	0.6645	0.662504	0.660998	0.602281
Tau 12 > S12	0.791375	0.777422	0.78605	0.790105	0.775357	0.790159	0.783459	0.790105	0.787732	0.785941	0.716125
$\epsilon_1 / (S1/E1)$ [Compression]	0.352112	0.345903	0.349742	0.351546	0.344984	0.35157	0.348589	0.351546	0.35049	0.349693	0.31863
$\epsilon_2 / (S2/E2)$ [Compression]	0.122179	0.120024	0.121356	0.121983	0.119706	0.121991	0.120956	0.121982	0.121616	0.12134	0.110561
ν_{12}	0.395688	0.388711	0.393025	0.395053	0.387679	0.39508	0.39173	0.395053	0.393866	0.392971	0.358062

The zero-degree plies continued to be the limiting factor in compression. For the last panel, the 0-degree plies passed the maximum stress criterion with a 0.927 and the Tsai Hill failure criterion with a 0.865. Comparatively, the 90-degree plies passed with a 0.277 and 0.177 respectively. In fact, the 90-degree plies never failed passing all failure criterion. This is likely due to the 90-degree plies having no fibers being compressed only the matrix which is comparatively pliable. The 45-degree and -45-degree plies also failed under the Tsai Hill criterion. While passing all other failure criteria, this is likely due to the nature of Tsai-Hill which looks at the interconnected failure of both characteristic directions.

Table 7: Model Output Structural Description for UAV Wing

Total Mass [lbm] of wing	328.2015126										
Ply Count	7	7	7	7	7	7	7	7	7	7	7
Effective Ply Count	7	7.7	8.4	9.1	9.8	10.5	11.2	11.9	12.6	13.3	14
Total Layup Thickness	0.2025	0.2165	0.2305	0.2445	0.2585	0.2725	0.2865	0.3005	0.3145	0.3285	0.3425
Ply Thickness	0.01	0.011	0.012	0.013	0.014	0.015	0.016	0.017	0.018	0.019	0.02
Composite Material	3	3	3	3	3	3	3	3	3	3	3
Core Thickness	0.0625	0.0625	0.0625	0.0625	0.0625	0.0625	0.0625	0.0625	0.0625	0.0625	0.0625
1	206										
2	187.2										
3	172.8										
4	160.8										
5	151.2										
6	141.6										
7	132										
8	124.8										
9	117.6										
10		110.4									
11		103.2									
12			96								
13			88.8								
14				81.6							
15				74.4							
16					67.2						
17						57.6					
18						48					
19							38.4				
20								28.8			
21									19.2		
22										9.6	
23											0

The structure produced by the application had a weight of 328.21 pounds. This is far below the 500 pounds allowed by the general 1/3rd wing lift rule for aircraft. Eight ribs were placed to make up the wing structure using six different composite layups. The key properties of these layups are recorded in rows 2 through 7 of table (7). Note the first four ribs use the same composite layup which finally fails between the fourth and fifth rib, at which point the application attempts to use the next composite doing so successfully. Between the fifth and sixth ribs, two composite steps are made. This happens again between the sixths and seventh as well as the seventh and eighth. Finally, a triple step is made for the last panel. The steps or skips over composite options are cases where the composite laminate is failing within the stack before a long enough characteristic length is found, which causes an instance of panel buckling. Further note that the application concluded before using the entire set of twenty potential composites. This is intentional as the range of enumerated composites provides a low end as prescribed by the minimum thickness of laminate available from the material provider and an upper end of thickness chosen to provide a wide range of potential layups with seven to twenty-one equivalent

plies. The application being able to conclude before using all twenty potential composites yields the lightweight structure seen in table (7).

4. FEA Validation

The structure developed by the model is the product of the conglomeration of many different principles of mechanical design, having been built from the foundation of flat panel stress analysis with the addition of element-by-element composite failure theory. To verify, the wing developed by the model Finite Element Analysis was used. The goal is to check for failure in the individual plies of the composite and to determine global buckling behavior. Additionally, the shell modeling process will confirm the whether the design limits used represent the behavior of an actual wing. Because the model was based off compression load failures, if the model fails in tension this approach would be deemed inappropriate for the design of a wing.

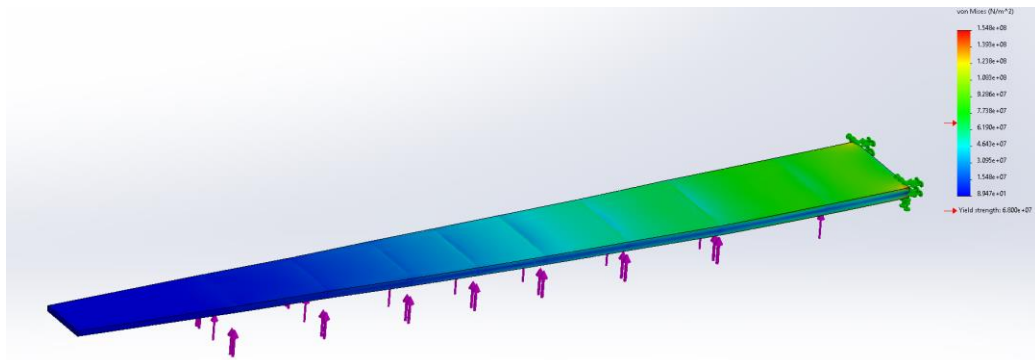


Figure 22: SOLIDWORKS Static Stress Analysis with Point Shear Loading

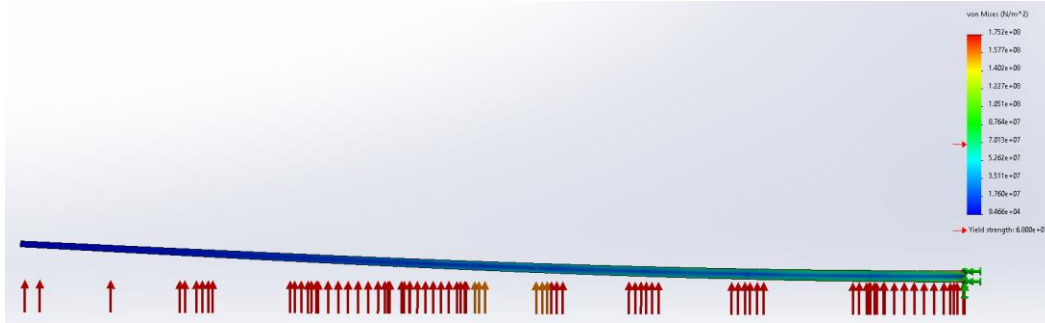


Figure 23: SOLIDWORKS wing model static loading failures analysis with distributed pressure

As previously mentioned, SOLIDWORKS was used for initial checks of the wing structure due to the speed with which the model could be drawn and taken through analysis. However, the data from this simulation was not relied upon or used beyond the preliminary testing process of the modelers ability to develop a reasonable wing structure. Fig (23-24) show the model under two different loading conditions. For the ANSYS model, only the second loading condition was used where each panel of the wings lower surface had an individual applied pressure. The point shear loading approach was used as a cursory investigation into the applicability of this analysis approach.

All further modeling was conducted in ANSYS. These figures show the critical flight load with a 1.5 Factor of Safety and the maximum maneuvering limit of three gees. The first figure of interest from ANSYS is the total deformation of the wing as seen in fig. (25). The wing deforms a total of 9.63 inches at the tip, having a fairly uniform flexure over the entire span. As an initial check, the distribution of deformation bodes well for the developed wing as no particular piece of the structure is bending on its own. The entire structure is flexing much like a beam. Further analysis of the wing is broken into three areas of interest. The Stress developed in the wing, the composite safety factor and the buckling load multipliers for the wing. The reactions were further investigated by

observing the behaviors in just the root panel which was identified was supporting the highest loads.

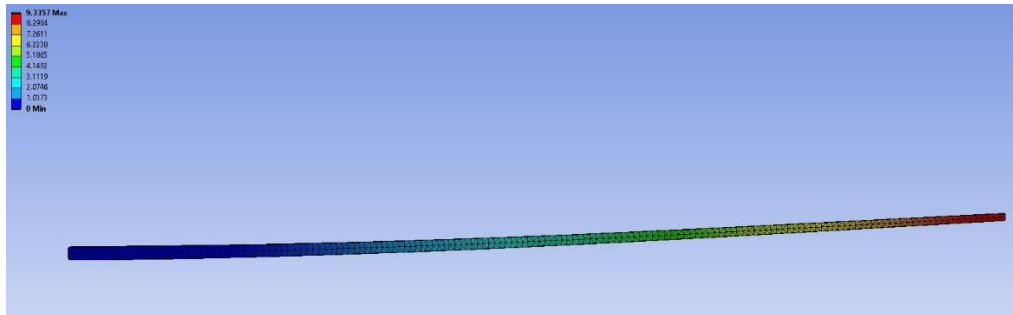


Figure 24: UAV wing Total Deformation [in]

Table 8: Carbon-Epoxy Failure Strength

S_1T [Psi]	S_1C [Psi]	S_12 [Psi]	S_2T [Psi]	S_2C [Psi]
217557	217557	9862.58	5801.52	35679.35

The first of the stresses to be observed would be the Equivalent Stress in the wing, or the Von-Mises Stress. As mentioned, the chosen composite for this wing is Carbon-Epoxy T300/N5208 which has failure strengths listed in table (8). These strengths are aligned along the spanwise direction meaning that for plies like 90 deg the 1 and 2 coordinate directions would be swapped. These failure strengths can be compared with the stresses observed in the individual ply figures. These do not apply to the full wing figures which have the stress distributed over the entire composite stack. The full wing model is immensely powerful for observing the distribution of stress over the entire platform. Equivalent (Von-Mises) Stress provides a useful “global” reaction of the wing and each ply to the applied load. However, its use is limited in the analysis of the composite stack's ability to support the applied load. As Von-Mises stress has limited application in the analysis of non-isotropic material lamina. This is where the normal stress in the laminate can be used to more accurately assess the lamina failures.

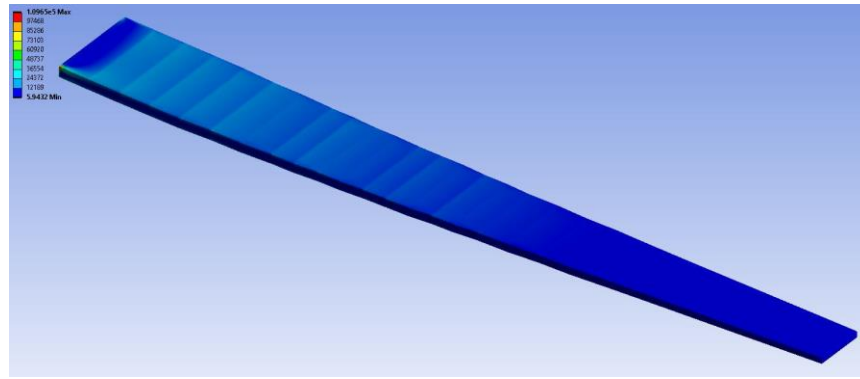


Figure 25: UAV wing Equivalent Stress [psi]

The equivalent stress shows the expected stacking of stress between the ribs. This behavior instills significant confidence in the approach used to develop the wing. Since panel buckling was iterated by increasing panel length and then “resetting” the stress and characteristic length by placing a rib. Each panel shows uniform stress increased between ribs except for the final root panel. Where there is a stress singularity at each corner of the root panel. This is likely due to the supports applied to the root face of the wing and the hard angles in the geometry which notoriously create stress singularity. To overcome this the maximum stress in the panel was taken slightly away from the singularity when they occur. In some cases, the second panel was analyzed to see the reactions in a panel with a uniform stress distribution.

The layup of the composite is [90, 45, 0, 0, 0, 0, -45]_s about a foam core panel. This composite layup was selected for its resistance to delamination and ply wrinkling. The stack zero-degree plies provide the primary structures stiffness in the spanwise direction. ANSYS ACP allows the user to see the reaction stresses within each ply of the composite on a panel-by-panel basis. The following figures show the root panels reaction for each composite ply, where “Top” indicates the ply is above the core and “Bot” indicates the ply is below the core in the stack-up.

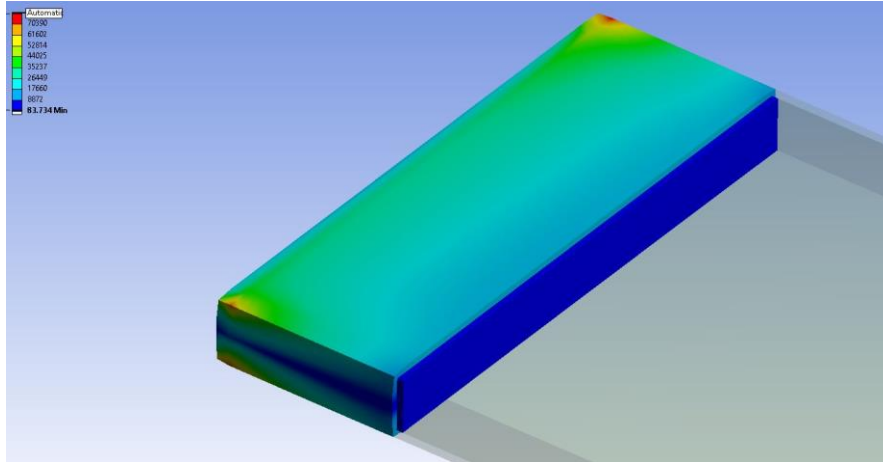


Figure 26: UAV Panel 1 Equivalent Stress Top 90 Deg. Ply [psi]

Starting with the first ply in the stack-up that being the Top 90-degree ply as seen in fig. (27). The equivalent stress is useful for seeing the overall heat map of the stress in the ply. Note the stress singularity in the corners near the root edges of the top and bottom panels of the wing. The 90-degree ply will have its fibers aligned in the chord wise direction. Note that for a unidirectional composite all the fibers in the laminate would align in a single direction. For woven composites, depending on the weave used the ratio of fibers aligned in the X or Y directions varies. In this case the ply is being compressed perpendicular to the aligned direction. While the equivalent stress figures can be helpful in seeing where areas of caution in the laminate are in the case of this project the material has been sized via buckling strength instead of strength-based sizing. In this case the composite excels with a maximum strength of 217,557 Psi. In the above figure the equivalent stress peaks at 70,400 Psi within the singularity. Clearly the composite is exceling when faced with a strength-based metric. The Normal Stress figures will be more illuminating regarding the composite's true laminates strength under the compressive loading seen by the top of the wing.

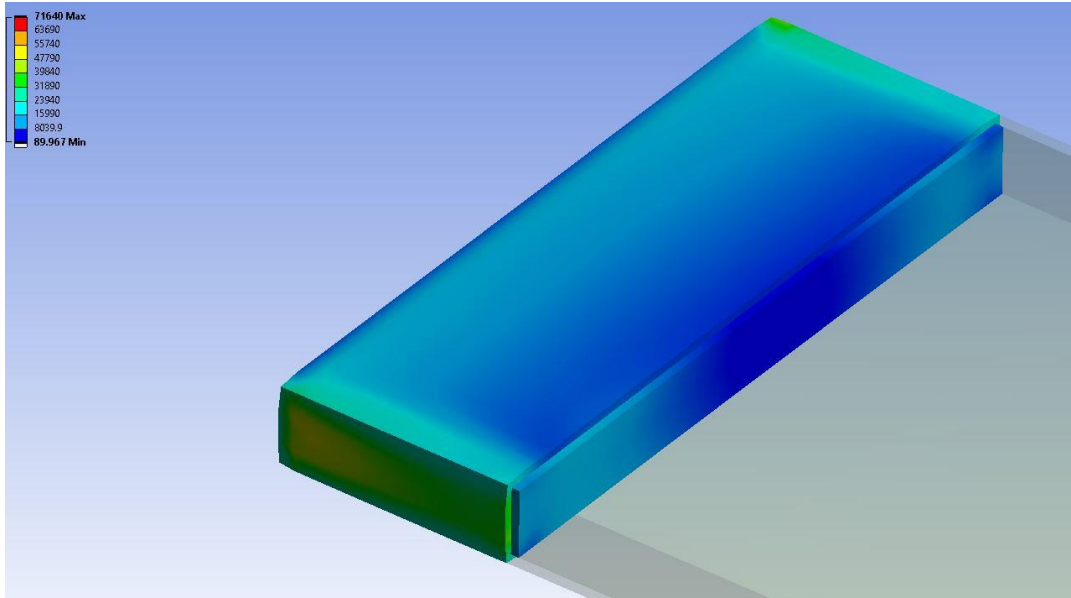


Figure 27: UAV Panel 1 Equivalent Stress Top 45 Deg. Ply [psi]

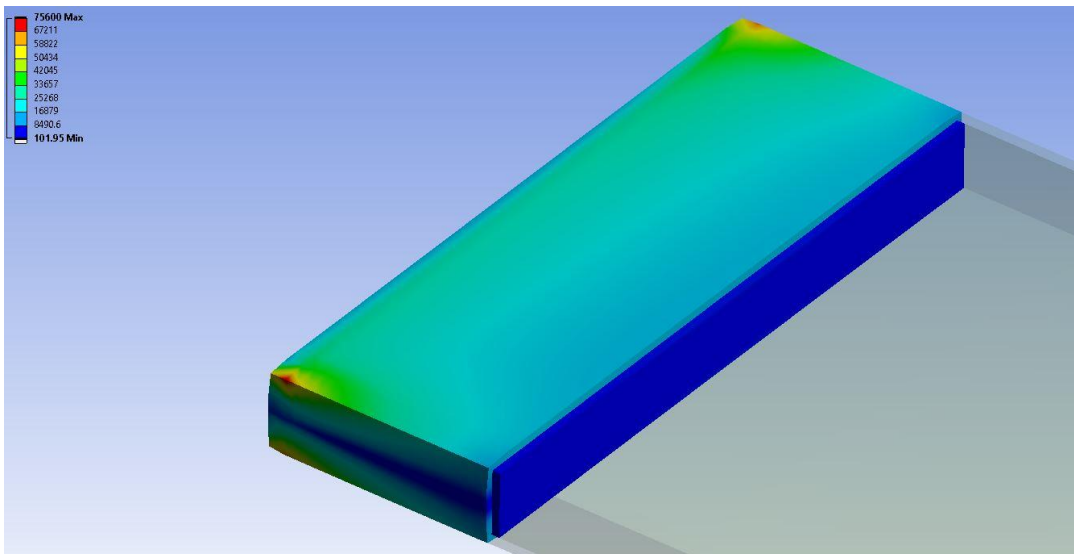


Figure 28: UAV Panel 1 Equivalent Stress Top 0 Deg. Ply [psi]

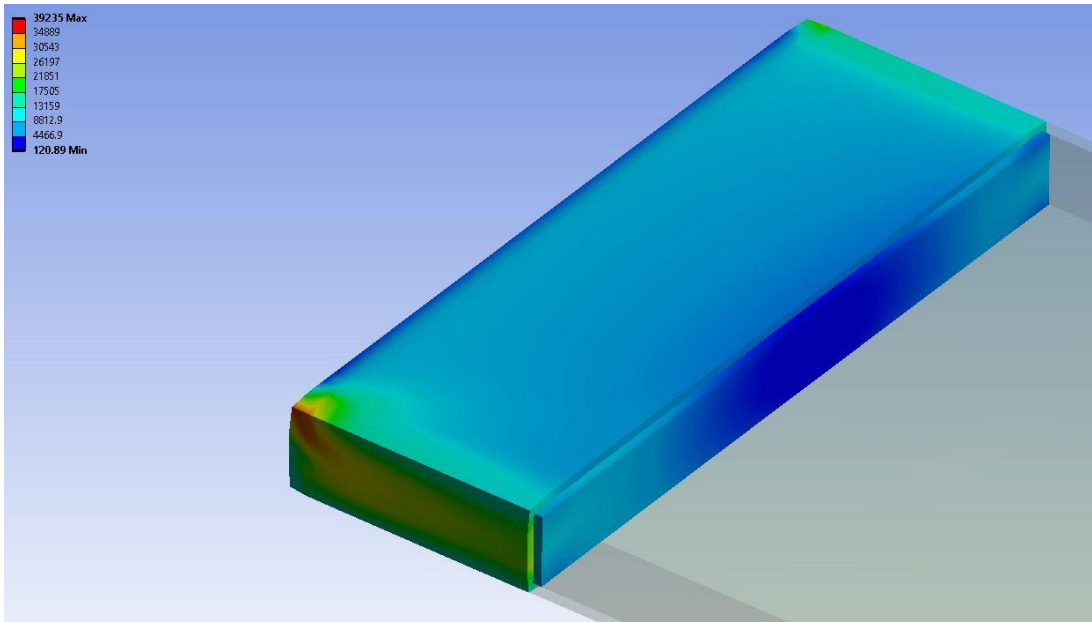


Figure 29: UAV Panel 1 Equivalent Stress Top -45 Deg. Ply [psi]

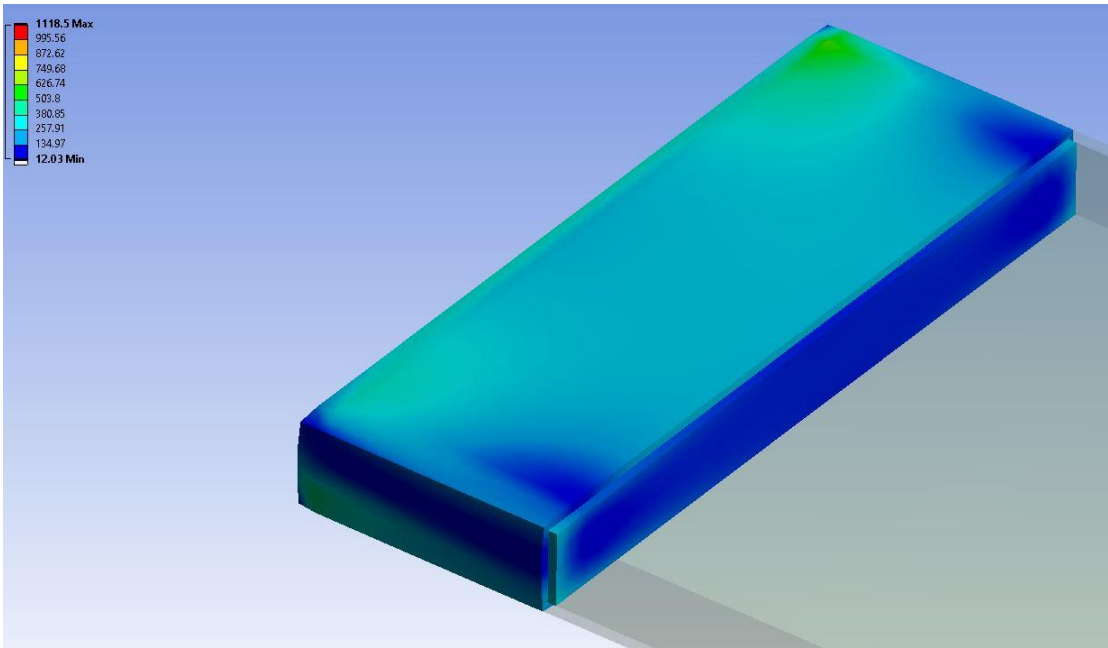


Figure 30: UAV Panel 1 Equivalent Stress Foam Core [psi]

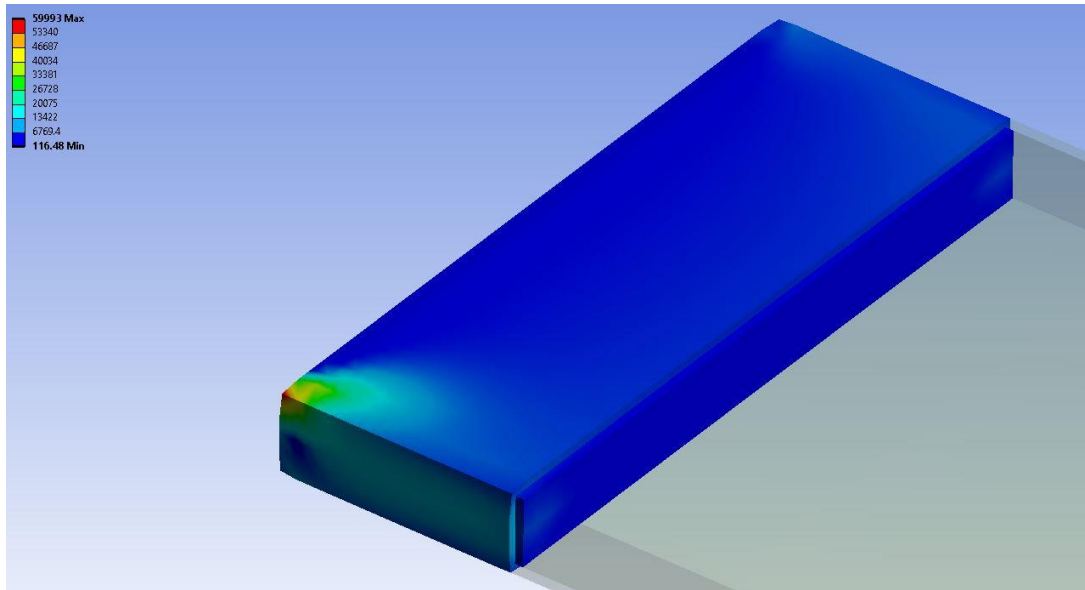


Figure 31: UAV Panel 1 Equivalent Stress Bot -45 Deg. Ply [psi]

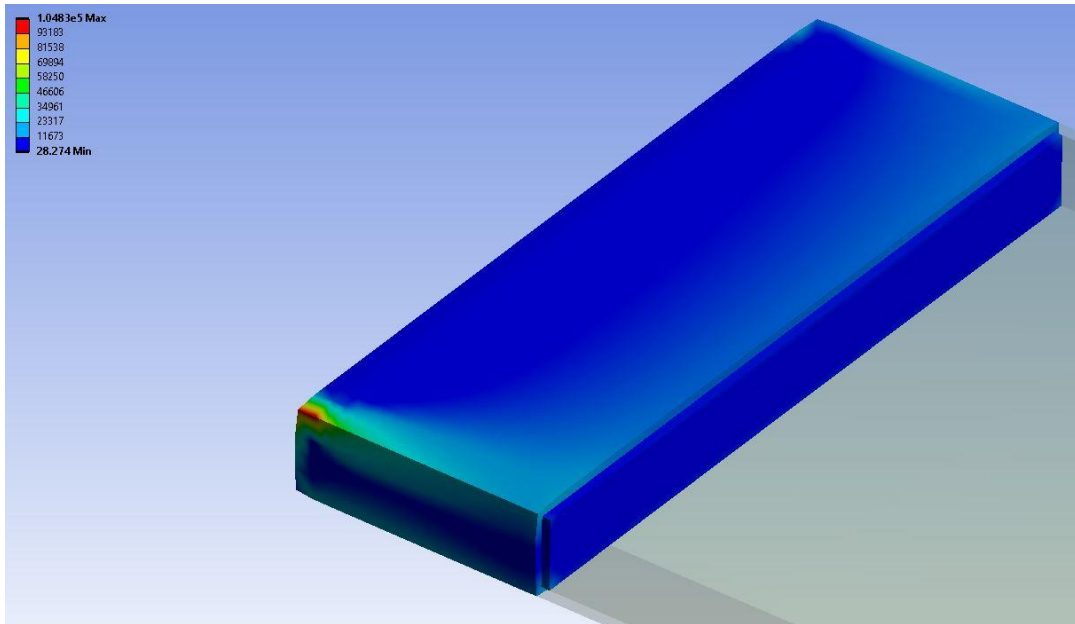


Figure 32: UAV Panel 1 Equivalent Stress Bot 0 Deg. Ply [psi]

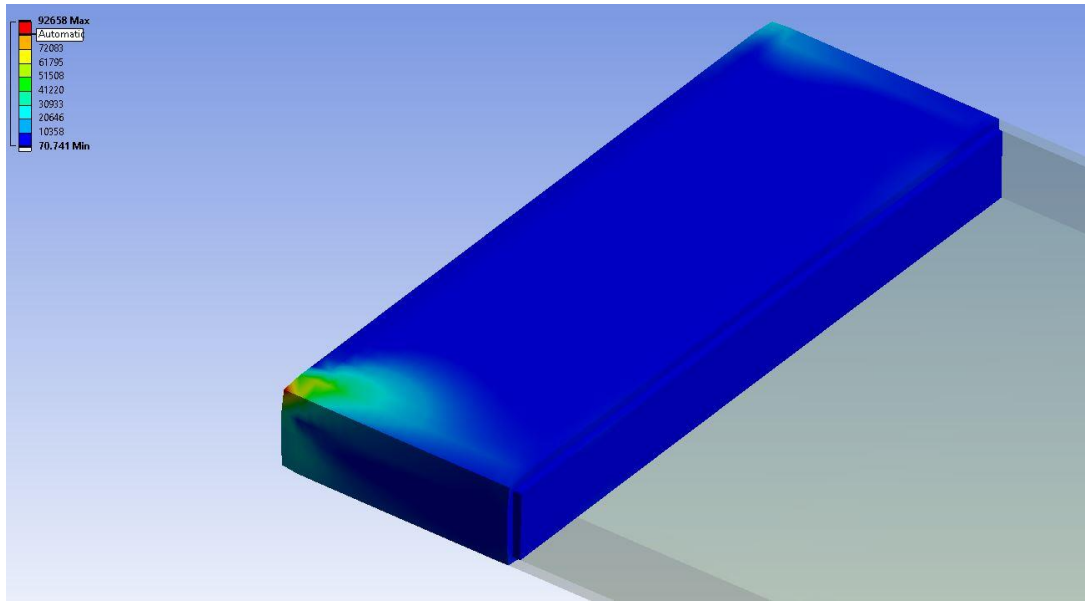


Figure 33: UAV Panel 1 Equivalent Stress Bot 45 Deg. Ply [psi]

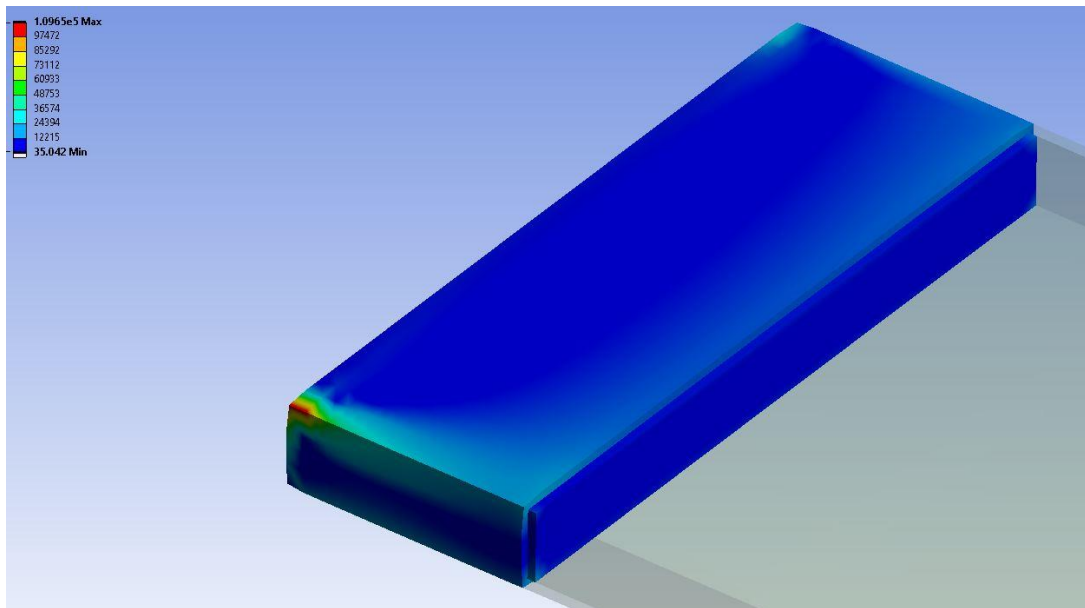


Figure 34: UAV Panel 1 Equivalent Stress Bot 90 Deg. Ply [psi]

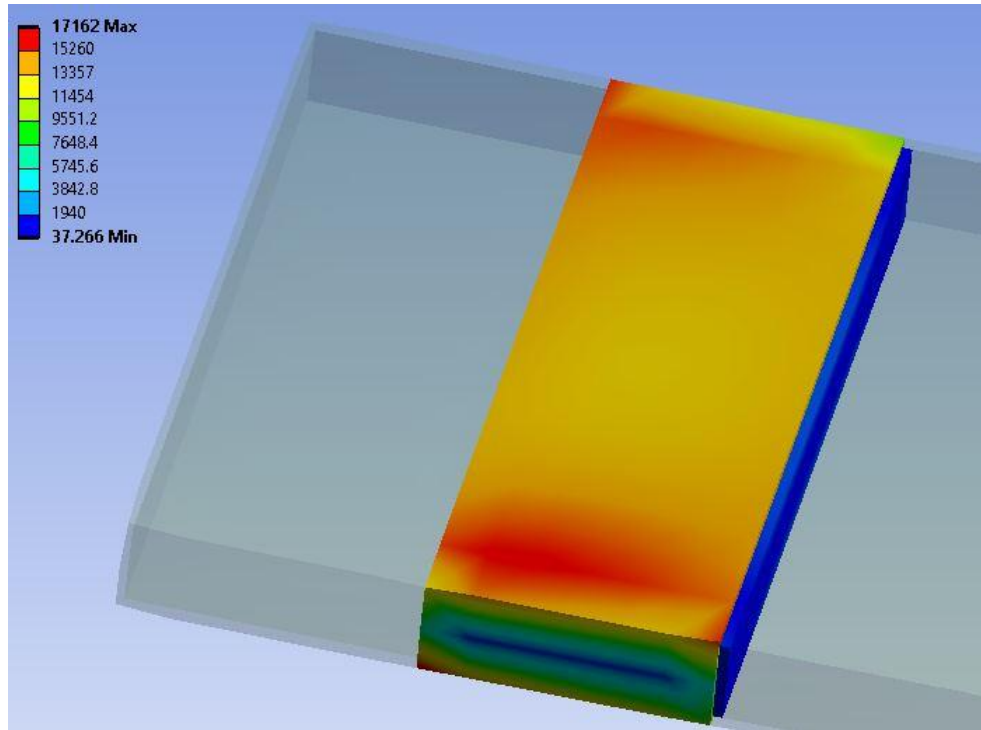


Figure 35: UAV Panel 2 Equivalent Stress Top 90 Deg. Ply [psi]

A recurring trend of the ply's reactions seen as equivalent stresses is that for the root panel there is a stress concentration at the supporting edges. When compared to the adjacent panel 2 which has no pronounced stress singularity, the severity of the issue becomes apparent. In a final structural design this issue would be mitigated by using radiuses and a wider mating surface between the root of the wing and the fuselage. In none of the presented figures does the equivalent stress approach a failure for the composite, the closest occurring in the bottom 90-degree ply which sees a load at 50% of the strength limit for the lamina. This analysis further cements the understanding of the limitations and unrealistic sizing seen when using equivalent stress as a primary sizing limitation.

The next set of figures show the normal stress in the wing in the spanwise direction. This is the critical direction for analyzing the composite lamina, as the magnitude of it

will be far greater than that of the chord wise direction. Further, in the spanwise direction the 90-degree ply will be facing the least optimal load direction. In the full wing model seen in fig. (37) the normal stress is nearly uniform, calling attention to no particular areas of the wing. As the root panel remains the most likely to experience failure the composite stack-up has been decomposed once more for ply-by-ply observation.

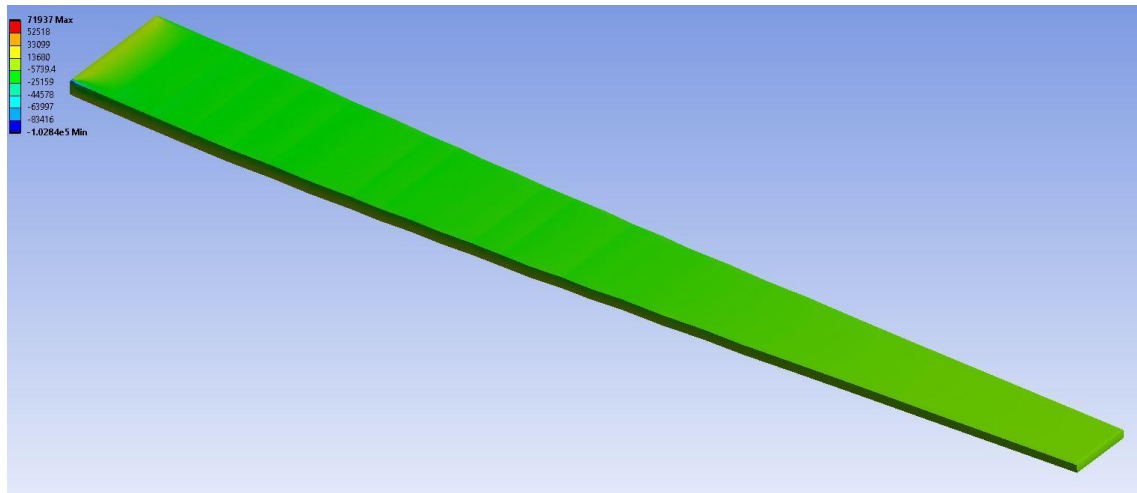


Figure 36: UAV Wing Normal Stress [psi]

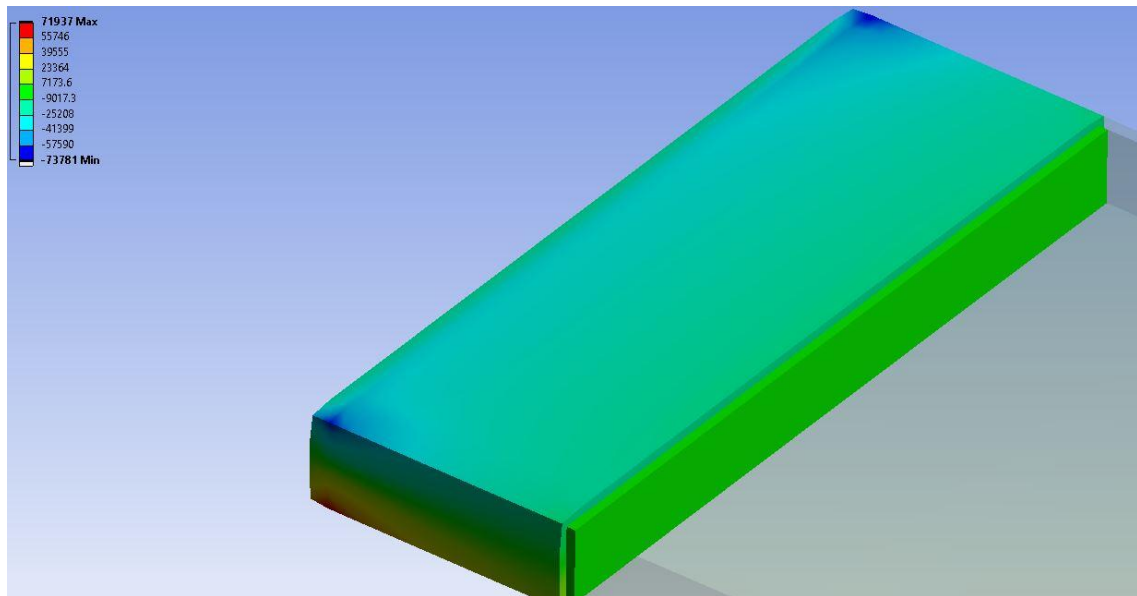


Figure 37: UAV Panel 1 Normal Stress Top 90 Deg. Ply [psi]

The maximum normal stress in each ply can be compared against the composite strength to determine if failure would occur in that ply. ANSYS does this itself in the Composite Failure Tool, however exploring the reactions in the plies in a more detailed approach such as this can be prudent. The top 90-degree ply seen in fig. (38) is the primary area of concern for the laminate as a whole. Approaching the stress singularity, the stresses just meet the panel strength at 33,715 Psi and exceed the panels strength closer to the center of the singularity. This will be revisited when observing the safety factor of the composite laminate, where the 90-degree top ply is the only ply to have failed in the stack up. Interestingly this behavior is indicative of a matrix failure where the composite matrix deteriorates under the applied strain, however this ply is not a critical structural ply, providing lateral stability to the laminate and little else. Further, this failure is only observed on the upper panel at the root, which would lead the engineering team to simply reinforce the laminate in this area of using design principles previously mentioned.

In the stack-up, no other ply approaches failure under the induced stress. This is likely due to the 45, 0, -45-degree plies are better aligned with the stress. The 0-degree ply was used as the primary design criteria for the composite iteration. The composites properties are built to accommodate the 0-degree ply and prevent their failure. As such, a failure in this ply would suggest a failure of the model in its development of the wing model.

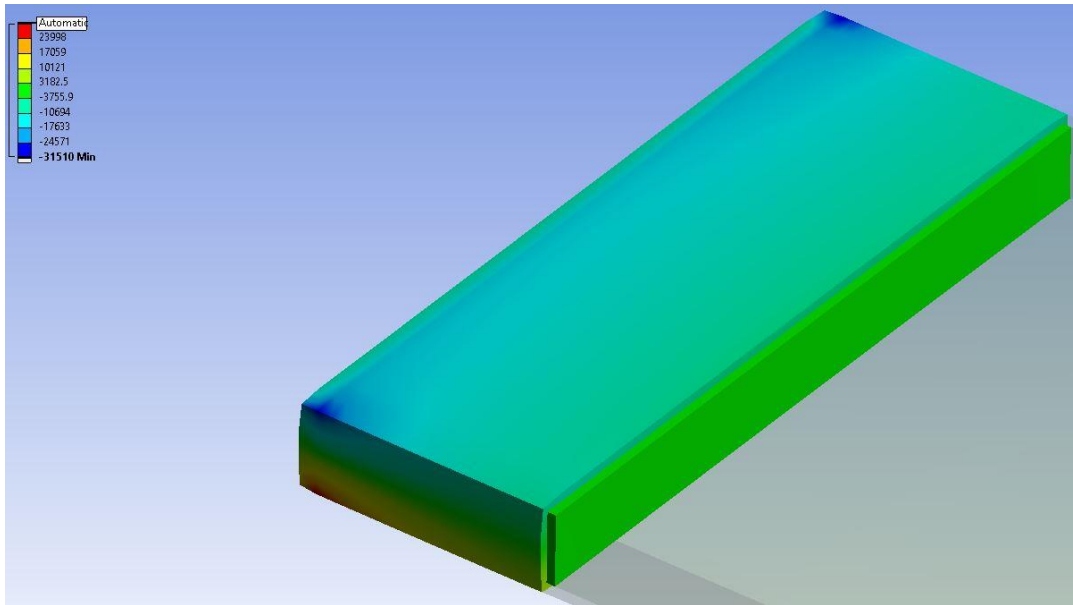


Figure 38: UAV Panel 1 Normal Stress Top 45 Deg. Ply [psi]

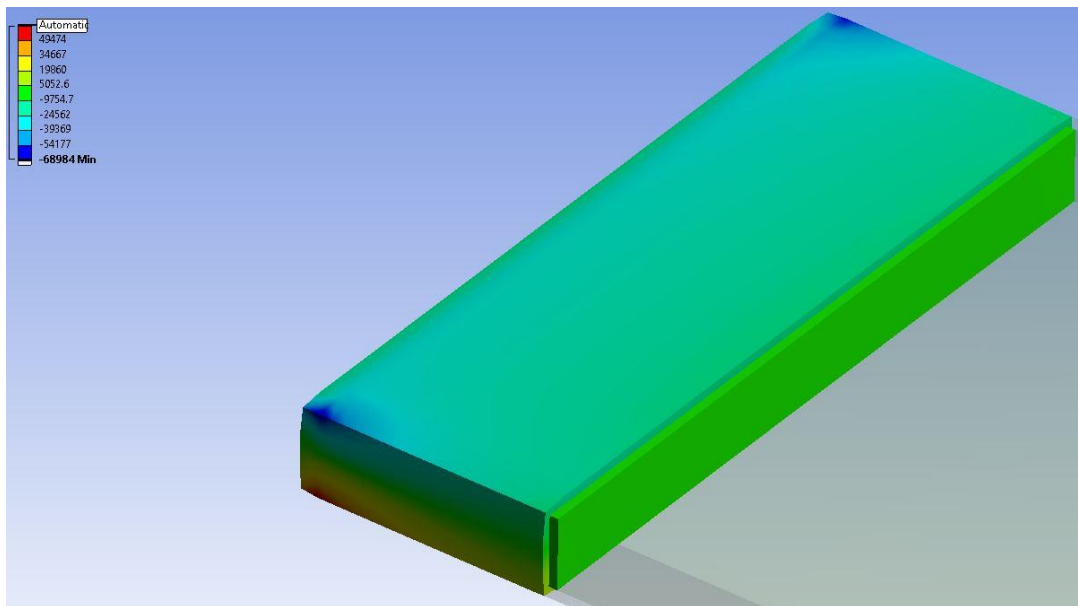


Figure 39: UAV Panel 1 Normal Stress Top 0 Deg. Ply [psi]

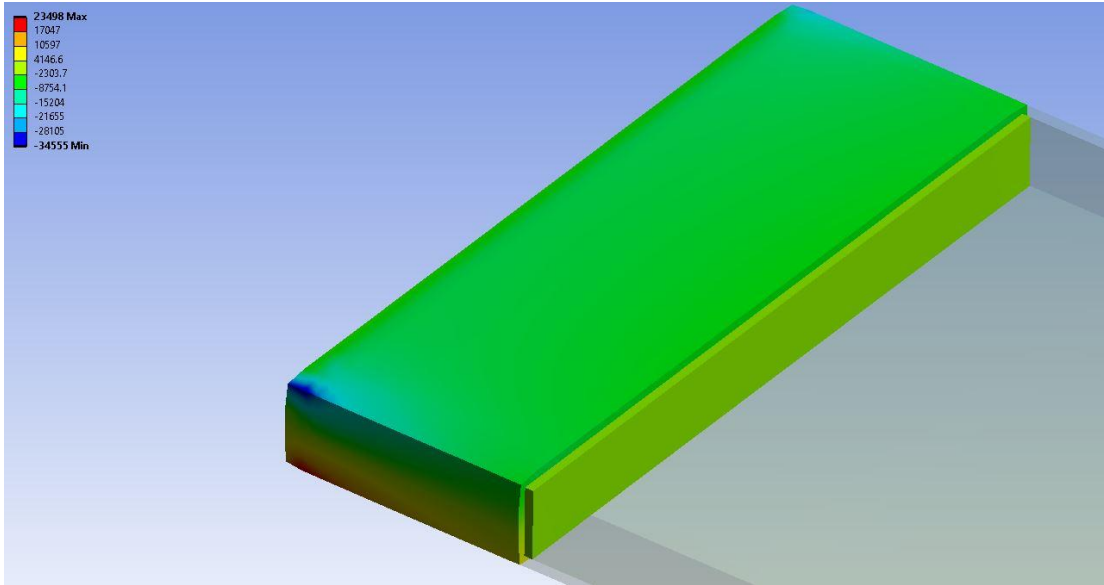


Figure 40: UAV Panel 1 Normal Stress Top -45 Deg. Ply [psi]

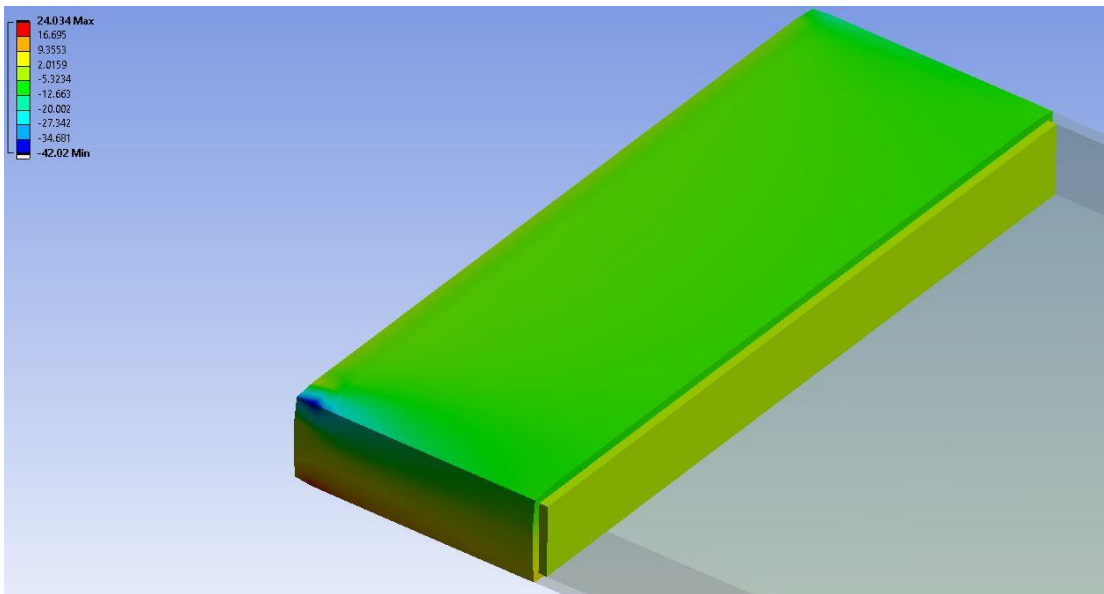


Figure 41: UAV Panel 1 Normal Stress Core [psi]

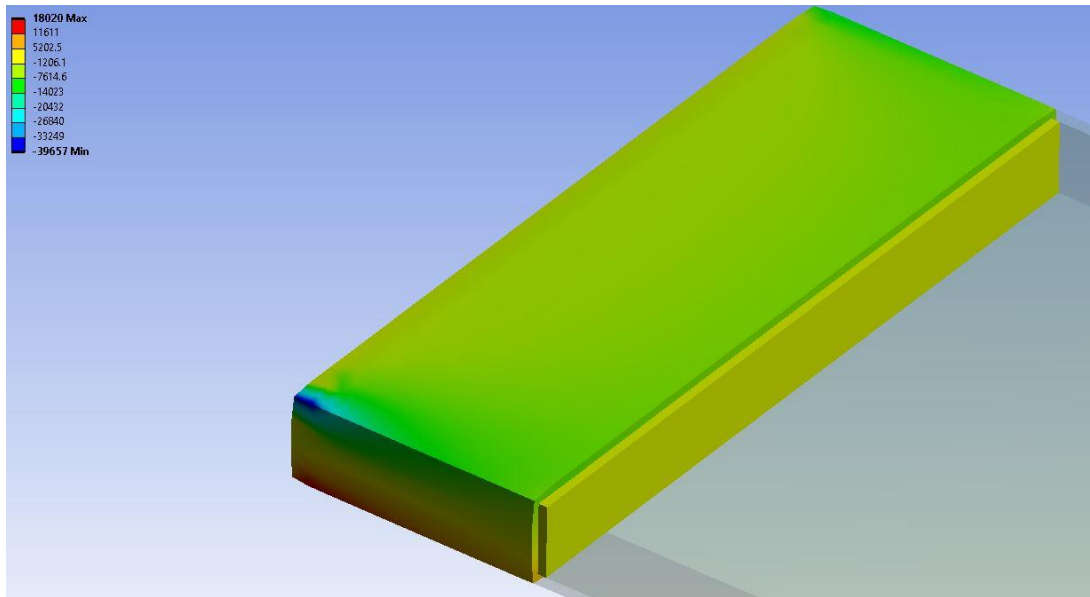


Figure 42: UAV Panel 1 Normal Stress Bot -45 Deg. Ply [psi]

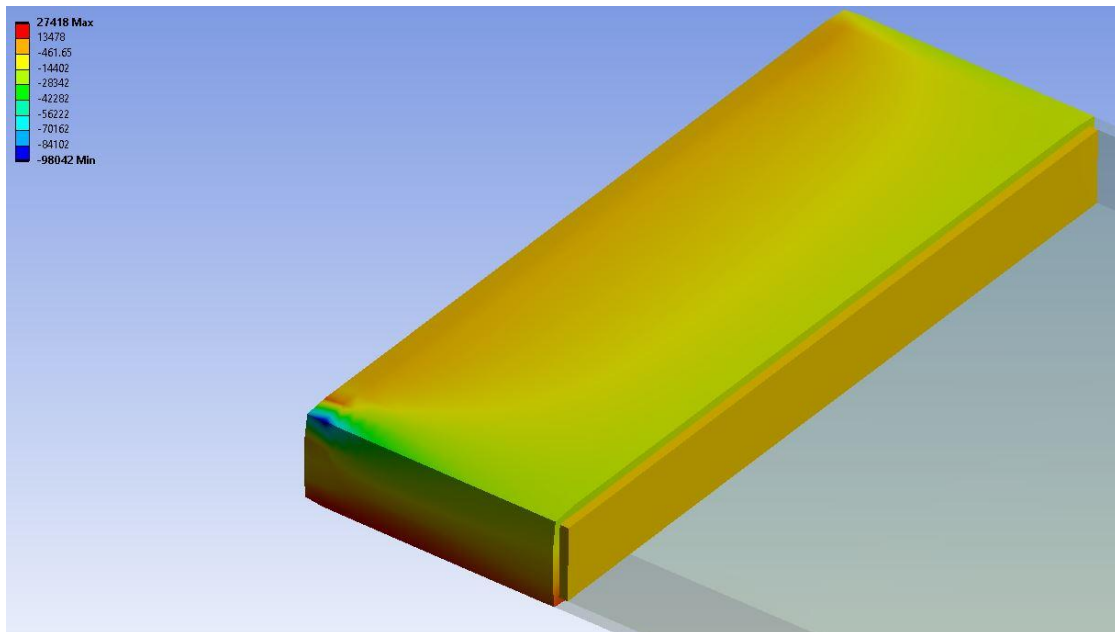


Figure 43: UAV Panel 1 Normal Stress Bot 0 Deg. Ply [psi]

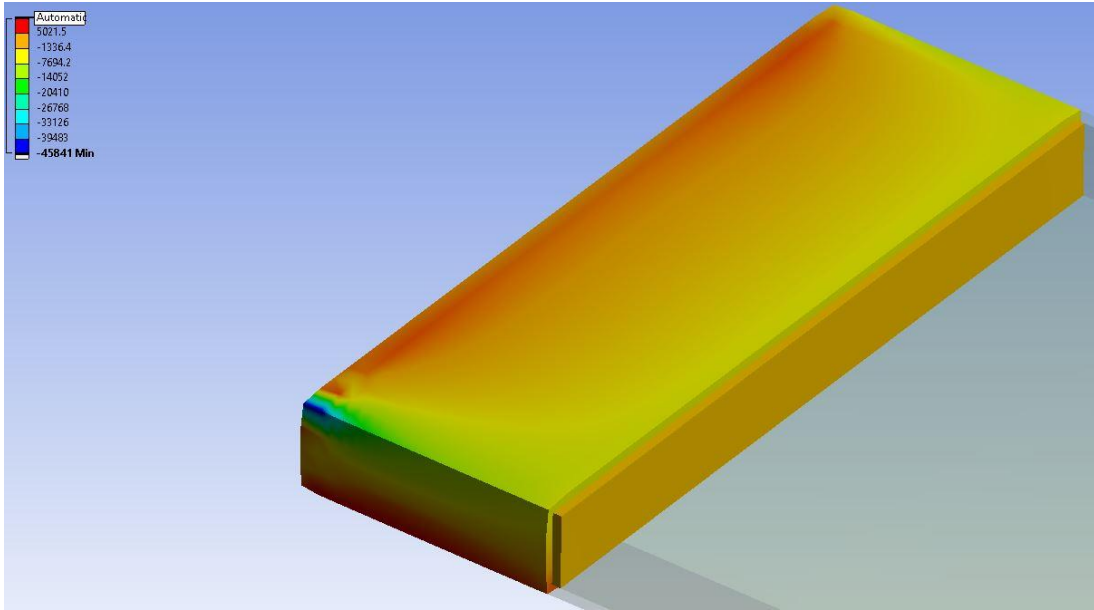


Figure 44: UAV Panel 1 Normal Stress Bot 45 Deg. Ply [psi]

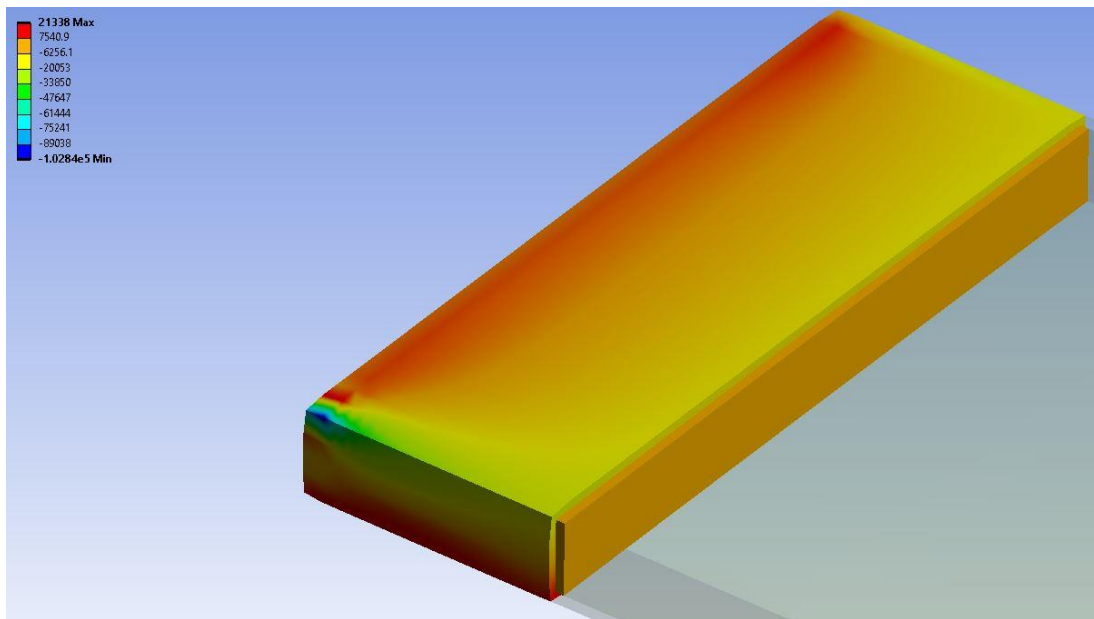


Figure 45: UAV Panel 1 Normal Stress Bot 90 Deg. Ply [psi]

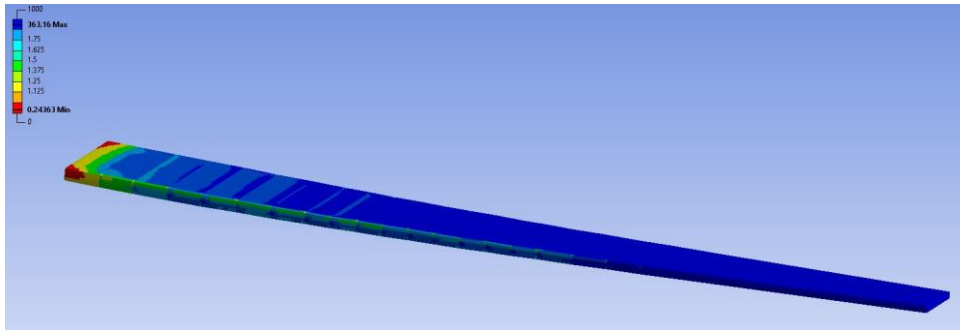


Figure 46: UAV wing composite Safety Factor

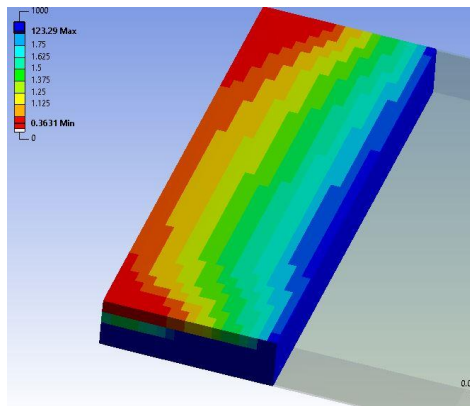


Figure 47: UAV wing composite Safety Factor Panel 1 Top 90 deg.

ANSYS has the capability to directly show the composite safety factor and the failure mode that results in the ply's failure. The color map indicates the analyzed strength of the given areas. For instance, the dark blue regions will require a load 123 times the applied certification load to fail; these regions will fail in some other mode unrelated to materials tensile, shear or compressive strength. Conversely, the dark red areas need a load only 0.36 times the applied certification load (only 54% of the design maximum loads); indicating these areas are currently failing for a ply in the laminate composite at only ~1.5-gee load factors without a safety-factor. This is a very localized phenomenon which would require further reinforcement before being released for production. Note that the red region of fig. (47) has a safety factor of 0.947 (142% of the design maximum loads) outside of the corner"

This is indicative of the composite “just” failing in the region. To build up the composite structure, a strengthening constant of 3 was added into the composite failure checks. This constant forced the model to develop a more pessimistic laminate. The inclusion of the constant was guided based on early ANSYS analysis where the composite was simply too weak to support the applied load. The same global failure behavior can be seen in fig. (48) for the Top 90-degree ply of panel 1. This confirms what was seen in the normal stress figures, where the 90-degree ply is a limiting factor of the design. Further investigation shows that ANSYS has identified the failure as Tsai-Hill, indicating that the ply is likely having an unbalanced strain due to the perpendicular loading it is supporting.

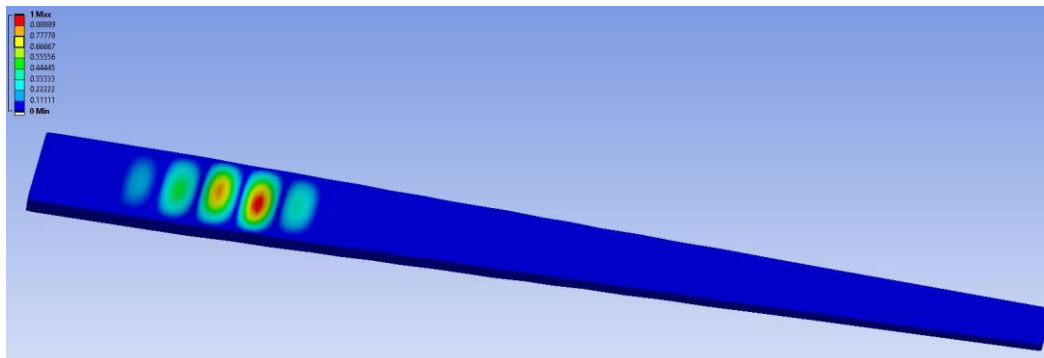


Figure 48: UAV wing Eigenvalue Buckling 0.97887

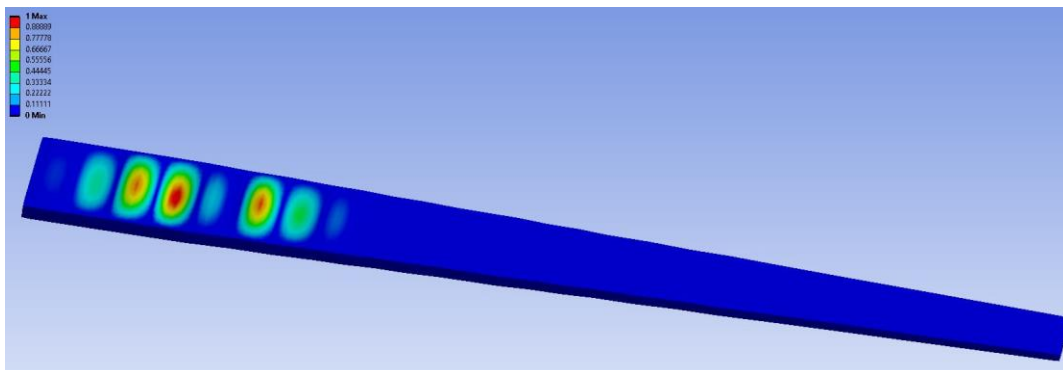


Figure 49: UAV wing Eigenvalue Buckling 1.0127

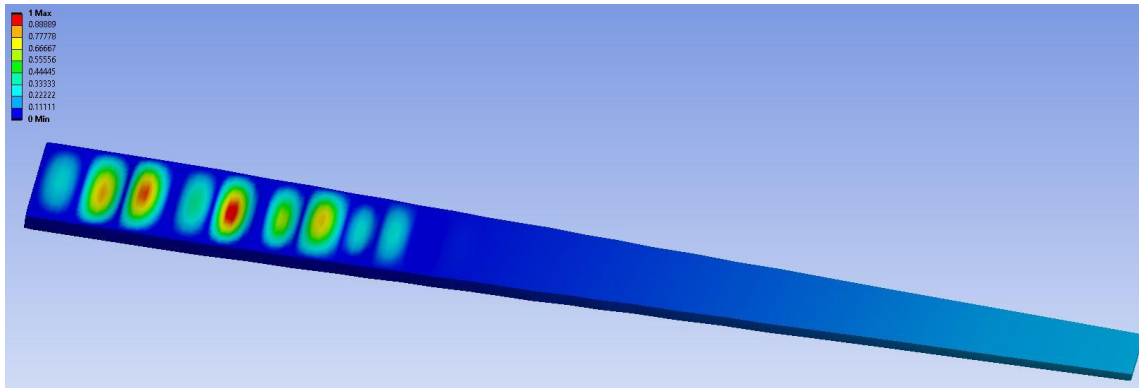


Figure 50: UAV wing Eigenvalue Buckling 1.0469

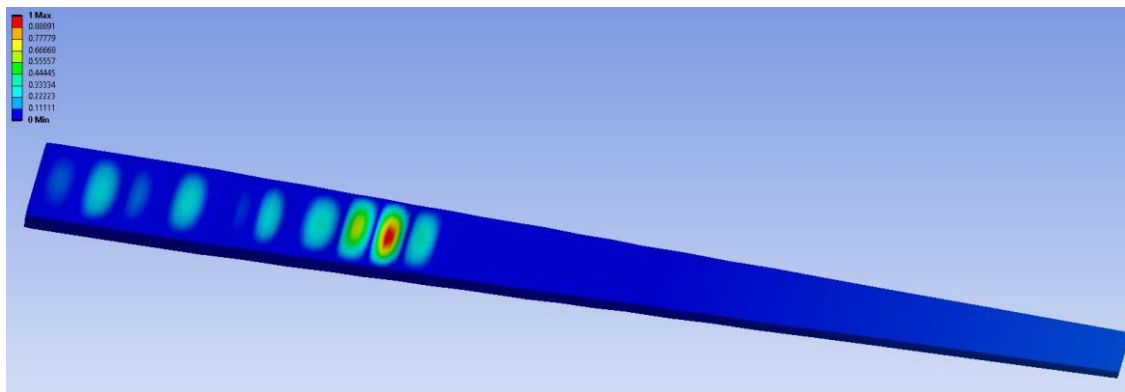


Figure 51: UAV wing Eigenvalue Buckling 1.0664

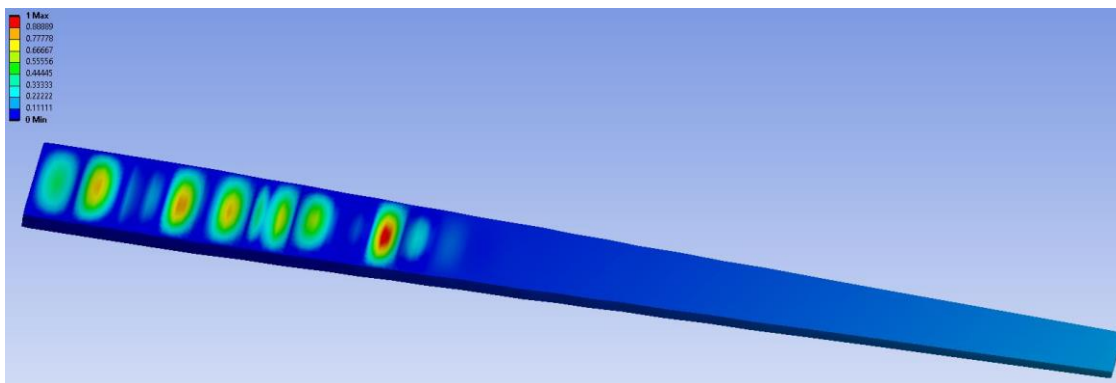


Figure 52: UAV wing Eigenvalue Buckling 1.0788

The final area of analysis is Eigenvalue buckling, the goal of which is to reveal global behavior of the wing. Figures (49-53) show several buckling modes which develop at their respective load multipliers. The onset of buckling occurs at a 0.979 load multiplier, which is in line with the target load multiplier for the wing. The goal for structure developed by the model would be to have a load multiplier near 1. The mode shape results seen in the first figure of the set shows buckling occurring several panels away from the root of the wing. Intuition would suggest that buckling would occur at the area of highest stress, often intuition is broken by computational analysis. The observed mode shape is well within reason and does not raise concerns regarding the applied fixity conditions or the structures development.

Table 9: Normal Stress Maximum Stress Criterion Tabulated

Maximum Stress Failure Criteria			
Panel Name	Panel Stress	S_1	S_2
	[psi]		
90	33715	0.155	0.945
45	30936	0.142	0.867
0	64282	0.295	0.450
-45	23498	0.108	0.659
Core	24	0.533	0.533
-45	39657	0.182	0.290
0	27418	0.126	0.768
45	11379	0.052	0.319
90	21338	0.098	0.598

After reviewing all the figures created in ANSYS, it is clear that the structure of the wing is performing within acceptable ranges. Buckling begins at 97% of the applied certification load (i.e., 145% of the design maximum load) and the laminate itself is

supporting the applied load. ANYSIS suggests the likely failure mode for the composite laminate will occur at the 90-degree ply as a Tsai-Hill failure. Upon further inspection, this ply also experiences face sheet wrinkling in the critical stress concentration areas. Face sheet wrinkling is a failure where the outer laminate of a stack-up delaminates from the other sheets and buckles independently of the rest of the laminate. Outside of the stress singularity, all the laminate plies support the applied load. Note that the applied load is the maximum failure load for the wing and would have to be supported for 3 seconds. Under this test, permanent deformation is expected but should be minimized. Under the criteria outlined in 14 CFR § 25.305 “The structure must be able to support limit loads without detrimental permanent deformation. At any load up to limit loads, the deformation may not interfere with safe operation...”^[16] This wing meets those criteria.

b. Jet with Low Aspect Ratio Wing Analysis

The second wing to be analyzed was selected to directly contrast the geometry of the UAV wing. In this case, a heavier aircraft with a shorter wing and higher airspeed creates considerably different design requirements for the model to handle. The goal of this wing geometry is to test the model with a wing outside of the initial trial testing range. The shorter and wider wing profile is more suited to supporting buckling loads, hence the likely failure mode of this wing will be the composite itself and not the panel buckling case. The difference in geometry could also lead to failure in modes unaccounted for in the model. Modeling a successful wing structure for this aircraft would prove the applications capabilities and further confirm the assumptions made in the process of its creation. Note that in the development of this wing the “tuning” constants were not changed. This was done explicitly as a test for the model’s ability to develop generalized structures.

1. Design Inputs

As with the UAV, the process of running the application is unchanged. Firstly, the aircraft geometry must be defined following reasonable approximations as informed by the end users' requirements and the experience of the design team. Note again that the dimensions of the fuselage are largely placeholders included for the convenience of the IPT and as a foundation for future enhancements to the model. Critical design variables begin with the wings reference surface area, which has been set to 300 square feet having a span of 25 feet and a taper ratio of 0.35. The sweep is set to 35 degrees. Sweep and taper ratio in this case create the characteristic wing profile of modern jets designed with maneuverability in mind. Note, this factors together create a relatively short "fat" wing with a low aspect ratio. Which should shift the design constraint away from panel buckling toward a composite laminate failure.

Table 10: Jet user design inputs

Fuselage Length	35	ft
Fuselage Width	48	in
Fuselage Height	48	in
Wing Area, Sref	300	sq. ft
Wingspan, b	25	ft
Wing TR	0.35	
Wing LE-Sweep	35	deg
Wing LE-FS	100	in
Aspect Ratio	2.0833	
Aircraft Lift	6000	Lbf at 1 gee
Design Mach #	0.606	
Design Alt	40000	ft
Design KTAS	400.4448	knots
Design G	6	
Design Lift	54000	Lbf at 3 gees

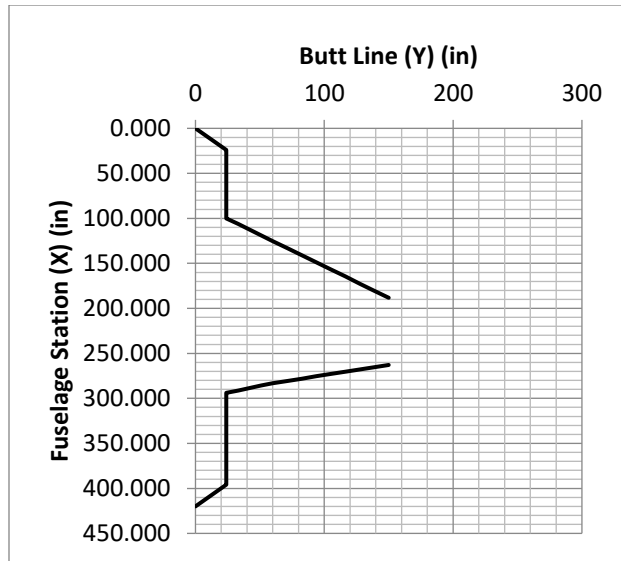


Figure 53: Jet Wing Profile Visualization

The design lift has been greatly increased to 6000 lbf which in conjunction with the 6-gee expected maneuvering limit will place significant flight loads on the wing. This also represents the higher flight capabilities of this aircraft class, and the potential payload it must carry. Furthermore, the flight speed and altitude have also been increased to 400 knots and 40,000 feet respectively. All the expressed design variables can be seen in table (10) which is representative of how they would be input into the application. A visualization of the aircraft wing profile can be seen in fig. (54).

2. Model Outputs

A complete run of the model develops the outputs seen in table (11) these show the composite used in the structure of the wing as well as the rib placement through the wing. In comparison to the UAV wing which is long and slender, the Jet wing is short and wide. This has resulted in a single composite laminate stack being used for the entire length of the wing. Note also that the composites failure modes are extremely low, the last saved values show the composite failure modes at the root. At this location, the composite is at

10% of failure, suggesting that the composite was not the limiting factor in the development of the structure.

Table 11: Jet wing Model Composite Failure Check

Tsai Hill Failure Criteria 0	0.106023
Tsai Hill Failure Criteria 90	0.021676
Tsai Hill Failure Criteria 45	0.111938
Tsai Hill Failure Criteria -45	0.111938
0 Degree	
Sigma 1 > S1C	0.324504
Sigma 2 > S2T	0.022854
Tau 12 > S12	0
$\epsilon_1 / (S1/E1)$ [Compression]	0.324675
$\epsilon_2 / (S2/E2)$ [Tension]	0.21675
ν_{12}	0
90 Degree Plies	
Sigma 1 > S1T	0.096829
Sigma 2 > S2C	0.103251
Tau 12 > S12	0
$\epsilon_1 / (S1/E1)$ [Tension]	0.101571
$\epsilon_2 / (S2/E2)$ [Compression]	0.112658
ν_{12}	0
45 Degree Plies	
Sigma 1 > S1C	0.087419
Sigma 2 > S2C	0.210858
Tau 12 > S12	0.250715
$\epsilon_1 / (S1/E1)$ [Compression]	0.111552
$\epsilon_2 / (S2/E2)$ [Compression]	0.038707
ν_{12}	0.125357
-45 Degree Plies	
Sigma 1 > S1C	0.087419
Sigma 2 > S2C	0.210858
Tau 12 > S12	0.250715
$\epsilon_1 / (S1/E1)$ [Compression]	0.111552
$\epsilon_2 / (S2/E2)$ [Compression]	0.038707
ν_{12}	0.125357

The wing uses six ribs to segment the panels in order to resist buckling, much less than was used for the UAV wing. The final wing developed is 1063 lbm, approximately 1/6th of the overall flight load. This wing weight is acceptably lightweight. Note that this wing was built using the same potential composites as the UAV wing. A ply thickness of 0.01 inches is on the lower end of available composite sheeting and the wing would be potentially built from a slightly thicker laminate to ease raw material availability.

Table 12: Model Output Structural Description for Jet Wing

Total Mass [lbm] of wing	1063.105
Ply Count	7
Effective Ply Count	7
Total Layup Thickness	0.2025
Ply Thickness	0.01
Composite Material	3
Core Thickness	0.0625
1	108
2	82.5
3	61.5
4	43.5
5	27
6	12
7	0

3. FEA Validation

The process to validate the wing structure in ANSYS is identical for this wing as it was for the UAV wing. The fixity conditions, loading method, and data collected all mirror what was done on the other wing. Unlike the UAV wing only the full wing figures are presented here as the reactions within the individual plies of the laminate mirror the same relationship as the previous wing. Further, the full wing figures are sufficient to articulate the performance of this wing structure. In the case of this larger wing, much of the reactions show more concentrated behavior in contrast to the global reactions of the slender wing.

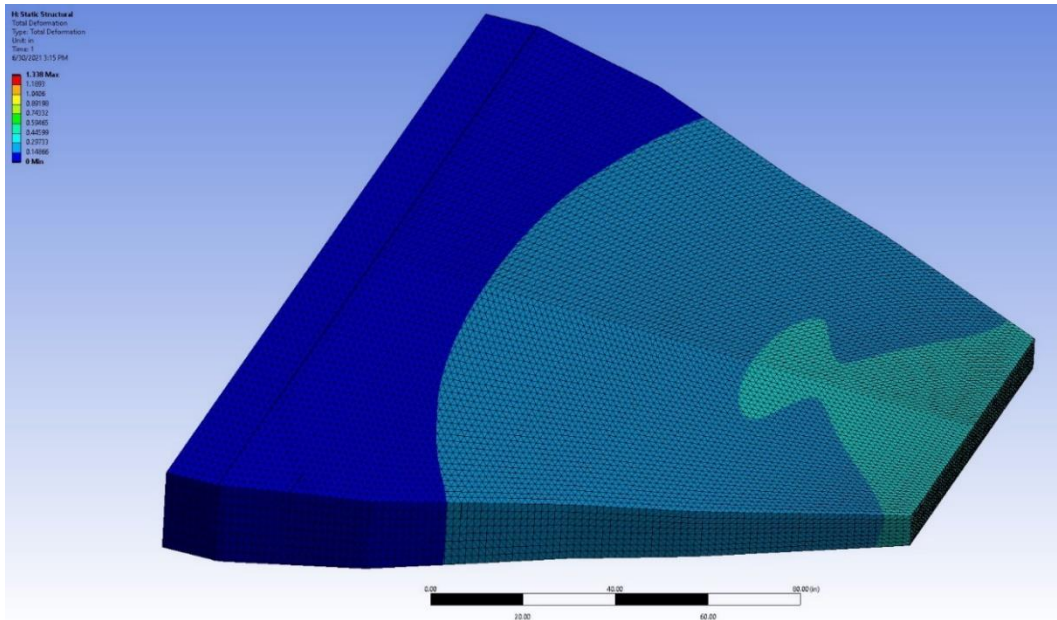


Figure 54: Jet wing Total Deformation [in]

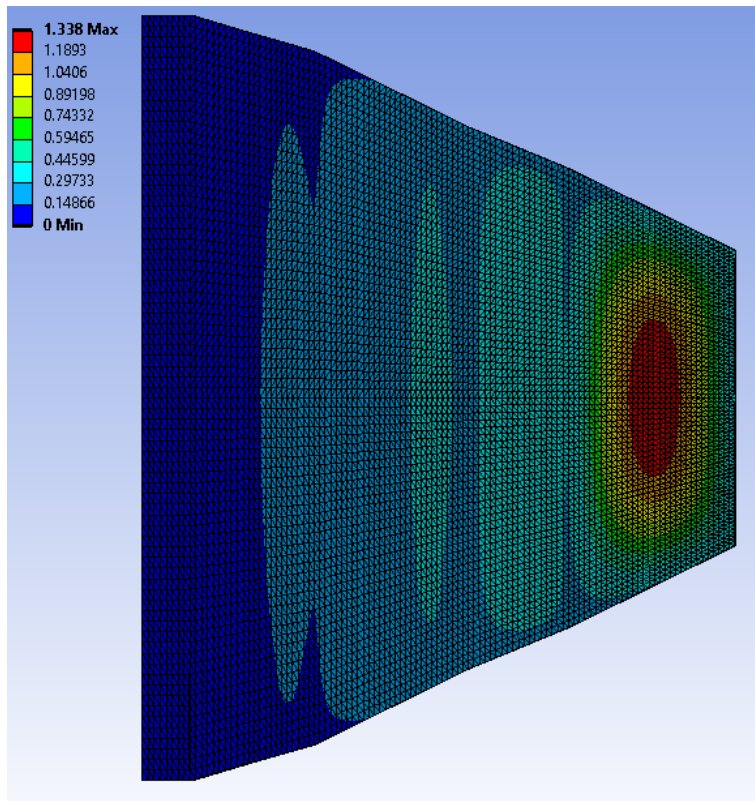


Figure 55: Jet wing Total Deformation (bottom of wing) [in]

Total deformation is a useful initial figure to see how the structure is reacting to the load without buckling. This is especially useful in cases where the deformation could change the performance of the structure. The total deformation of the wing is shown fig. (55) where the wing deflects a total of 1.338 inches and again in fig. (56) which shows the bottom of the wing. A view of the bottom of the wing was included in this case as the deformation over the span is not analogous to a beam. The final panel on the bottom of the wing experiences what appears to be plate deformation. Plate deformation was not an accounted for failure mode within the model. In the case of this wing, the surface area of the planform is several times greater than that of the thin wing. It follows that a large section of unsupported sheet would undergo plate deformation. The following figures will reveal whether this unpredicted type of deformation results in a composite or buckling failure.

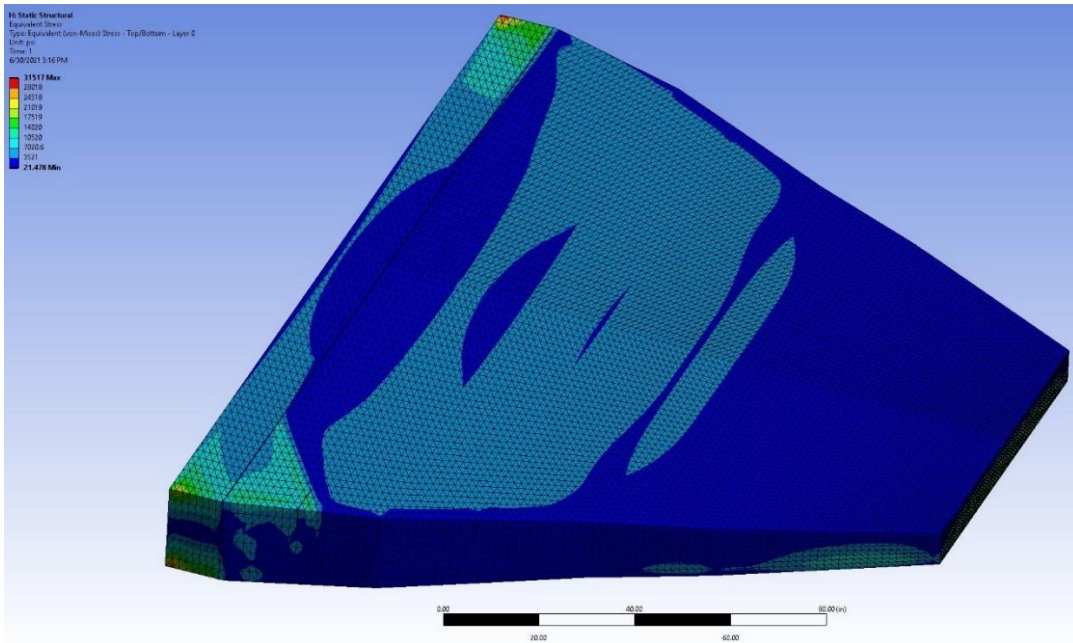


Figure 56: Jet wing Equivalent Stress [psi]

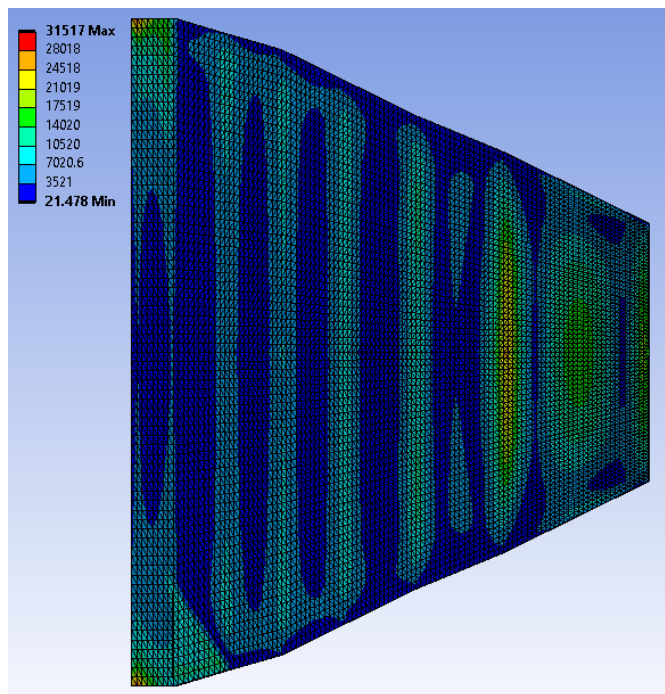


Figure 57: Jet wing Equivalent Stress (bottom of wing) [psi]

While the usefulness of Equivalent (Von-Mises) Stress for understanding the failure in a composite is limited. The heat map of the stress in the wing can be used to identify areas for further investigation on the wing. Fig. (57-58) show the top and bottom of the wing with the equivalent stress modeled onto its surface. Similar to the previous wing model, there are stress singularities at the corners of the supported panels. In the case of this wing, the bottom of the structure is more interesting than the top. The UAV wing behaved as predicted and is limited by the compression strength of the top panels. This wing experiences high stresses across the bottom panels. The top of the wing shows the stress due to the deflection of the wing which would drive the buckling equations used to develop the structure. The bottom continues to show how the pressure applied to the greater unsupported surface area of this wing is driving a plate deformation in the larger panels. Also note that many of the stress concentrations are near the placed ribs.

The second set of figures shows the Normal Stress in the wing structure this set includes fig. (59-60). The normal stress in the x direction shows the same trend as the equivalent stress. The top of the wing is uniformly stressed while the bottom of the wing shows the stress stacking expected on the top. A significant negative stress is seen where the impression on the panel is occurring. This is indicative of the composite resisting the strain of the deformation. The observed normal stresses are well below the max stress of 217,557 psi.

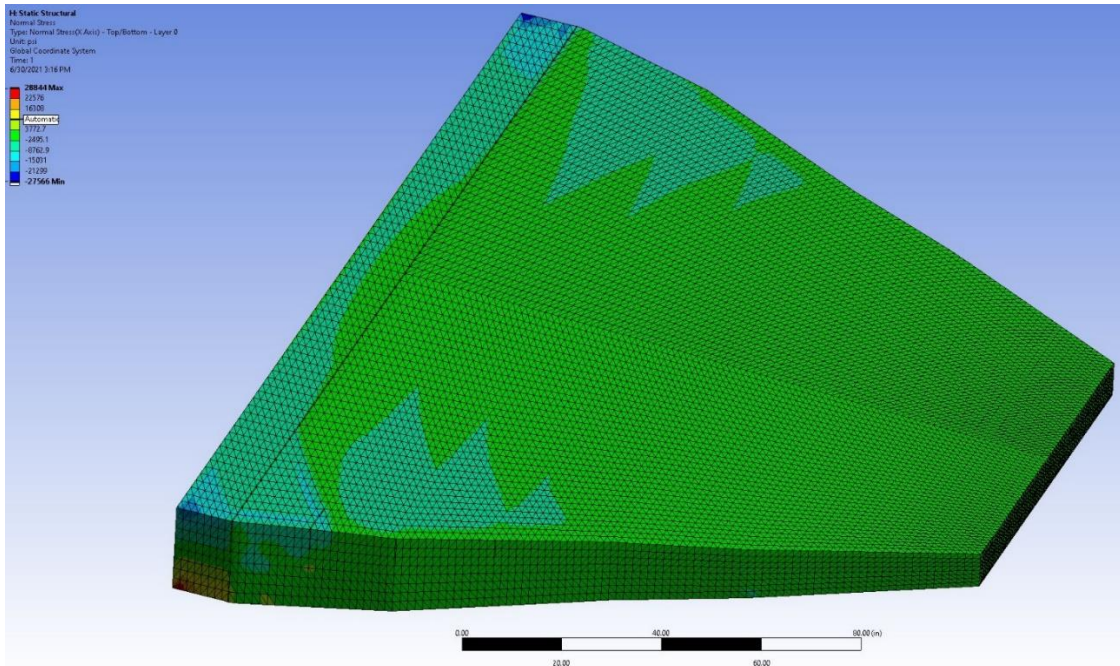


Figure 58: Jet wing Normal Stress [psi]

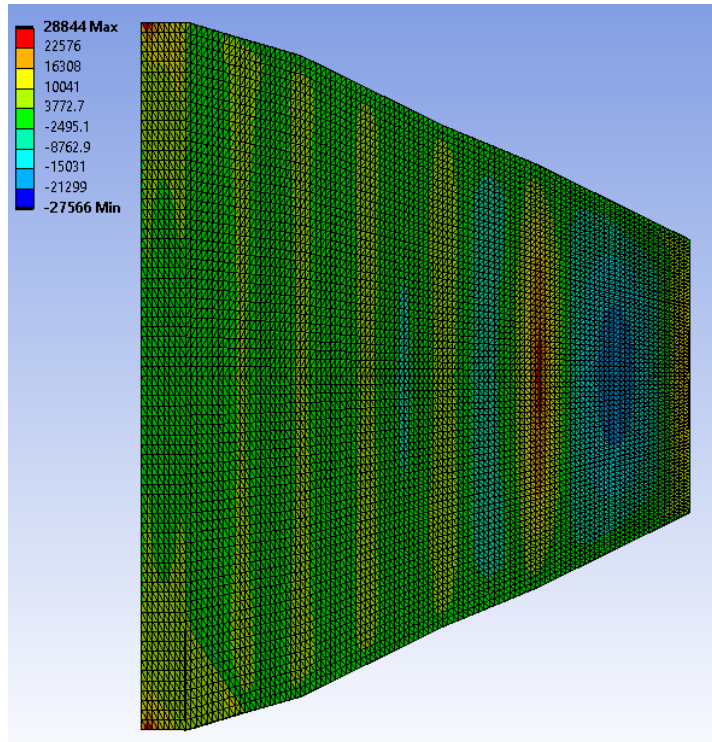


Figure 59: Jet wing Normal Stress (bottom of wing) [psi]

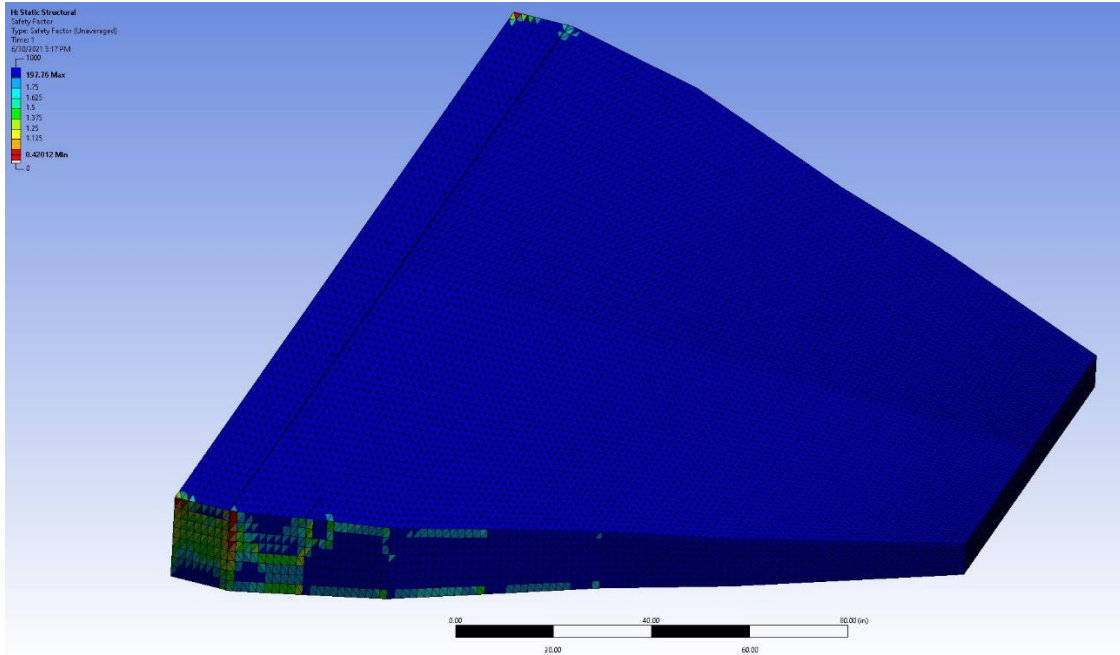


Figure 60: Jet wing Composite Safety Factor

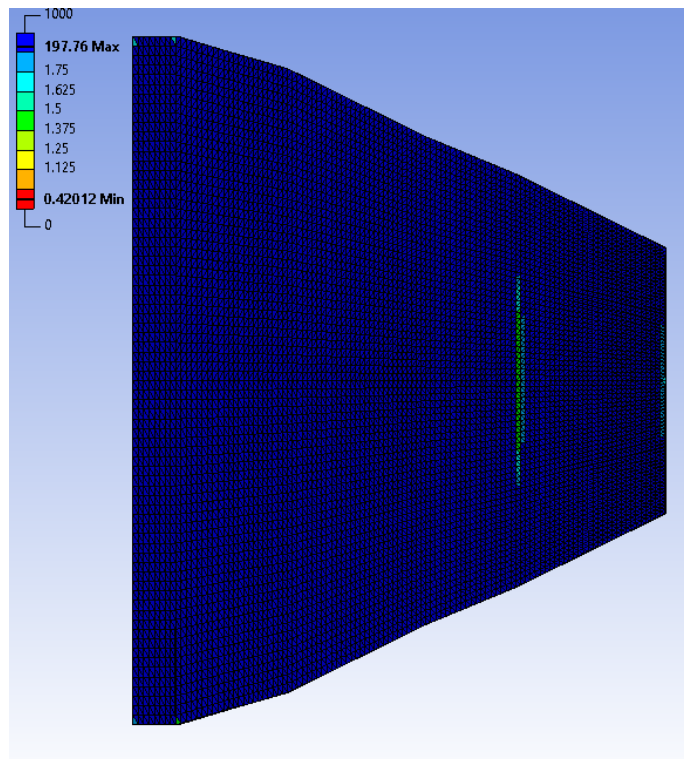


Figure 61: Jet wing Composite Safety Factor (bottom of wing)

The composite safety factor shows the areas ANSYS has identified as failing to support the structural loads. Failure occurs at the connection of the final rib to the root panel as well as at the corners of the support panel as seen in fig. (61). Note that in fig. (62) of the bottom of the wing the area of plate deformation is well within the strength of the composite. In fact, much of the wing is overbuilt with a peak safety factor of nearly 200. The wing weight could potentially be reduced by reducing the initial thickness of the composite laminate ply. However, there is a lower bound to the available thickness of composite lamina, of which 0.01 inches represents a soft floor. As with the UAV wing, the issues of composite strength predominate center on the 90-degree ply and could be resolved by softening the transition between the fuselage and the wing root.

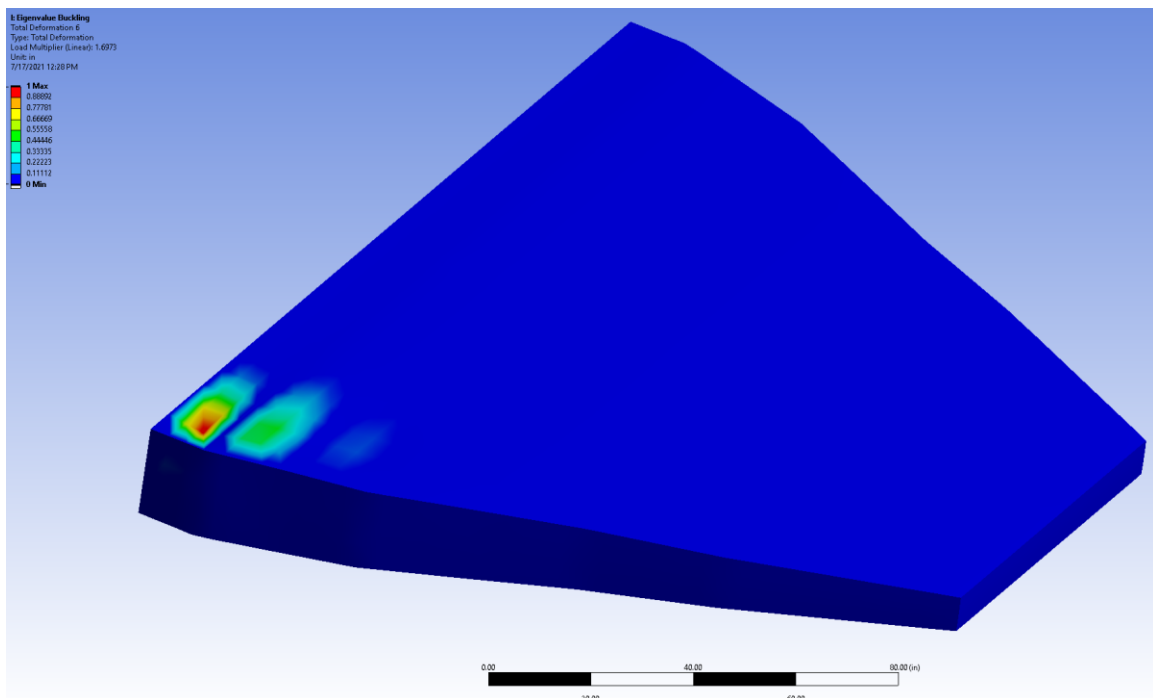


Figure 62: Jet wing Eigenvalue Buckling 1.675

Eigenvalue buckling is useful to see the global reaction of the structure to the applied load. The jet wings first buckling mode can be seen in fig. (63) where the structure fails under a 1.675 load multiplier. The output eigenvalue is an indicator of likely failure, in this case a load multiplier above the applied load. This suggests that the structure would not buckling under the current critical loading. This provides a degree of confidence in the developed wing. The higher buckling load multiplier observed in this wing likely occurred because the buckling of a panel depends on its characteristic length and width as a ratio. This structure is comparatively wide with respect to its length lending it a high resistance to buckling.

The processing of the figures developed in ANSYS for the maneuvering jet wing present potential limitations to the modeler's ability to develop low aspect ratio wings. As previously mentioned, this wing shows plate deformation of the bottom wing panel. This deformation does not lead to any failure modes in the wing. However, it is not optimal for the wing to maintain its profile and aerodynamic characteristics. Potential solutions include the addition of stiffeners in this region or the creation of further checks within the model that check for non-optimal deformations. Omitting the panel deformation, the wing passes all checks. However, further analysis should be done to confirm the global buckling characteristics of the wing. The structure developed serves the function of providing initial sizing, weight, and structural predictions early in the design process.

CHAPTER 6

CONCLUSION

Upon initial review, composites have favorable material properties for use in aerospace design because they typically have a very high modulus of elasticity and extreme tensile strength while also being lightweight and non-reactive. However, composites require a fundamentally different design approach than that of traditional metallic wings. The design precedent for small aircraft wings made of metallics is to optimize around the buckling failure mode ^[6]. Through this project it has been found that composite wings require a secondary failure check for the potential laminate failures ^[4]. Additional composite failures not accounted for in the model include plate buckling, shear crimping, and face sheet wrinkling. The potential drawbacks of composites are exacerbated by the fact that aircraft are expected to last for several thousands of hours without failure. Further, parts including the wings are often rebuilt instead of being replaced, which introduces concerns about fatigue and potential lifespan issues of a composite wing.

In practice, the use of fully composite primary structures is rare, and anecdotally tends to be overweight when compared to the initial design promises. This is likely due to the use of strength-based sizing, which dimensions the wing using the tensile failure mode. This is a failure mode in which the composites excel. However, strength-based sizing contradicts the established aircraft design principle of buckling as the limiting failure mode for lightweight aircraft ^[14]. Additionally, structures in industry take advantage of more complex laminate layups using strips of composite “tape” in critical areas to strengthen the wing as well as stackups that vary not only in the spanwise direction but also chord wise. To approach the strength of a more complex structure using

the simplified laminate, a composite scaling factor was used in addition to the already included 3.6 K factor used in the critical buckling force equation. The constant was set to 3, which created a more pessimistic composite structural sizing that could support the applied critical loading.

Despite the potential drawbacks of composite laminates when used for primary structures, the wings developed still succeeded during analysis. The goal for the created model and the accompanying analysis was to create a tool for design teams to employ in the conceptual design phase that provides in-depth information about structural sizing and rib spacing. Using the concept of a napkin sketch where in the early steps of the design process an engineer can develop a wing structure that can be used to inform critical design decisions. Enabling this by providing an accurate approximation of the structural weight, composite sizing, and structural geometry. The tool is not intended to develop a final wing structural design. To this end, the model has performed well and developed reasonable wing structures. The wings are realistically weighted and when checked through ANSYS, the wings appropriately support the applied load while being on the edge of failure by having a safety factor close to one. To refine the model, further functionality could be added; in the case of the maneuvering jet aircraft, the low aspect ratio wings development could benefit from the addition of failure criteria for plate buckling and shear crimping.

REFERENCES

[1] MIL-STD 499

[2] Yeh, H., Murthy, H., “An Investigation of Failure Criterion for New Orthotropic Ceramic Matrix Composite Materials” *Journal of Reinforced Plastics and Composites*, Vol 28, No. 4/2009 pp. 441-459

[3] Froud, G.R. “Your sandwich order, Sir?” *Composites*, July 1980, pp. 133-138

[4] Roylance, D., “Laminated Composite Plates” Department of Materials Sciences and Engineering Massachusetts Institute of Technology Cambridge, Ma 02139, February 10, 2000

[5] Sun, C.T., Quinn, B.J., Tao, J., Oplinger, D.W., William j., “Comparative Evaluation of Failure Analysis Methods for Composite Laminates”, DOT/FAA/AR-95/109 May 1996

[6] Kolesov, N., Takahashi, T., “Design and Validation of Buckling Dominated Wing Structures for Small Unmanned Aerial Systems”, 2020

[7] 14 CFR § 25.613 (2021)

[8] Niu, M., “Buckling and Stability of Structures,” *Airframe Structural Design*, 2nd ed., Hong Kong Conmilit Press LTD, Hong Kong, 2011, pp. 118-161.

[9] 14 CFR § 04 et seq (1938)

[10] 14 CFR § 23 et seq (2021)

[11] 14 CFR § 25 et seq (2021)

[12] MIL-HDBK-5J

[13] Sedaghati, R., “Wing-Box Structural Design Optimization” Department of Mechanical and Industrial Engineering Concordia University. Ref. No: CRIAQ 4.1-Task 6, June 2006

[14] Takahashi, T.T., Lemonds, T., “Transport Category Wing Weight Estimation Using an Optimizing Beam-Element Structural Formulation” AIAA Paper 2014

[15] 14 CFR § 25.337 (2021)

[16] 14 CFR § 25.305 (2021)

[17] 14 CFR § 04.200 (1945)

[18] 14 CFR § 04.201 (1945)

[19] 14 CFR § 25.303 (2021)

[20] 14 CFR § 04.202 (1945)

[21] 14 CFR § 04.203 (1945)

[22] 14 CFR § 04.210 (1945)

[23] 14 CFR § 04.2130 (1945)

[24] 14 CFR § 04.2111 (1945)

[25] 14 CFR § 04.2110 (1945)

[26] 14 CFR § 25.301 (2021)

[27] Ainsworth, J., Collier, C., “Airframe Wingbox Preliminary Design and Weight Prediction” Society of Allied Weight Engineers, 2020

[28] Appendix B - Plate Buckling Under Uniaxial Compression, Mechanics of Optimal Structural Design: Minimum Weight Structures David W. A. Rees, 2009 John Wiley & Sons, Ltd. ISBN: 978-0-470-74623-3

[29] Hutchins, C., Missoum, S., Takahashi, T.T., “Fully Parameterized Wing Model for Preliminary Design,” AIAA Paper 2010-9120, Sept. 2010.

[30] Takahashi, T.T., Lemonds, T., “Prediction of Wing Structural Mass for Transport Category Aircraft Conceptual Design,” AIAA Paper 2015-3374, 2015.

[31] Anderson, B., “Conceptual Fuselage Design with Direct CAD Modeling” Arizona State University, May 2017

[32] Alonso, J.J., Martin, J.R.R.A., Reuther, J.J., Haimes, R., Crawford, C.A., “High-Fidelity Aero-Structural Design Using a Parametric CAD-Based Model,” AIAA Paper 2003-3429. Jun. 2003.

[33] 14 CFR § 25.302 (2021)

[34] Rastogi, N., Ghosh, D. K., Vanderplaats, G. N., “Discrete Optimization Capabilities in Genesis Structural Analysis and Optimization Software,” AIAA Paper 2002-5646, Sept. 2002.

[35] Beam, S., “Collier Comes Back to His Future at Langley” NASA [online], http://www.nasa.gov/centers/langley/news/researchernews/rn_collier.html [retrieved 4 November 2020].

[36] “Our Products” HyperSizer [online], <http://hypersizer.com/about/> [retrieved 4 November 2020].

[37] “Orion” Lockheed Martin [online], <https://www.lockheedmartin.com/en-us/products/orion> [retrieved 4 November 2020]

[38] "genesis" Vanderplaats [online], <http://www.vrand.com/products/genesis/> [retrieved 4 November 2020]

[39] Kurus, N., "Unique Design Discoveries for a Modern Mach 1.3 Airliner Including Anomalies in the Shock Wave Formation Along a Highly Swept Blunt Leading Edge Wing" Arizona State University, December 2020

[40] G. Arnold, "A morning at Boeing," 9 April 2009. [Online], <http://geoffarnold.com/?p=3124> [retrieved 7 June 2021]

[41] What are the Effects of the Boeing 787s Very Flexible Wings [Online], <https://aviation.stackexchange.com/questions/838/what-are-the-effects-of-the-boeing-787s-very-flexible-wings> [retrieved 7 June 2021]

APPENDIX A
MATERIAL PROPERTIES TABLES

Table 2.1 Mechanical properties of representative reinforcing fibers [1-2]

Fiber	Density (g/cm ³)	Tensile Modulus (GPa)	Tensile Strength (MPa)	Diameter (μm)
<u>Glass</u>				
E-glass	2.54	72.4	3450	3-20
S-glass	2.49	85.5	4590	8-13
<u>Carbon</u>				
T300	1.75	230	3530	7-8
AS4	1.77	241	4130	6-7
IM6	1.74	276	5130	
UHM	1.85	441	3450	
<u>Aramid</u>				
Kevlar 29	1.44	62	2760	12
Kevlar 49	1.44	124	3620	12
<u>Boron</u>				
100 μm	2.61	400	3450	100
140 μm	2.47	400	3450	140
200 μm	2.39	400	3450	200
<u>Ceramic</u>				
Al ₂ O ₃	3.95	379	1380	20±5
SiC (CVD)	3.3	430	3500	140
SiC (pyrolysis)	2.6	180	2000	10-20

Table 2.2 Mechanical properties of representative matrix materials [1]

Matrix Material	Density (g/cm ³)	Tensile Modulus (GPa)	Tensile Strength (MPa)	Flexural Modulus GPa
<u>Thermosets</u>				
Epoxy 9310/9360 @23°C	1.2	3.12	75.8	
Epoxy 9310/9360 @149°C	1.2	1.4	26.2	
Epoxy 9420/9470 (A) @23°C	1.16	2.66	57.2	
Epoxy 9420/9470 (B) @23°C	1.16	2.83	77.2	
Polyimides	1.46		120	3.5-4.5
Phenolics	1.30		50-55	
Polyester	1.1-1.4	2-4.4	34.5-104	
<u>Thermoplastic</u>				
PEEK	1.30	3.24	92	4.0
Polyetherimide	1.27	3.0	105	3.5
Polysulfone	1.25	2.48	75	2.8
Polyamide-imide	1.38		95	5.0
Polyphenylene sulfide	1.32	3.3	70	4.0
<u>Aluminum alloys</u>				
1100	2.7	63	86	
2024	2.7	71	240	
5052	2.7	68	135	

Table 3.3 Comparison of properties – unidirectional composites and metals [1]

Material	Fiber Volume Fraction	Density (g/cm ³)	Longitudinal Tensile Modulus (GPa)	Longitudinal Tensile Strength (MPa)	Specific Tensile Strength	Specific Modulus
Boron-Epoxy B-4/N5505	0.50	2.00	204	1260	630	102
Carbon-epoxy T300/N5208	0.70	1.60	181	1500	938	113
Carbon-epoxy AS/H3501	0.66	1.60	138	1447	904	86
Carbon-epoxy IM6/epoxy	0.66	1.60	203	3500	2188	127
Carbon-PEEK AS4/APC2	0.66	1.60	134	2130	1331	84
Aramid-epoxy Kevlar 49/Epoxy	0.60	1.46	76	1400	959	52
Glass-epoxy E-glass/epoxy	0.45	1.80	38.6	1060	589	21
4340 Steel		7.8	207	990	127	27
2014-T6 Al		2.8	72	460	164	26
Ti-6Al-4V		4.5	110	930	207	24

Table 7.1 Typical strengths of unidirectional composites (MPa)

Type	Material	V_f	Long Tens S_{1T}	Long Comp S_{1C}	Trans Tens S_{2T}	Trans Comp S_{2C}	Shear S_{12}
B(4)/5505	Boron-epoxy	0.50	1260	2500	61	202	67
T300/5208	Carbon-epoxy	0.70	1500	1500	40	246	68
AS/3501	Carbon-epoxy	0.66	1447	1447	52	206	93
Scotchply 1002	Glass-epoxy	0.45	1062	610	31	118	72
Kevlar 49/Epoxy	Aramid-epoxy	0.60	1400	235	12	53	34
AISI 4130 ¹	Alloy steel		1240	1240	1240	1240	745
2024-T3	Aluminum alloy		448	448	448	448	276

Note: ¹Heat treat to 180 ksi (1240MPa)

APPENDIX B
EXCEL MODEL EXAMPLES

Composite Name	1	2	3	4	5	6	7	8	9	10	11	12	13	14	15	16	17	18	19	20
Core Material	12	12	12	12	12	12	12	12	12	12	12	12	12	12	12	12	12	12	12	12
Symmetric Composite																				
Material	3	3	3	3	3	3	3	3	3	3	3	3	3	3	3	3	3	3	3	3
Ply Thickness	0.01	0.011	0.012	0.013	0.014	0.015	0.016	0.017	0.018	0.019	0.02	0.021	0.022	0.023	0.024	0.025	0.026	0.027	0.028	0.03
Number of Plies (S)	10	10	10	10	10	10	10	10	10	10	10	10	10	10	10	10	10	10	10	10
Ply Orientation																				
0 Degree	1	1	1	1	1	1	1	1	1	1	1	1	1	1	1	1	1	1	1	1
90 Degree	1	1	1	1	1	1	1	1	1	1	1	1	1	1	1	1	1	1	1	1
45 Degree	1	1	1	1	1	1	1	1	1	1	1	1	1	1	1	1	1	1	1	1
-.45 Degree	1	1	1	1	1	1	1	1	1	1	1	1	1	1	1	1	1	1	1	1
Effective Ply Thickness	7	7	7	7	7	7	7	7	7	7	7	7	7	7	7	7	7	7	7	7
Layup																				
10	1	1	1	1	1	1	1	1	1	1	1	1	1	1	1	1	1	1	1	1
9	1	1	1	1	1	1	1	1	1	1	1	1	1	1	1	1	1	1	1	1
8	1	1	1	1	1	1	1	1	1	1	1	1	1	1	1	1	1	1	1	1
7	90	90	90	90	90	90	90	90	90	90	90	90	90	90	90	90	90	90	90	90
6	45	45	45	45	45	45	45	45	45	45	45	45	45	45	45	45	45	45	45	45
5	0	0	0	0	0	0	0	0	0	0	0	0	0	0	0	0	0	0	0	0
4	0	0	0	0	0	0	0	0	0	0	0	0	0	0	0	0	0	0	0	0
3	0	0	0	0	0	0	0	0	0	0	0	0	0	0	0	0	0	0	0	0
2	0	0	0	0	0	0	0	0	0	0	0	0	0	0	0	0	0	0	0	0
1	-45	-45	-45	-45	-45	-45	-45	-45	-45	-45	-45	-45	-45	-45	-45	-45	-45	-45	-45	-45
Core thickness	0.06	0.06	0.06	0.06	0.06	0.06	0.06	0.06	0.06	0.06	0.06	0.06	0.0625	0.0625	0.0625	0.0625	0.0625	0.0625	0.0625	0.0625
1	-45	-45	-45	-45	-45	-45	-45	-45	-45	-45	-45	-45	-45	-45	-45	-45	-45	-45	-45	-45
2	0	0	0	0	0	0	0	0	0	0	0	0	0	0	0	0	0	0	0	0
3	0	0	0	0	0	0	0	0	0	0	0	0	0	0	0	0	0	0	0	0
4	0	0	0	0	0	0	0	0	0	0	0	0	0	0	0	0	0	0	0	0
5	0	0	0	0	0	0	0	0	0	0	0	0	0	0	0	0	0	0	0	0
6	45	45	45	45	45	45	45	45	45	45	45	45	45	45	45	45	45	45	45	45
7	90	90	90	90	90	90	90	90	90	90	90	90	90	90	90	90	90	90	90	90
8	1	1	1	1	1	1	1	1	1	1	1	1	1	1	1	1	1	1	1	1
9	1	1	1	1	1	1	1	1	1	1	1	1	1	1	1	1	1	1	1	1
10	1	1	1	1	1	1	1	1	1	1	1	1	1	1	1	1	1	1	1	1

Mat.	Name	E1 [psi]	E2 [psi]	v12	v21	G12 [psi]	S_1T	S_1C	S12	S_2T	S_2C	Density [lbm/in^3]
1	Test	2000000	1200000	0.3	0.018	1000000	1000	600	70	50	120	
2	Boron-E B(4)/5505	29587752	1775265	0.3	0.018	700000	182747.9	362595	9717.546	8847.318	29297.68	0.0722546
3	Carbon-E T300/N5208	26251878	1493891	0.28	0.015934	700000	217557	217557	9862.584	5801.52	35679.35	0.05780368
4	Carbon-E AS/H3501	20015244	1200915	0.3	0.018	700000	209870	209870	13488.53	7541.976	29877.83	0.05780368
5	Carbon-E IM6/epoxy	29442714	1766563	0.32	0.0192	700000	0	0	0	0	0	0.05780368
6	AS4/APC2	19435092	1166106	0.3	0.018	700000	0	0	0	0	0	0.05780368
7	Kevlar 49/Epoxy	11022888	661373.3	0.3	0.018	700000	203053.2	34083.93	4931.292	1740.456	7687.014	0.05274586
8	Glass-epoxy	5598467	335908	0.3	0.018	700000	0	0	0	0	0	0.06502914
9		0	0	0.3	#DIV/0!		0	0	0	0	0	
10		0	0	0.3	#DIV/0!		0	0	0	0	0	
11	PVC Foam Core	217557	13053.42	0.3	0.018		0	0	0	0	0	0.00162
12	FR-3703 Polyurethane	1250	1250	0.3	0.3	2000	75	45	40	75	45	0.00173611
13	FR-3740 Polyurethane	72200	72200	0.3	0.3	61000	2750	4500	2000	2750	4500	0.02314816
14	FR-6710 Polyurethane	10000	10000	0.3	0.3	10900	280	560	225	280	560	0.00578704
15	FR-6725 Polyurethane	51300	51300	0.3	0.3	35600	1100	3100	1000	1100	3100	0.0144676

Layers	Orientation	Thickness [in.]	Z-Cordinates	0	-45	45	90
10	1	0.02	-0.23125	0	0	0	0
9	1	0.02	-0.21125	0	0	0	0
8	1	0.02	-0.19125	0	0	0	0
7	90	0.02	-0.17125	0	0	0	0.02
6	45	0.02	-0.15125	0	0	0.02	0
5	0	0.02	-0.13125	0.02	0	0	0
4	0	0.02	-0.11125	0.02	0	0	0
3	0	0.02	-0.09125	0.02	0	0	0
2	0	0.02	-0.07125	0.02	0	0	0
1	-45	0.02	-0.05125	0	0.02	0	0
Total Thickness =		0.14		0.08	0.02	0.02	0.02
Core Material Properties							
Layers	Density	Stiffness	Thickness	1/2 Thick	Z-Cor.		
1	0.001736112		0.0625	0.03125	-0.03125		
Skin (Lower)							
Layers	Orientation	Thickness [in.]	Z-Cordinates	0	-45	45	90
1	-45	0.02	0.05125	0	0.02	0	0
2	0	0.02	0.07125	0.02	0	0	0
3	0	0.02	0.09125	0.02	0	0	0
4	0	0.02	0.11125	0.02	0	0	0
5	0	0.02	0.13125	0.02	0	0	0
6	45	0.02	0.15125	0	0	0.02	0
7	90	0.02	0.17125	0	0	0	0.02
8	1	0.02	0.19125	0	0	0	0
9	1	0.02	0.21125	0	0	0	0
10	1	0.02	0.23125	0	0	0	0
Total Thickness =		0.14		0.08	0.02	0.02	0.02
Structure Total Thickness =			0.3425	0.18248			
Ply Total Thickness =			0.28	0.81752			

Sheet	Zp (B)				Core
	0	-45	45	90	
-10	0	0	0	0	
-9	0	0	0	0	
-8	0	0	0	0	
-7	0	0	0	-0.00645	
-6	0	0	-0.00565	0	
-5	-0.00485	0	0	0	
-4	-0.00405	0	0	0	
-3	-0.00325	0	0	0	
-2	-0.00245	0	0	0	
-1	0	-0.00165	0	0	-0.00098
1	0	0.00165	0	0	0.00098
2	0.00245	0	0	0	
3	0.00325	0	0	0	
4	0.00405	0	0	0	
5	0.00485	0	0	0	
6	0	0	0.00565	0	
7	0	0	0	0.00645	
8	0	0	0	0	
9	0	0	0	0	
10	0	0	0	0	
Totals	0	0	0	0	0

Zp (D)					
Sheet	0	-45	45	90	Core
-10	0	0	0	0	
-9	0	0	0	0	
-8	0	0	0	0	
-7	0	0	0	0.00156	
-6	0	0	0.001199094	0	
-5	0.000884094	0	0	0	
-4	0.000617094	0	0	0	
-3	0.000398094	0	0	0	
-2	0.000227094	0	0	0	
-1	0	0.000104094	0	0	3.1E-05
1	0	0.000104094	0	0	3.1E-05
2	0.000227094	0	0	0	
3	0.000398094	0	0	0	
4	0.000617094	0	0	0	
5	0.000884094	0	0	0	
6	0	0	0.001199094	0	
7	0	0	0	0.00156	
8	0	0	0	0	
9	0	0	0	0	
10	0	0	0	0	
Totals	0.00425275	0.000208188	0.002398188	0.00312	6.1E-05

Basic Loading	
Nx	-36283.30693
Ny	0
Nz	0
Mx	0
My	0
Mz	0

Stiffness Matrix (Q)		
0 Deg.		
26369523.96	420164.1276	0
420164.1276	1500586.17	0
0	0	700000
90 Deg.		
1500586.17	420164.1276	0
420164.1276	26369523.96	0
0	0	700000
45 Deg.		
7877609.595	6477609.595	6217234.446
6477609.595	7877609.595	6217234.446
6217234.446	6217234.446	6757445.468
neg. 45 deg.		
7877609.595	6477609.595	-6217234.446
6477609.595	7877609.595	-6217234.446
-6217234.45	-6217234.45	6757445.468
Core		
1373.626374	412.0879121	0
412.0879121	1373.626374	0
0	0	61000

Extensional Stiffness (A)		
A _{ij} = sum(Q _{ij})p(Z _p -Z _{p-1})		
4909441.9	602267.3486	0
602267.349	1925169.365	0
0	0	684408.1
Coupling Stiffness (B)		
0	0	0
0	0	0
0	0	0
Flexural Stiffness (D)		
45787.7314	6660.876456	4538.581
6660.87646	36432.34784	4538.581
4538.58115	4538.581146	7593.339

Laminate Stiffness						
4909441.899	602267.3486	0	0	0	0	0
602267.3486	1925169.365	0	0	0	0	0
0	0	684408.137	0	0	0	0
0	0	0	45787.73	6660.87646	4538.581146	0
0	0	0	6660.876	36432.3478	4538.581146	0
0	0	0	4538.581	4538.58115	7593.338775	0
2.11818E-07	-6.6265E-08	0	0	0	0	0
-6.6265E-08	5.40165E-07	0	0	0	0	0
0	0	1.4611E-06	0	0	0	0
0	0	0	2.35E-05	-2.748E-06	-1.2384E-05	0
0	0	0	-2.7E-06	2.9978E-05	-1.6276E-05	0
0	0	0	-1.2E-05	-1.628E-05	0.000148825	0

Surface Strain & Surface Curvature	
ε _x ⁰ [in]	-0.00768547
ε _y ⁰ [in]	0.00240431
γ _{xy} ⁰	0
K _x	0
K _y	0
K _{xy}	0

Top Surface					Compression	Tension	Compression	Tension		
ϵ_x	-0.00768547	Stress	Sigma x	-201651.85 Psi	S_1/E1	0.0082873	S_1/E1	0.036	0.06	
ϵ_y	0.00240431		Sigma y	378.718169 Psi	S_2/E2	0.0238835	S_2/E2	0.036	0.06	
γ_{xy}	0		Tau xy	0 Psi	S_12/G12	0.0140894	S_12/G12	0.02	0.02	
Core					Failure Criteria					
ϵ_x	-0.00768547	Stress	Sigma x	-9.5661704 Psi	Maximum Stress	Tsai Hill	0.045840274	Maximum Strain	0.2134851	
ϵ_y	0.00240431		Sigma y	0.13553688 Psi		Sigma 1	0.212581564			0.0400718
γ_{xy}	0		Tau xy	0 Psi		Sigma 2	0.001807158			0.0000000
0 degree Ply					Maximum Stress	Tau 12	0	Maximum Strain	0.6191099	
ϵ_1	-0.00768547	Stress	Sigma 1	-201651.85 Psi		Tsai Hill	0.865003736			0.9273795
ϵ_2	0.00240431		Sigma 2	378.718169 Psi		Sigma 1	0.926892043			0.6191099
γ_{12}	0		Tau 12	0 Psi	Sigma 2	0.065279128	0.0000000			
90 degree Ply					Maximum Stress	Tau 12	0	Maximum Strain	0.3217898	
ϵ_2	-0.00768547	Stress	Sigma 2	-10522.498 Psi		Tsai Hill	0.176849101			0.2901201
ϵ_1	0.00240431		Sigma 1	60171.3638 Psi		Sigma 1	0.276577466			0.3217898
γ_{12}	0		Tau 12	0 Psi	Sigma 2	0.294918442	0.0000000			
45 degree Ply					Maximum Stress	Tau 12	0	Maximum Strain	0.3580625	
ϵ_x	-0.00768547	Stress	Sigma x	-44968.91 Psi		Tsai Hill	0.913261593			0.3186297
ϵ_y	0.00240431		Sigma y	-30843.224 Psi		Sigma 1	0.249696197			0.1105608
γ_{xy}	0		Tau xy	-32834.177 Psi	Sigma 2	0.602280579	0.3580625			
-45 degree Ply					Maximum Stress	Tau 12	0.716124991	Maximum Strain	0.3186297	
ϵ_x	-0.00768547	Stress	Sigma x	-44968.91 Psi		Tsai Hill	0.913261593			0.1105608
ϵ_y	0.00240431		Sigma y	-30843.224 Psi		Sigma 1	0.249696197			0.3186297
γ_{xy}	0		Tau xy	32834.1772 Psi	Sigma 2	0.602280579	0.1105608			
						Tau 12	0.716124991	Check	0.3580625	